1. SITE 1[1]

The Shipboard Scientific Party[2]

SITE REPORT

Setting and Purpose

The general geological setting of the Gulf Coast States has been summarized by Eardly (1951), King (1959), Halbouty (1967), and Murray (1961).

The pre-Mesozoic history of the continental shelf of the Texas-Louisiana gulf coast is essentially unknown, principally because of its depth of burial. The Jurassic is well represented by evaporites and shales obtained from drilled wells on shore, and has been projected seawards by seismic reflection and refraction results. The Tertiary and Pleistocene sections make up the bulk of the continental shelf sediments and are largely clastic, and are probably largely the products of the erosion that followed the Laramide revolution. The layers thicken and plunge gulfwards, and additional layers are frequently added as wedges into this configuration. Salt domes occur as diapirs in these overlying sediments (Shepard, 1937; Parker and Curray, 1956; Lankford and Curray, 1957; Neumanń, 1958; Curray, 1960; and Halbouty, 1967). Gravity surveys have confirmed this interpretation (Joesting and Frautschy, 1947; Nettleton, 1957). Buried reefs along the shelf edge have also been suggested on the basis of seismic profiler records (Matthews, 1963).

The continental slope extends from the shelf edge, about 140 kilometers from the present coast line, to the Sigsbee Scarp (Figure 1), approximately 180 kilometers farther towards the Gulf. This is a broad and fairly gentle slope which has been described as hummocky and affected by slumping (Gealy, 1955; Ewing, Worzel, Ericson, and Heezen, 1955). This outbuilding and slumping must be a regular part of this slope building, as the contemporary faulting described by Hardin and Hardin (1961) suggests. The upper part of the continental slope, on the basis of seismic profiler and gravity data (moore and Curray, 1963; Ewing and Antoine, 1966; and Jones and Antoine, 1968) has been interpreted as intruded by salt structures. More recently, salt domes have been outlined by seismic profiling and drilled (Lehner, 1968). This suggests that the hummocky terrain is in part due to slumping and in part due to diapiric intrusion.

The seismic refraction studies first began in 1953 and reported in a series of papers (Ewing, Worzel, Ericson, and Heezen, 1955; Ewing, Antoine, and Ewing, 1960; Antoine and Ewing, 1963) showed that sediments with velocities in the range 2.3 to 3.6 km/sec vary in thickness from 12 to 15 kilometers beneath the shelf to about 6 to 7 kilometers beneath the slope just shoreward of the Sigsbee Scarp. Beneath a layer of 5.3 to 5.6 km/sec is found. Near the Sigsbee Scarp no further laying was encountered, although large shots were fired at intermediate and great distances. This lack of return was first interpreted as a salt or limestone layer underlain by a great thickness of lower velocity sediments (Ewing, Worzel, Ericson, and Heezen, 1955); later it was interpreted as a ridge of salt, possibly responsible for the Sigsbee Scarp (Ewing, Antoine, and Ewing, 1960), and more recently as one of a series of successive ridges, each formed seaward of the previous one by lateral stresses engendered by the accumulating slope sediments (Antoine and Ewing, 1963; Ewing and Antoine, 1966).

Recent profiling of a number of investigators (unpublished) suggests the presence of salt ridges whose tops are warped seawards by the lateral pressures of the accumulating slope sediments.

Figure 2 shows a reflection record section provided by a committee, which was the representaitve of the oil companies (Chevron, Conoco, Gulf, Humble, Mobil, and Texaco), from a Western Geophysical Company Survey in the vicinity of Hole 1. The section shoreward of the Sigsbee Escarpment is interpreted as supporting the latter hypothesis. However, seaward of the scarp there is disturbed layering tremination abruptly just beneath the scarp. Perhaps, this represents beds which have slumped from the continental slope, crossed the Sigsbee Scarp and been deposited in a disturbed but nearly horizontal position in the Sigsbee Basin just beyond the scarp.

Three drilling sites were recommended by the committee: one considerably north of the scarp, one just above the scarp, and a third just below the scarp, Hole 1 was drilled near the third site. This location was chosen

[1]Lamont-Doherty Geological Observatory of Columbia University contribution No. 1363.

[2]M. Ewing and J.L. Worzel, Lamont-Doherty Geological Observatory of Columbia University, Palisades, New York; A.O. Beall, Continental Oil Company, Ponca, City Oklahoma; W.A. Berggren, Woods Hole Oceanogarphic Institution, Woods Hole, Massachusetts; D. Bukry, U.S. Geological Survey, La Jolla, California; C.A. Burk, Mobil Oil Company, Princeton, New Jersey; A.G. Fischer, Princeton University, Princeton, New Jersey; and, E.A. Pessagno, Jr., Southwest Center for Advanced Studies, Dallas, Texas.

primarily for engineering tests and also to, obtain a location in moderately deep water for testing the ship positioning system.

Hole 1 was drilled at latitude 25°51.5′ N, lognitude 92°11.0′ W. The water depth was 2827 meters (9275 feet) corrected for sound velocity and transponder depth. The hole was drilled to a depth of 770.5 meters (2528 feet) subbottom, and no sediments older than Pleistocene were reached. Detailed geophysical description of Site 1 awaits the results of the site survey to be made during *Vema* Cruise 26 in March and April, 1969.

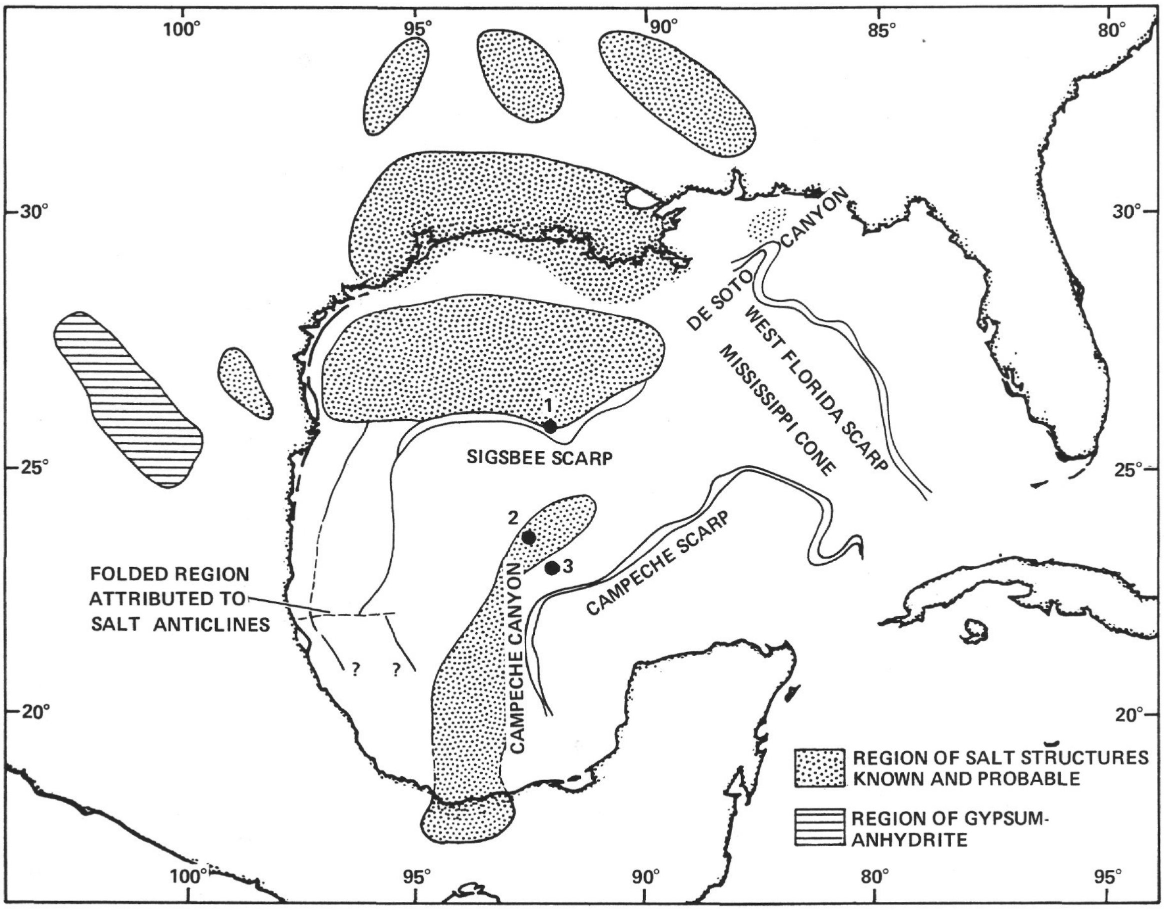

Figure 1. *Physiographic diagram of Gulf of Mexico, showing locations of Sites 1, 2, and 3.*

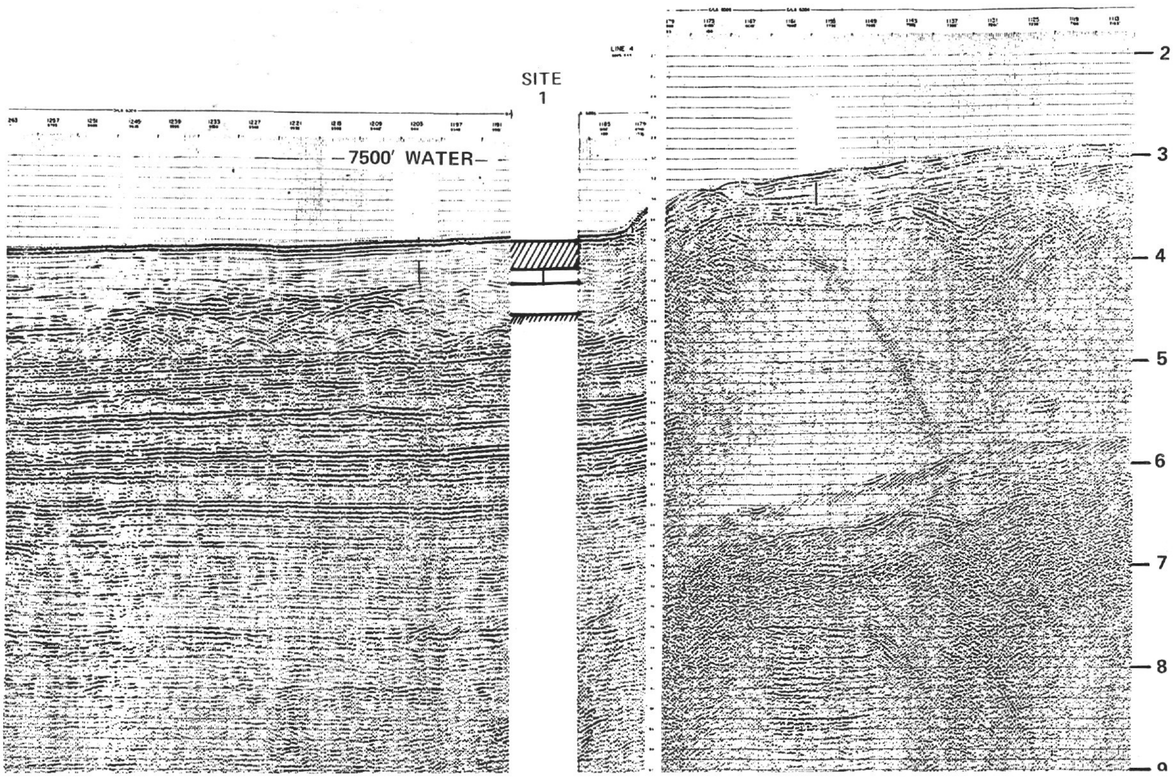

Figure 2. *Profiler record near Site 1.*

Interpretation of Down-Hole Logs

Three suites of logs were recorded at Site 1: an in-pipe neutron-gamma log; an open-hole gamma ray and qualitative gamma-gamma (density) log; and, a conventional resistivity log in the open hole. Analysis of these logs demonstrates the general lack of correlation of the in-pipe neutron-gamma log as compared to the open-hole devices. For this reason, the neutron-gamma log was not used for further analysis. This same conclusion was later independently reached by the JOIDES Advisory Panel on Well Logging (see Chapter 8).

Interpretation of down-hole logs from shallow, near surface borings is complicated by the unconsolidated nature of the sediments. Experience in the interpretation of such logs is generally lacking and examples from the literature are rare. Furthermore, most previous examples have involved shallow water or land situated drilling localities where fresh-water invasion is likely.

Results of open-hole logs from Site 1 are shown here at a reduced scale (Figure 3). From examination of the various curves, it is obvious that a moderately good correlation exists between resistivity, gamma ray, and gamma-gamma responses. Short normal resistivity values range from a minimum of about 0.6 ohmmeter up to over 2.0 ohmmeters at the base of the section. Ignoring the rather large scale variations in resistivity within specific segments of the log, there is an overall tendency for resistivity to increase with depth. Resistivity values as determined from the lateral curve, a deep investigating tool, are consistently higher than the short normal resistivity. This difference is increased in low resistivity zones as delineated by the short normal curve, suggesting invasion of drilling fluid (see Chapter 8). It is the authors' contention, however, that such zones represent enlarged hole diameter. This point will be elaborated subsequently.

On the assumption that only the higher resistivity values are truly representative of formation resistivity, a comparison can be made with resistivity values from shallow depths on the northern Gulf of Mexico continental shelf. Although values of drilling fluid resistivity were not attainable, conditions under which shallow segments of continental shelf borings are drilled and logged are similar to those of Hole 1 with one important exception. That exception involves temperature differences of both the drilling fluid and of the formation, especially near the sea floor. Short normal resistivity values for muds at depths of 1000 to 2000 feet on the outer continental shelf (off Louisiana) range between approximately 1.0 and 1.4 ohmmeters. This can be contrasted with resistivities from Hole 1 of 1.5 to 2.0^{+} ohmmeters. It is suggested that this difference arised from the appreciably lower formation and drilling fluid temperatures at Hole 1, and not to a basic difference in lithology. Contributions to higher resistivity from the drilling mud should be comparable to drilling mud resistivities of continental shelf borings.

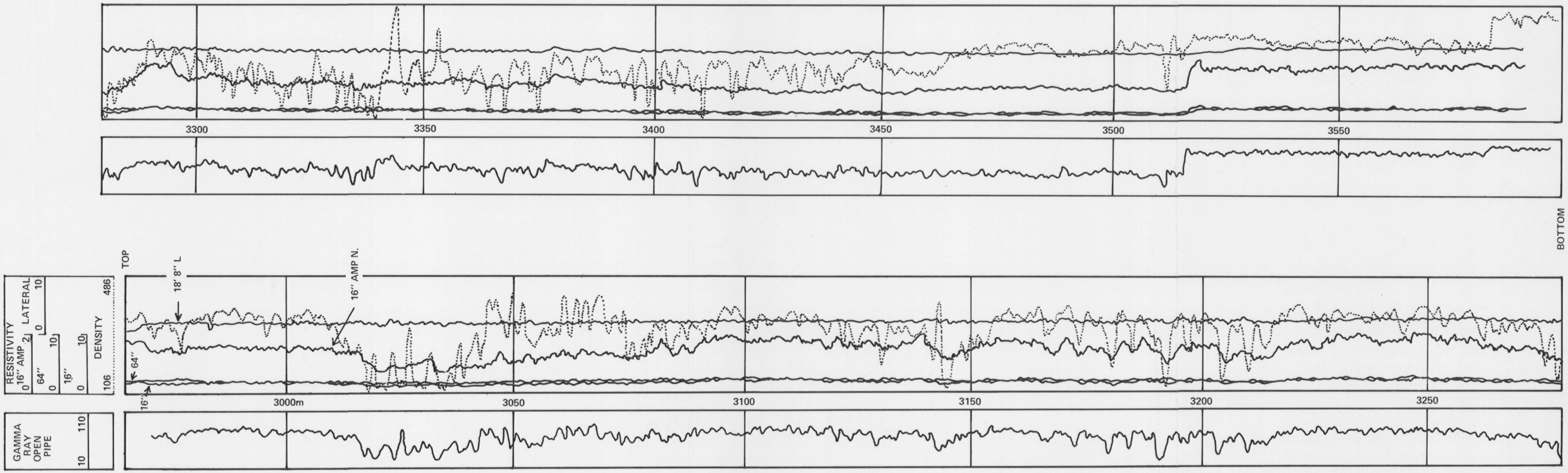

Figure 3 *Composite electric log, gamma gamma density log and natural gamma radiation log for Hole 1.*

Inspection of gamma ray and gamma-gamma curves shows a general increase of gamma-ray count and gamma-gamma density with depth, corresponding to the resistivity increase (Figure 3). The gamma-ray curve shows a good correspondence with that obtained from natural gamma-ray measurements of core (see Figure 4). Gamma-gamma density shows a more or less constant increase with depth except in the uppermost segment of the curve.

The general increases described above are in agreement with both the overall tendency of the sediments to become more consolidated with depth and the possibility of greater enlargement of the borehole in the upper part (see Chapter 8).

From a consideration of the sediments recovered by coring, the physical measurements performed on the cores, and the general sedimentological interpretation of these sediments and their postulated depositional setting, it appears highly unlikely that major thicknesses of "sand" could be present within the sequence.

In unconsolidated sands and muds, bulk densities of quartzrose sands are generally higher than the interbedded muds. A maximum "effective" porosity approaching 40 per cent in unconsolidated quartzrose sandstones has been well documented in the literature. As consolidation proceeds and water is expelled from the more easily compacted muds, a point is gradually reached where bulk density of the muds is higher than that of interbedded "effectively" porous sands. "Effective" porosity refers to intergranular porosity within sands not occupied by clay infill. At depths of less than 1000- to 2000 feet, bulk densities of muds are generally less than those obtained from related sands, as evidenced from the quartzrose sands of shallow depth from Site 3.

In considering the low resistivity zones previously mentioned, these zones apparently do not represent the proper combination of curve responses for sand; that is, gamma-gamma density should be higher, not lower. From cursory extrapolation of measured bulk densities of muds from the cores (which gives a very poor plot), the low resistivity zones would have an absurdly high porosity. The authors originally postulated foraminiferal ooze as the most likely lithology to give such a log response. Simple calculations as to percentage of open foraminifera tests and sediment water content have negated this postulation, since it too involves an extremely high porosity as compared to gamma-gamma density.

Therefore, it is concluded that large variations in borehole diameter are responsible for departures toward low resistivity, low gamma-ray count, and low gamma-gamma density values. If future down-hole logging programs include a bore-hole caliper, corrections for this variation can be made. At present, however, one can only postulate that the log would be more or less monotonous showing a general increase of response with depth, basically reflecting consolidation of a mud sequence.

In contrast to the above described curve responses, these are two thin intervals which are characterized by spikes of high gamma-gamma density with accompanying moderate or low resistivity values and high gamma-ray count. These zones occur from 3040 to 3072 meters (subrotary table) and 3338 to 3350 meters. These spikes could be interpreted as quartz-sand-rich zones were it not for the high gamma-ray count. It is concluded that such zones represent small hole diameter, possible more consolidated claystone intervals with resistivity lower than normal due to lack of non-clay mineral impurities (i.e., truly clays). Otherwise, these anomalies are unexplained.

Summary of Drilling and Coring at Site 1

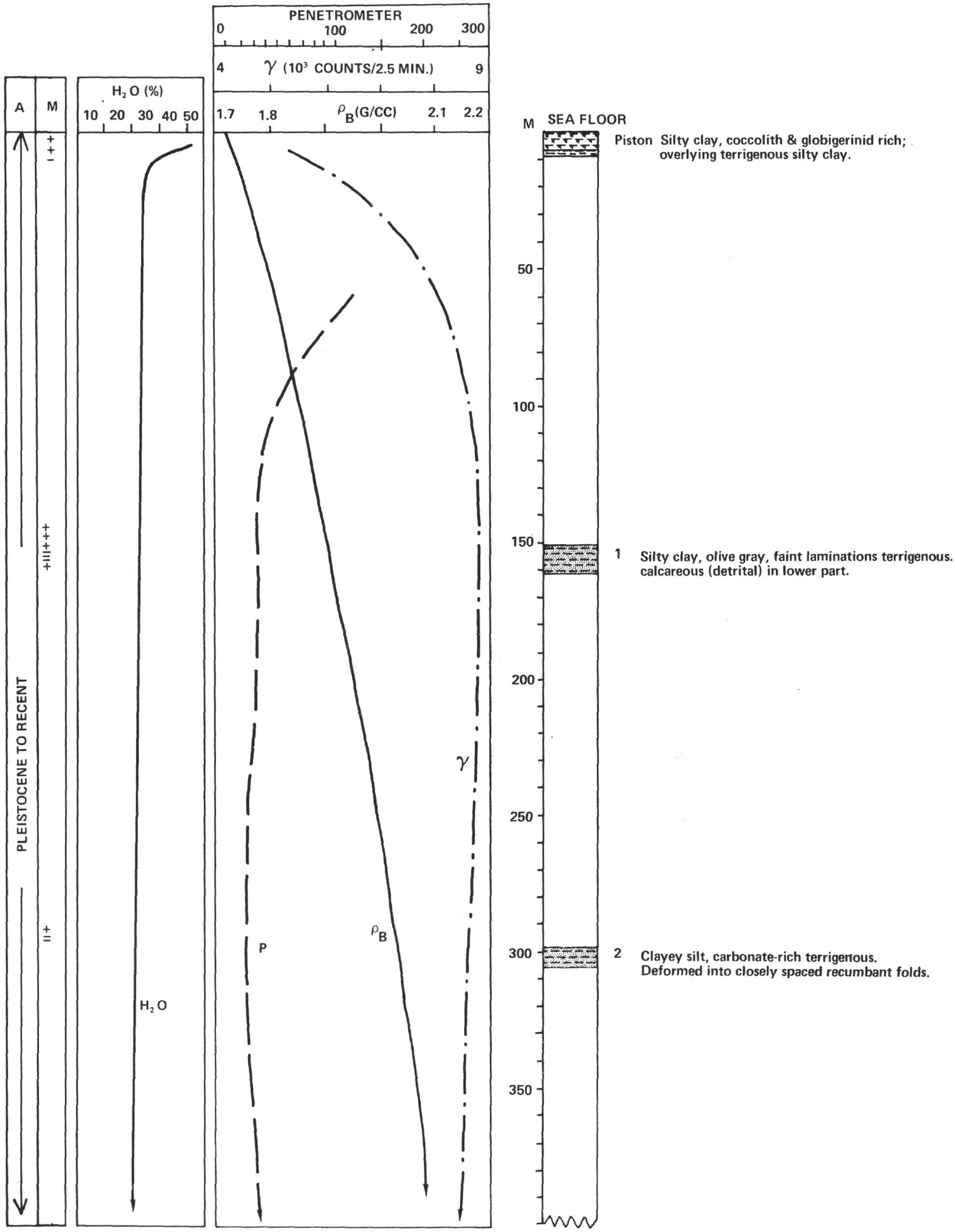

Figure 4. *Summary of Drilling and Coring at Site 1.*

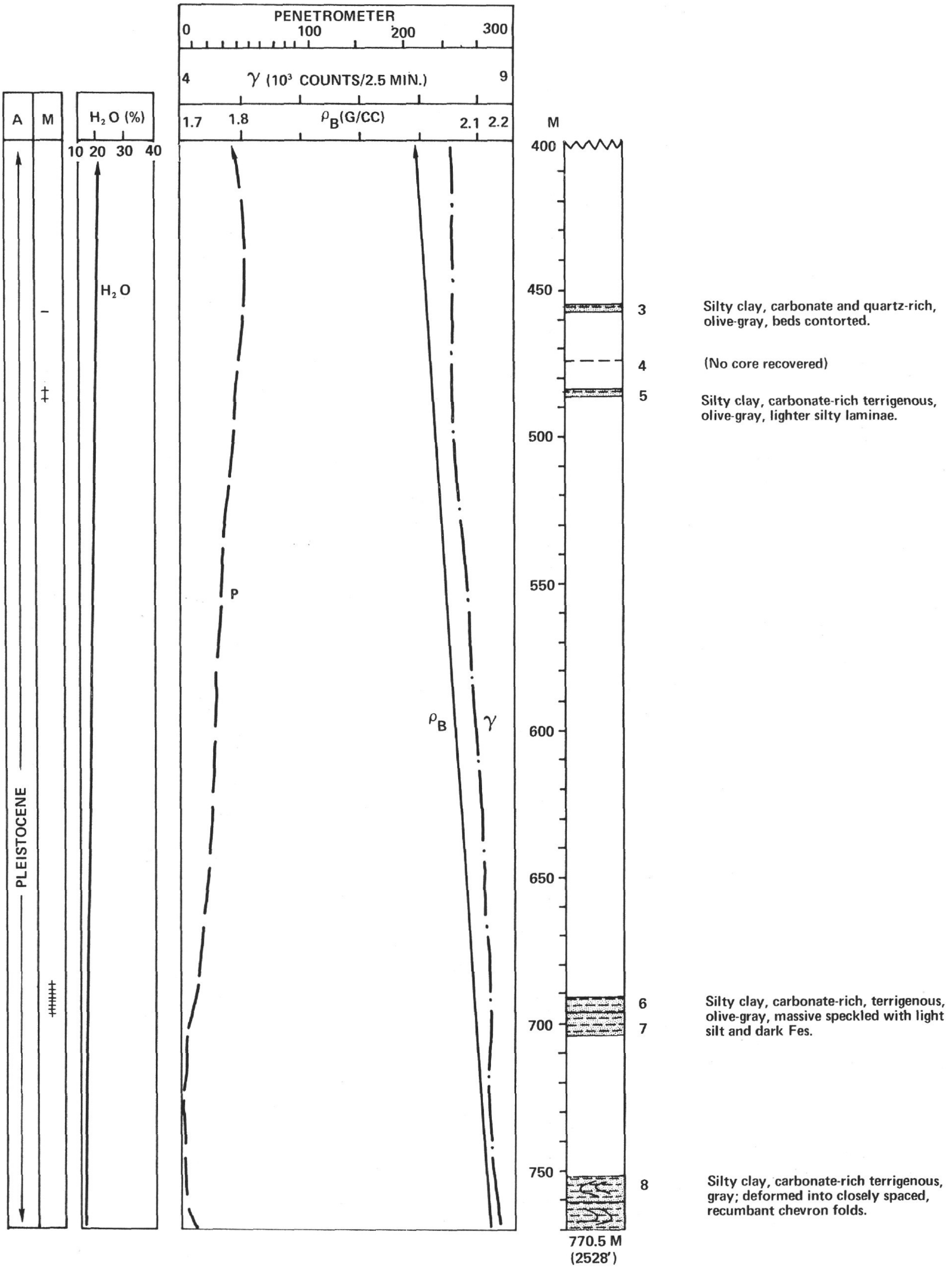

Figure 4. *Continued.*

The Cores Recovered from Site 1

Figures 5 through 13 are the graphic summaries of the cores recovered at Site 1.

These figures show, for each core:

(1) The stratigraphic age.
(2) The paleomagnetic results – normal (+) or reversed (–).
(3) The natural gamma radiation (full line).
(4) The bulk density was determined by the GRAPE (Gamma Ray Attenuation Porosity Evaluation) equipment (broken line).
(5) The length of the core in meters measured from the top of the core and the subbottom depth of the top of the cored interval.
(6) The lithology (see key which follows).
(7) The positions of the tops of each core section.
(8) Some notes on the lithology.

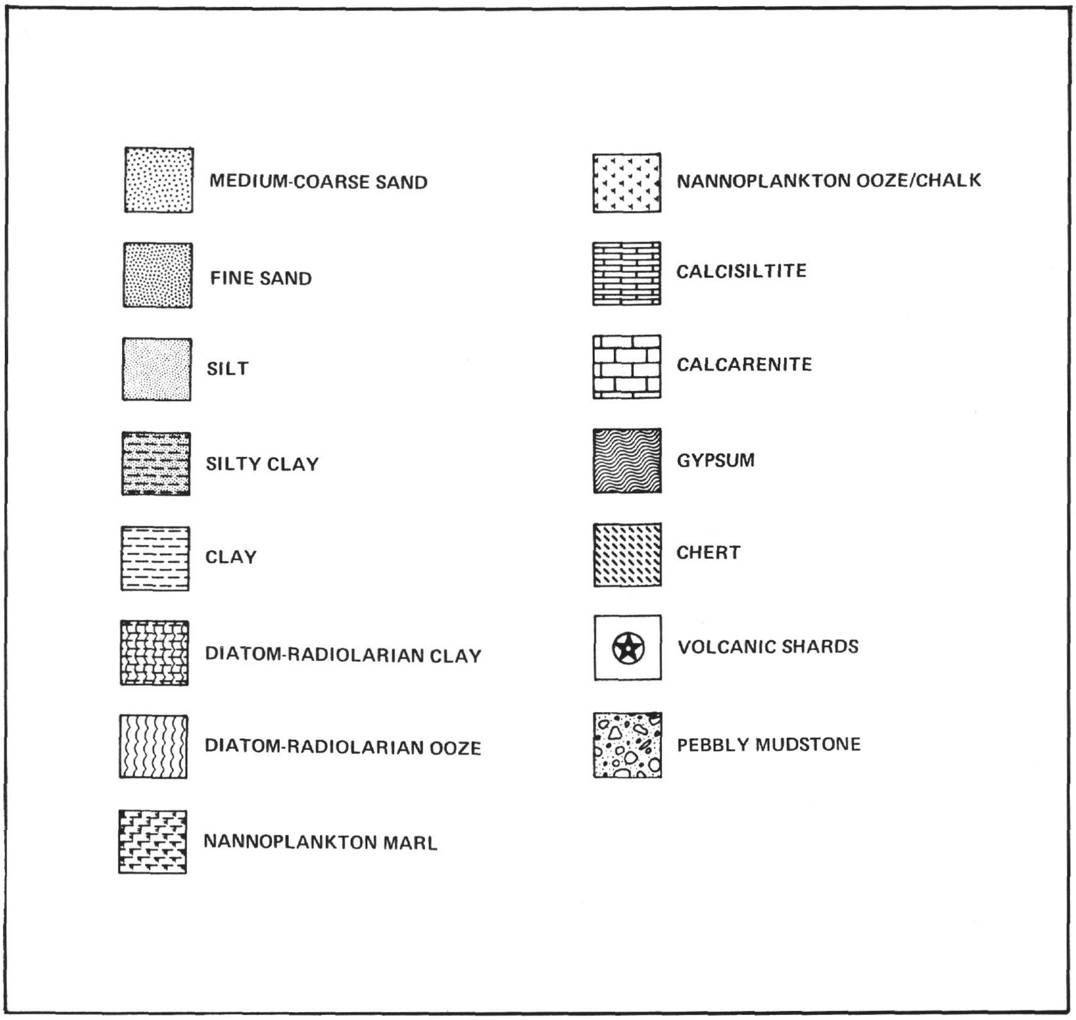

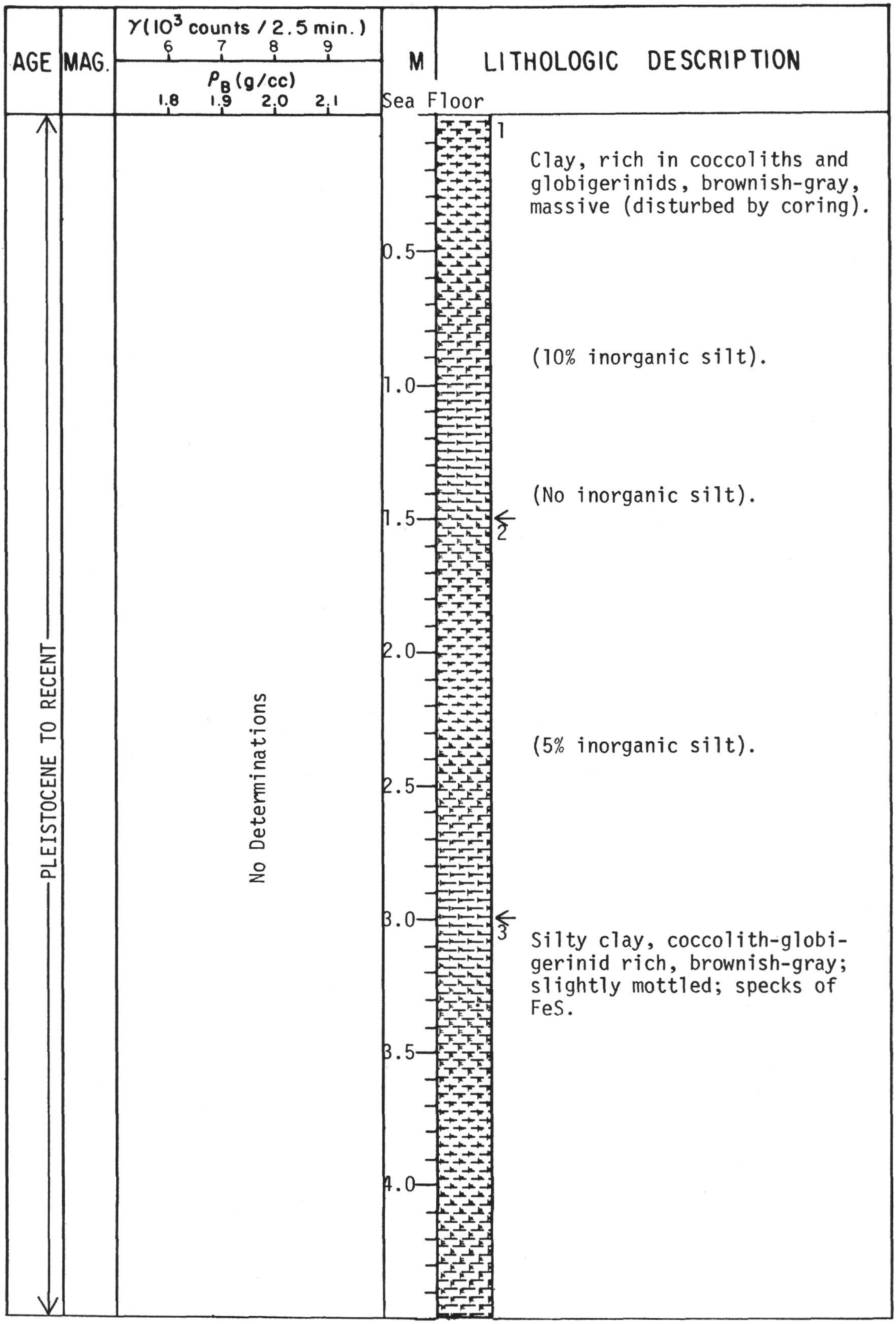

Figure 5. *Hole 1, Piston Core.*

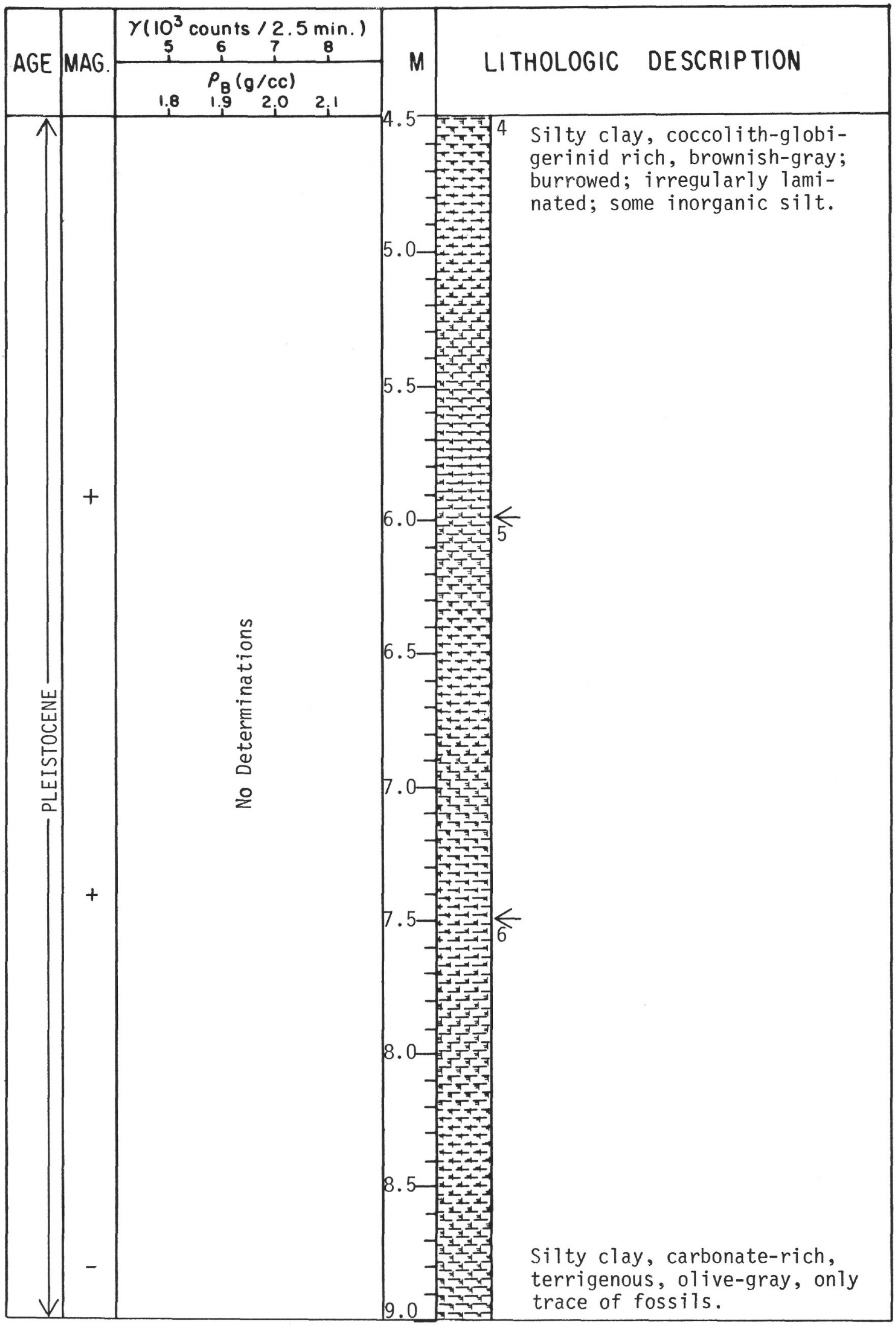

Figure 5. *Continued.*

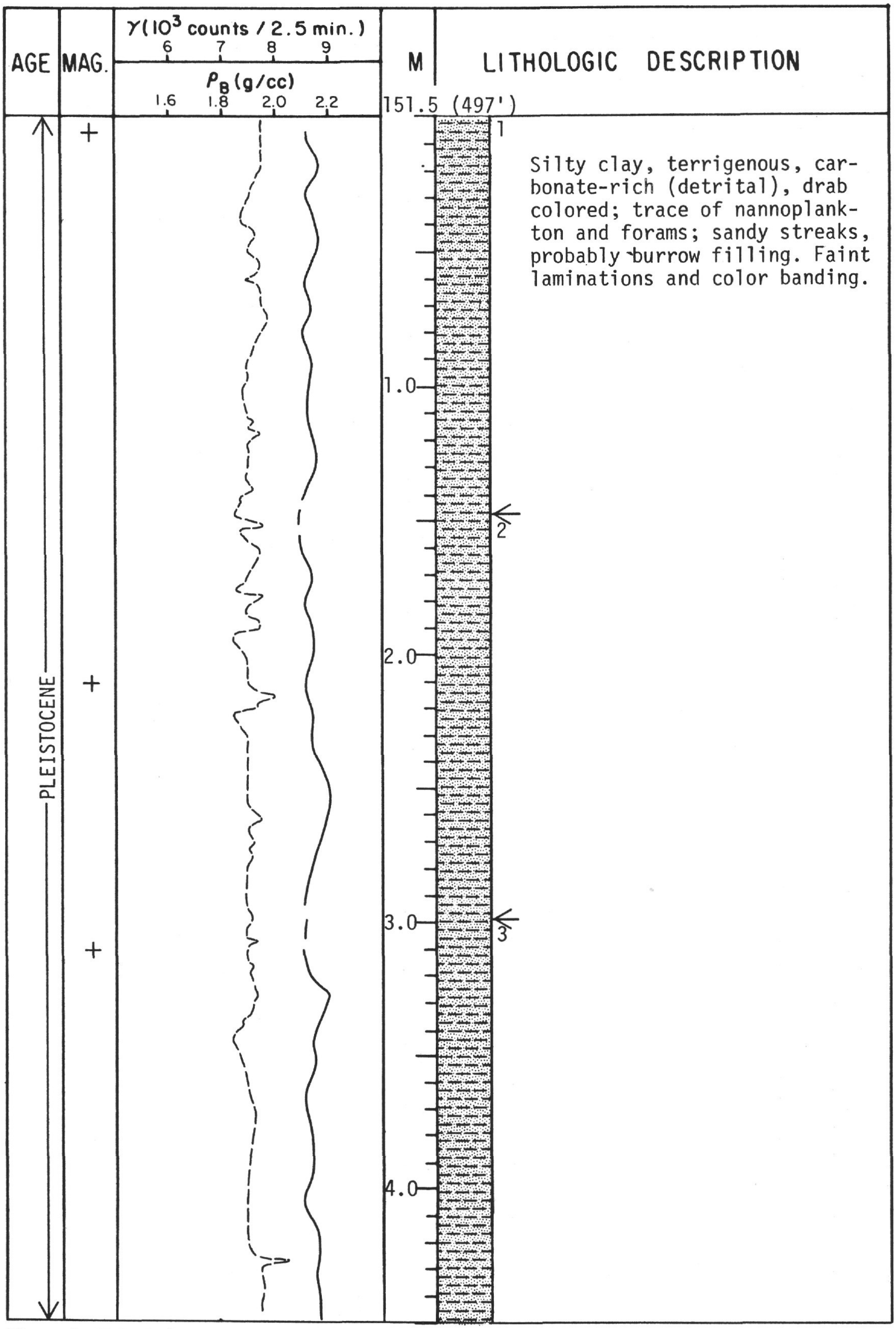

Figure 6. *Hole 1, Core 1.*

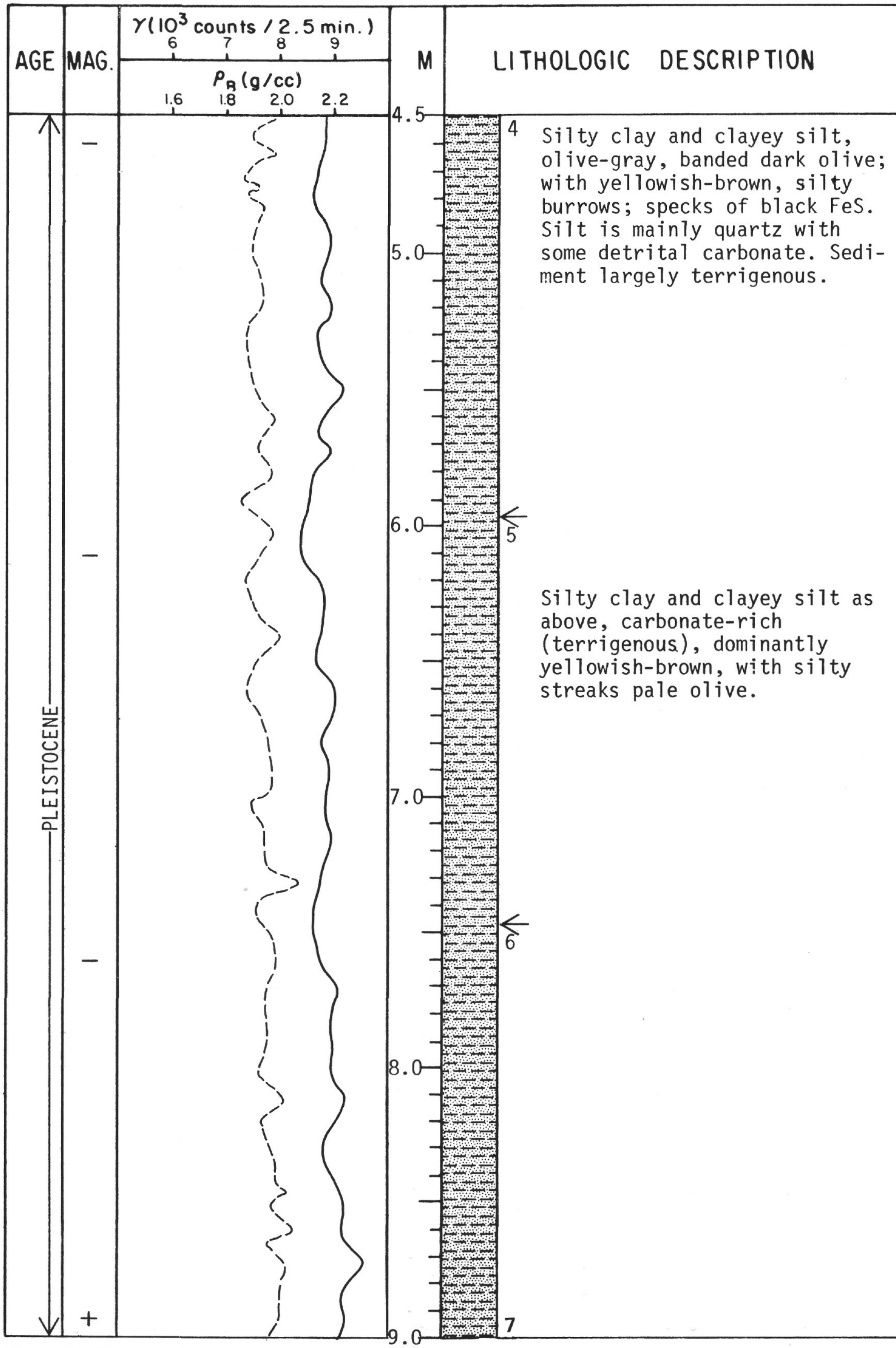

Figure 6. *Continued.*

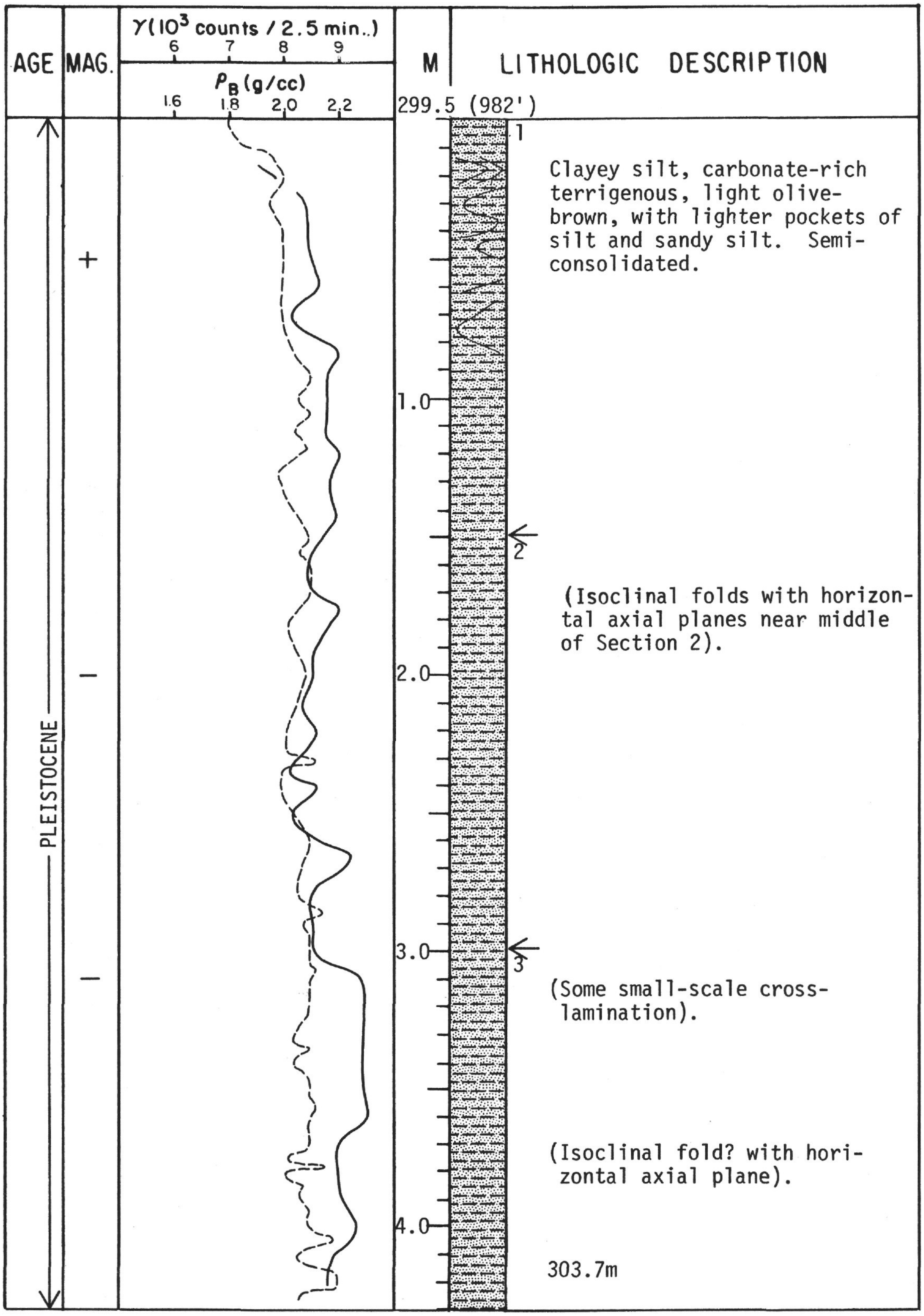

Figure 7. *Hole 1, Core 2.*

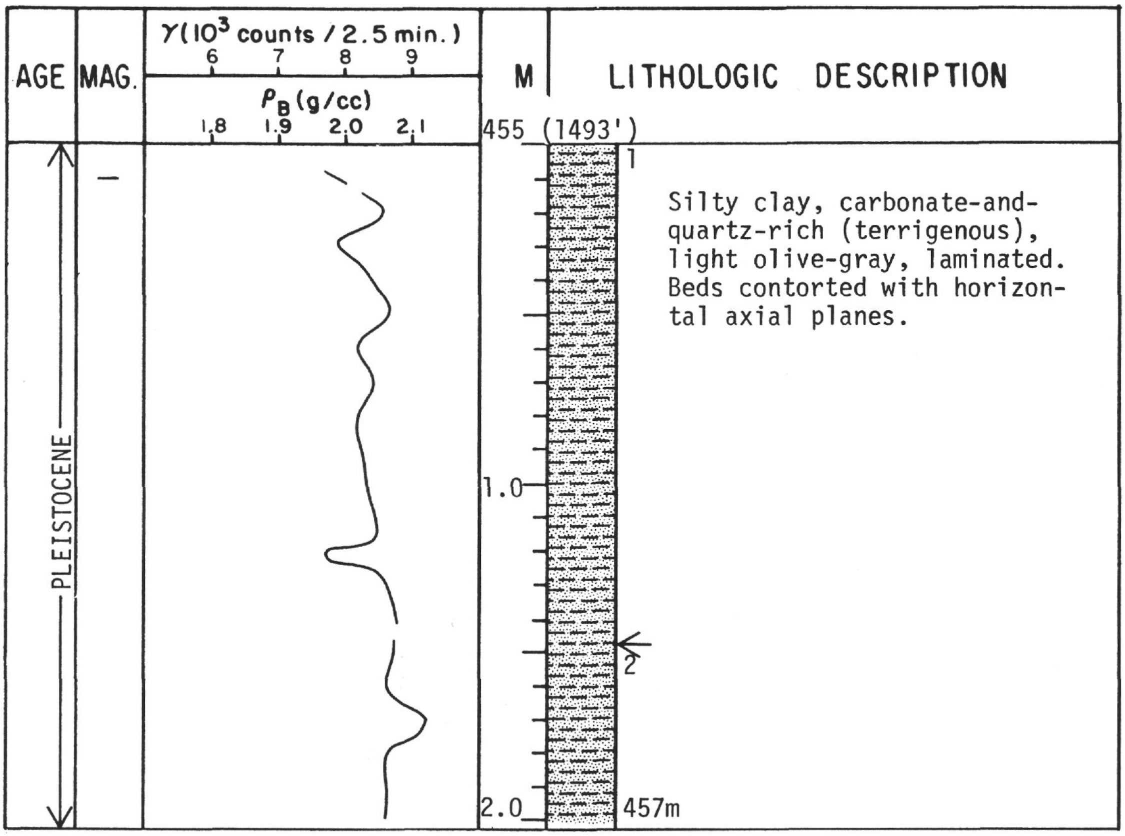

Figure 8. *Hole 1, Core 3.*

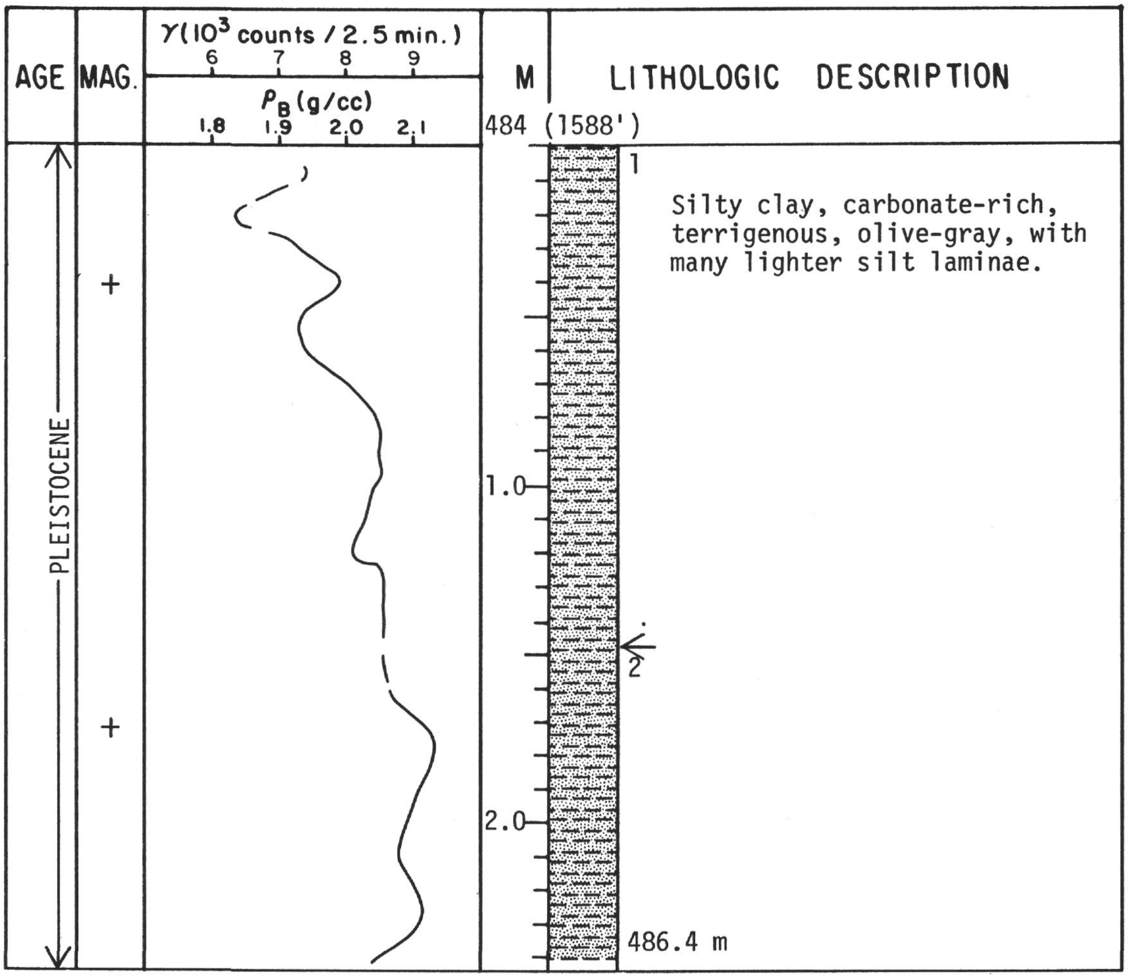

Figure 9. *Hole 1, Core 5.*

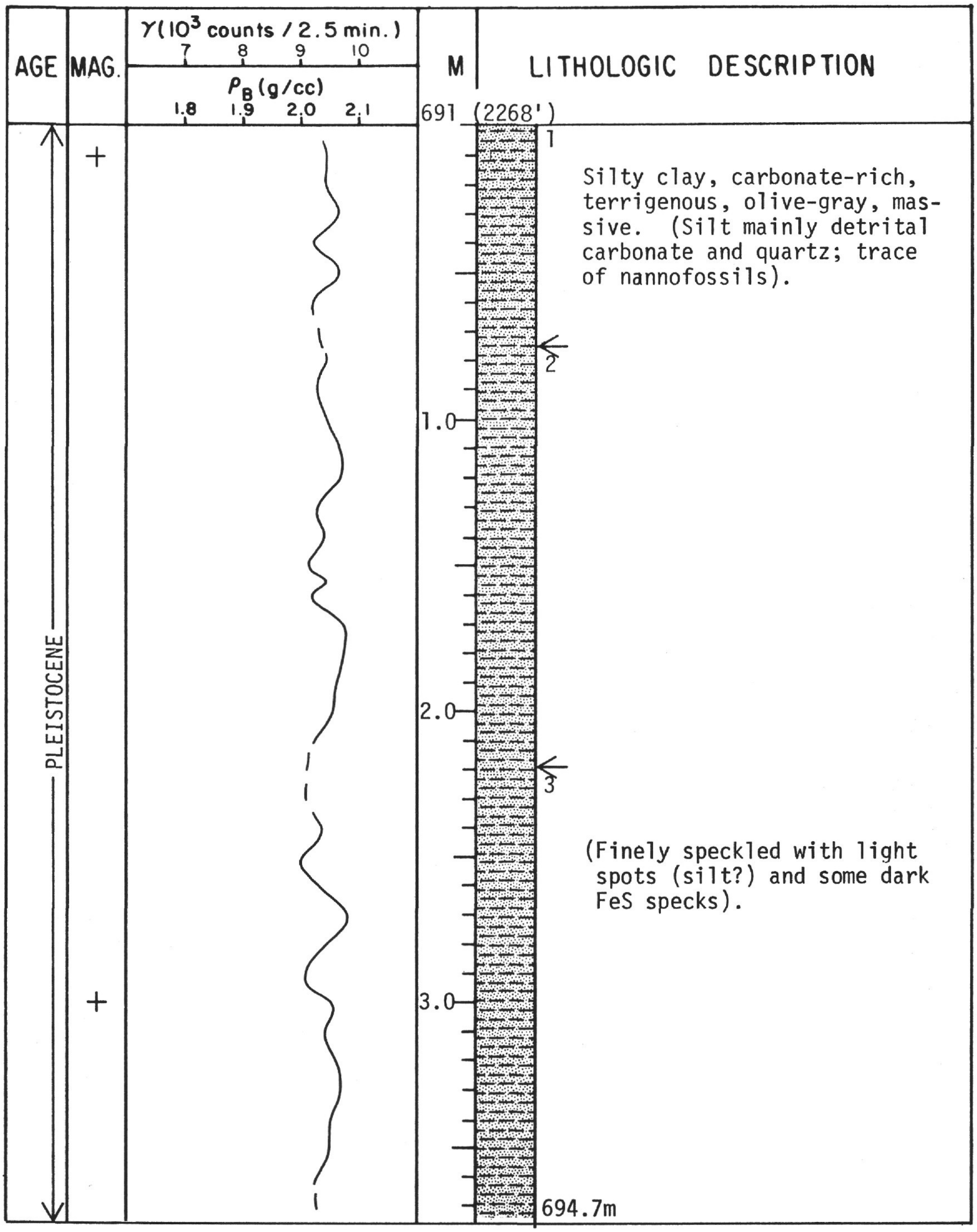

Figure 10. *Hole 1, Core 6.*

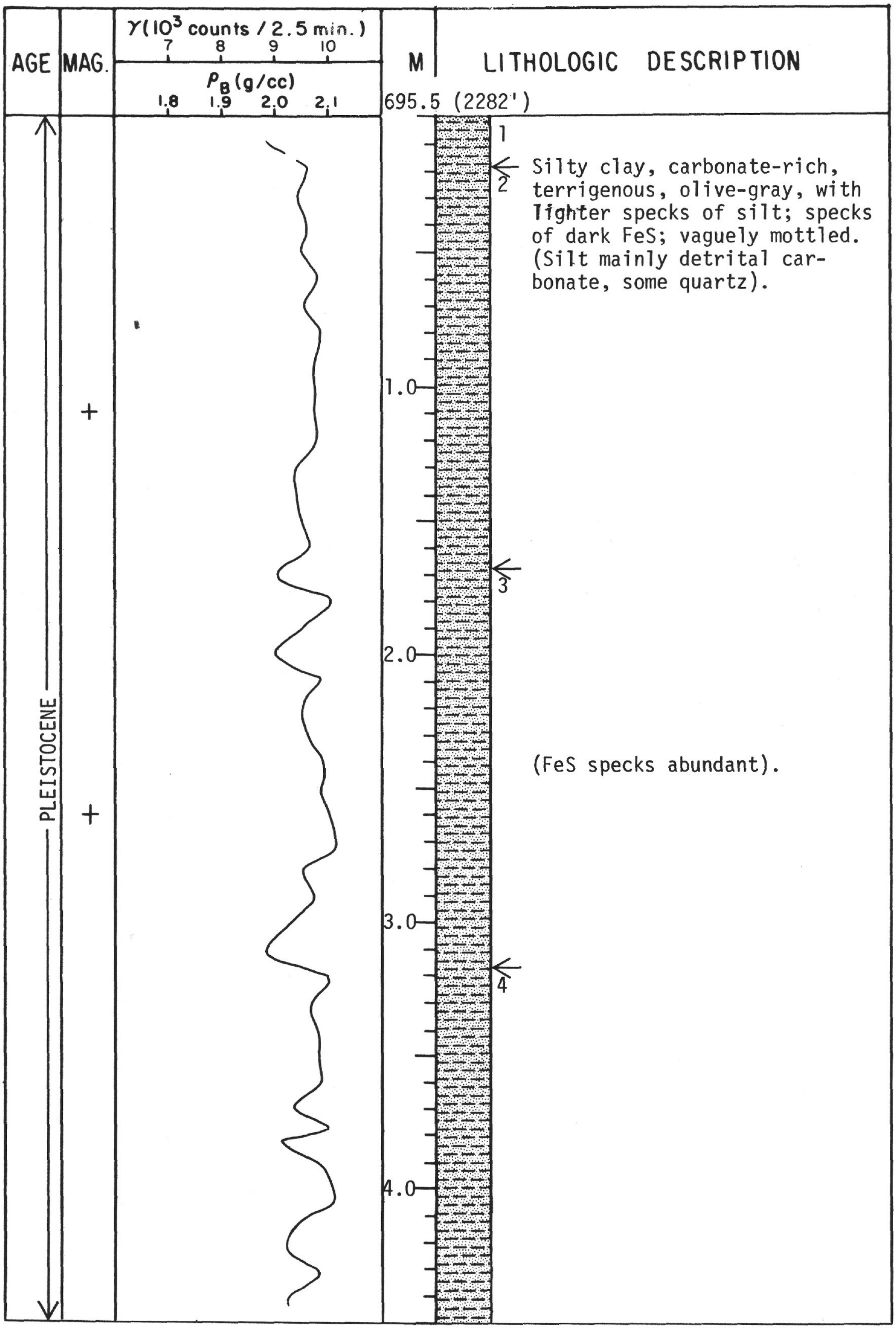

Figure 11. *Hole 1, Core 7.*

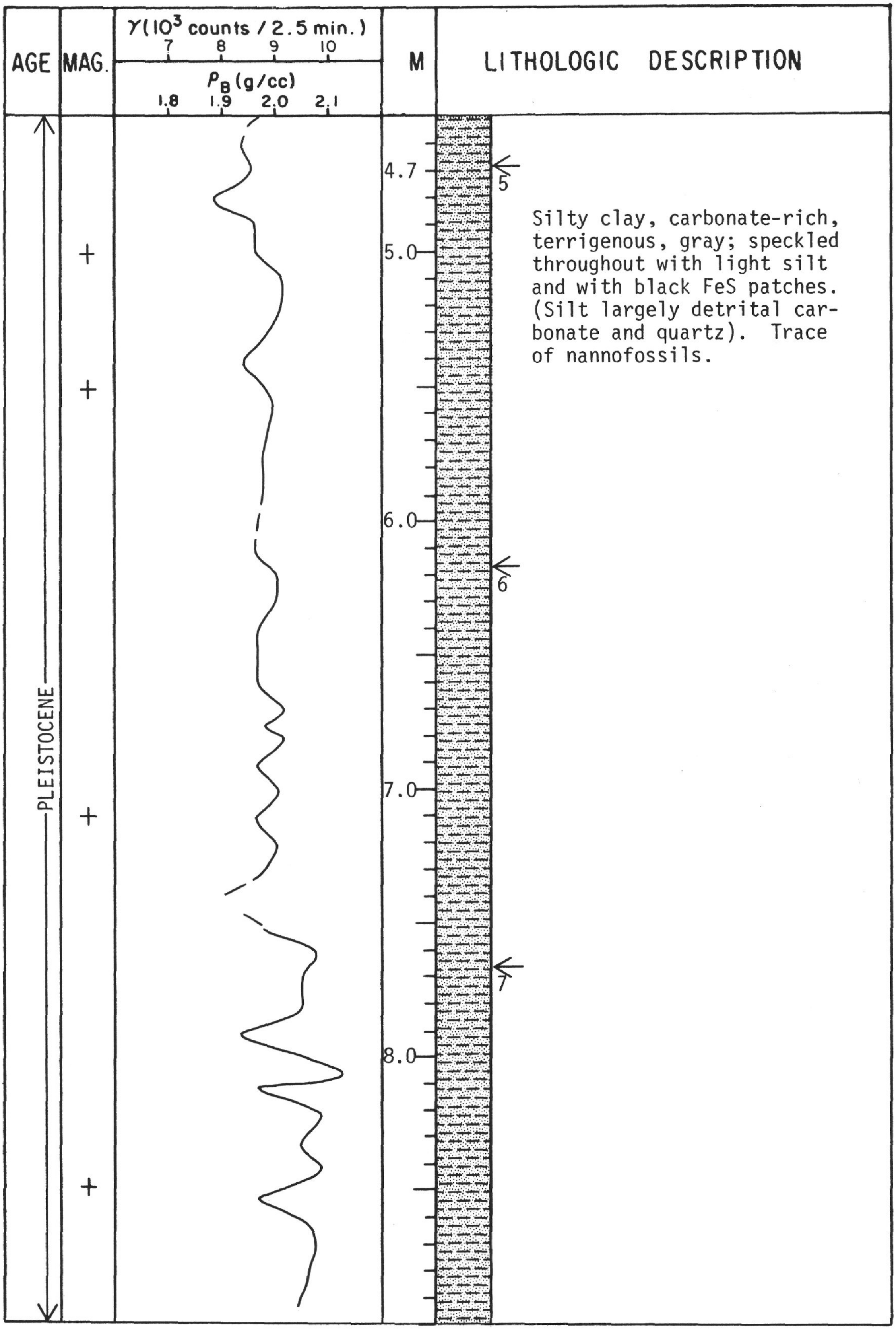

Figure 11. *Continued.*

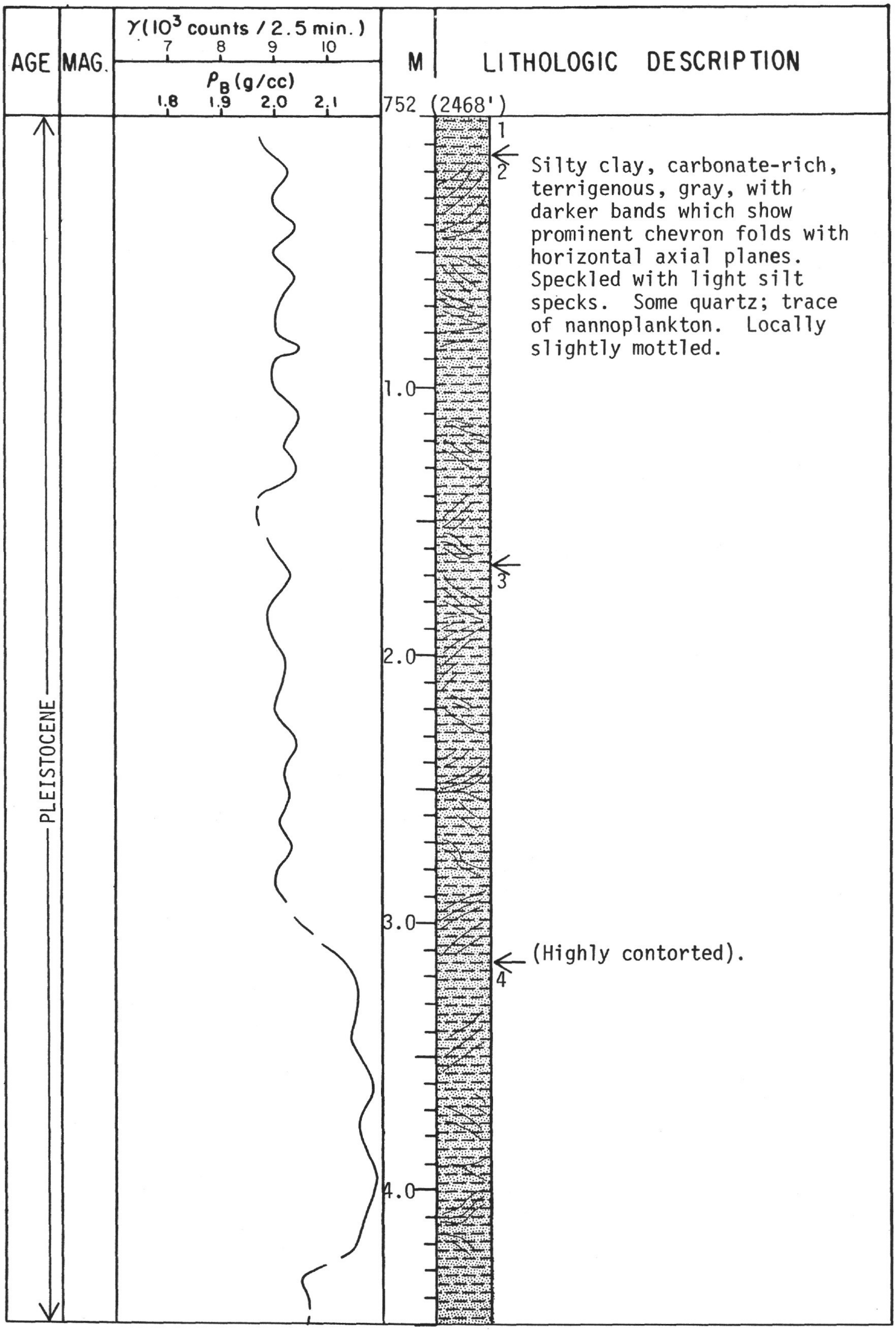

Figure 12. *Hole 1, Core 8.*

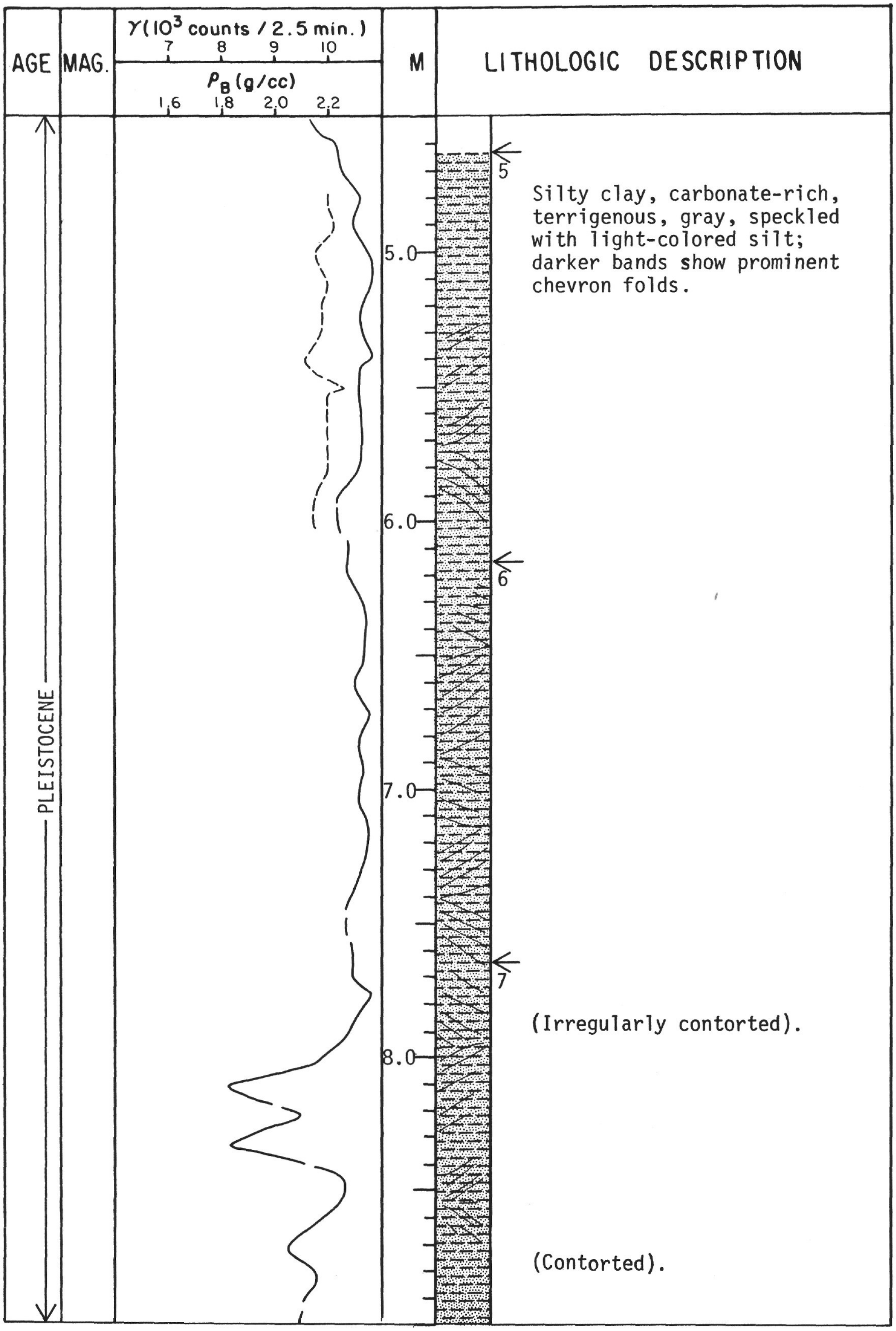

Figure 12. *Continued.*

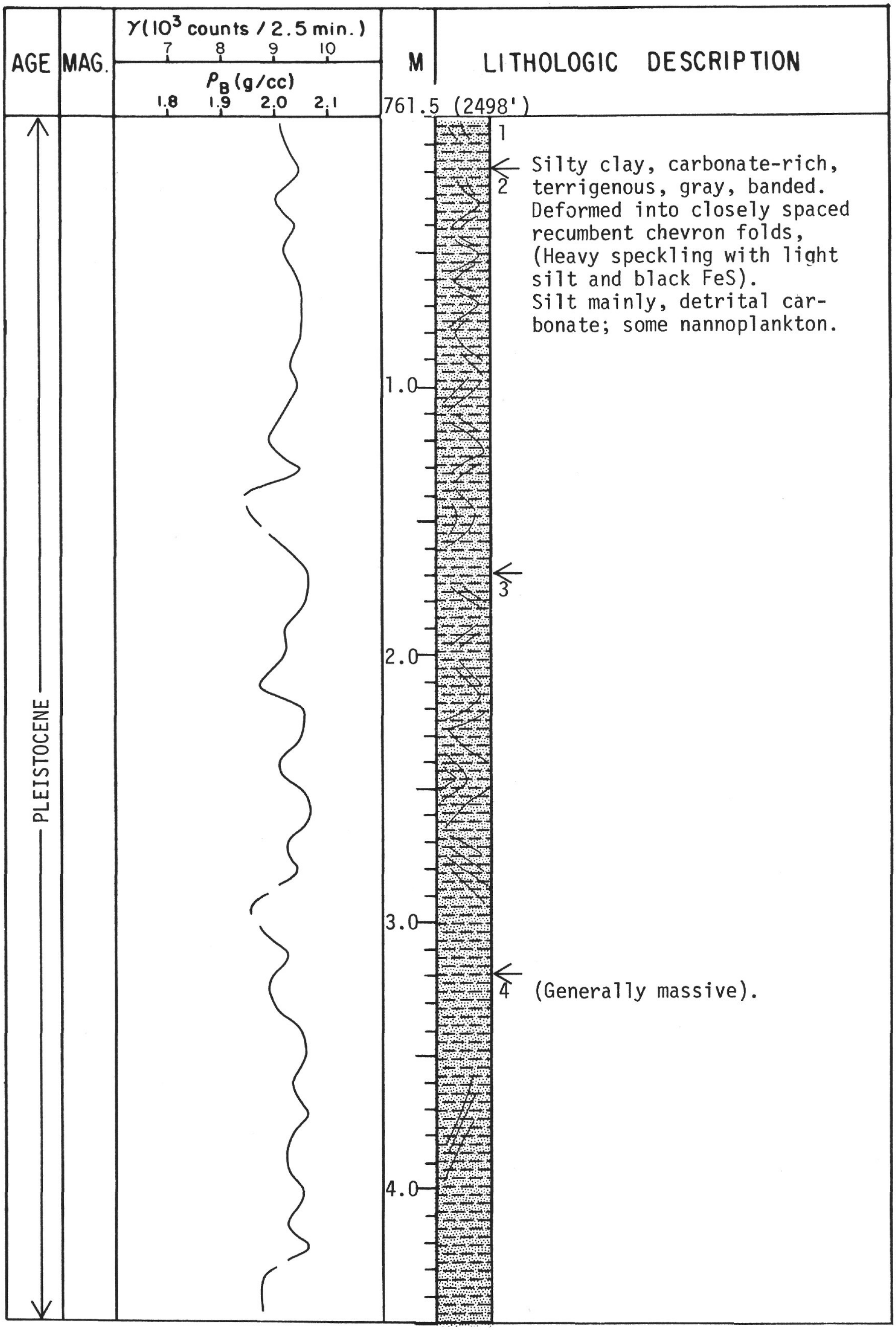

Figure 13. *Hole 1, Core 9.*

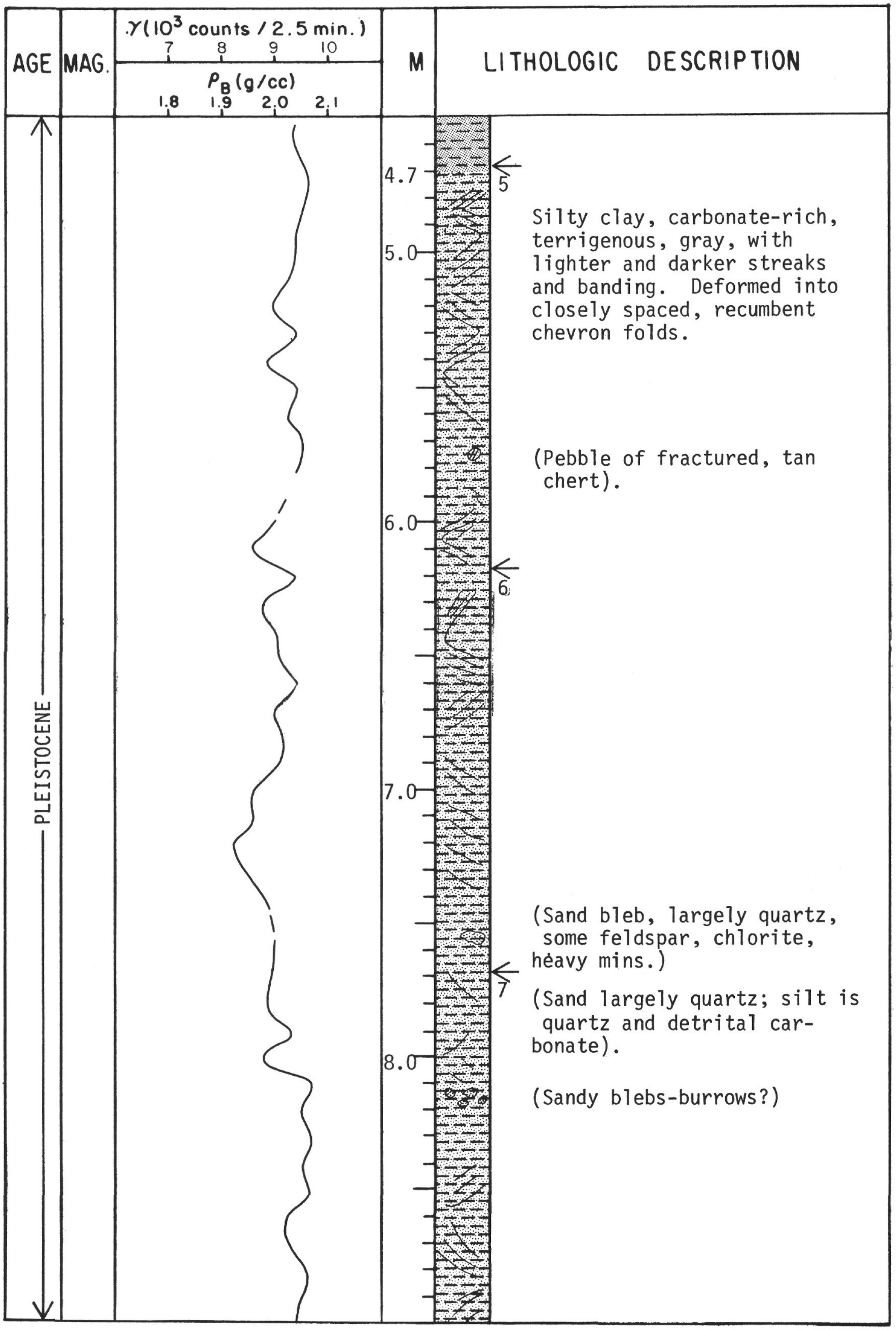

Figure 13. *Continued.*

The Cores Recovered from Site 1

Figures 14 through 57 show details of the individual core sections of the cores from Site 1.

Each figure shows:

(1) A scale of centimeters from the top of each section.
(2) An X radiograph of the core section (where available).
(3) A photograph of the core section.
(4) The lithology (see key).
(5) The positions of smear slides (x).
(6) Notes on the lithology, carbon content, expressed as a percentage of total sediment (see Chapter 11), the water content (see Chapter 10) and the grain size (see Chapter 9). Colors are given with reference to the GSA Rock Color Chart.

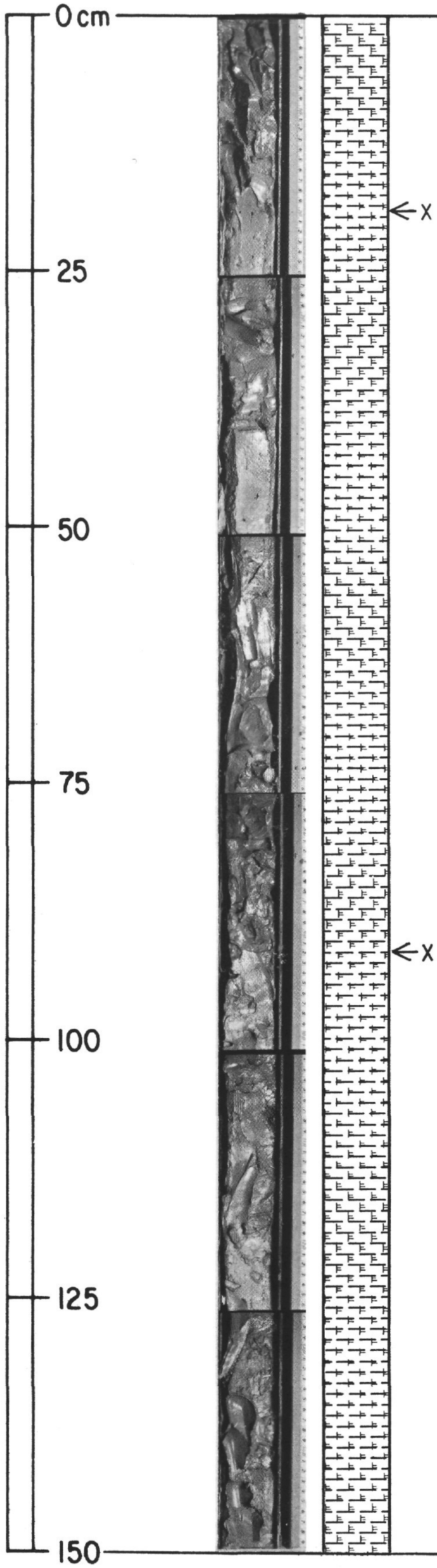

Clay, coccolith-globigerinid-rich, brownish-gray, massive, disturbed in cutting.

(2.5Y 5/2)
Sand 0.2; silt 20.3; clay 79.5.
Total C 3.4; Org. C 0.6; $CaCO_3$ 23.7.
Water content 60.6.

(5Y 5/2)

10% inorganic silt; nannoplankton > forams, trace sponges and Radiolaria.

(5Y 6/2)

(5Y 6/1)

Sand 1.2; silt 15.3; clay 83.5.

Figure 14. *Site 1, Piston Core 1, Section 1.*

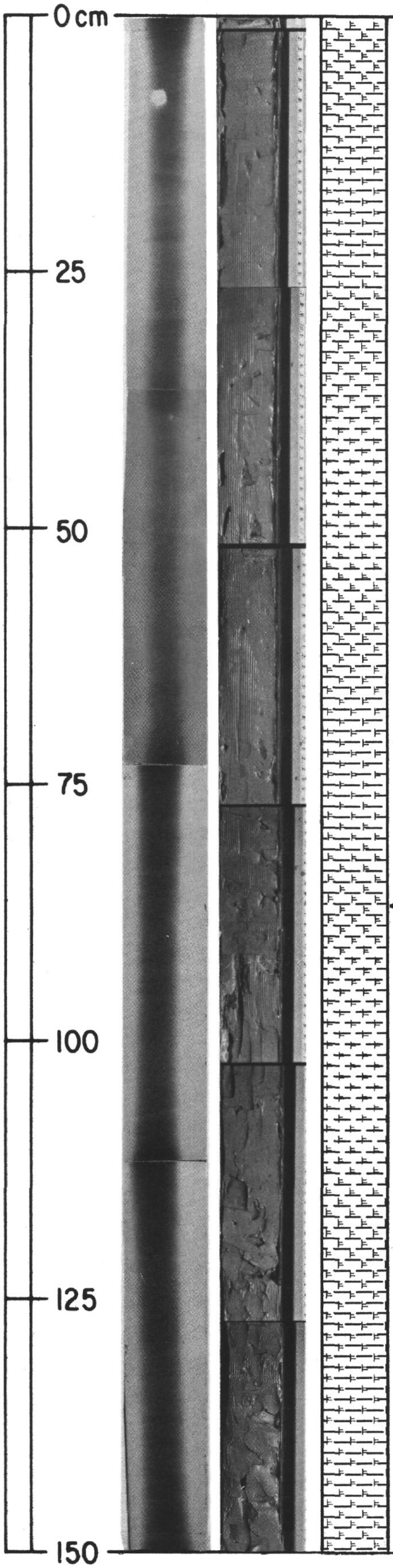

Clay, coccolith-globigerinid-rich, brownish-gray (5Y 5/2), massive.

←X 5% inorganic silt; forams> nannoplankton.

Sand 1.1; silt 20.2; clay 78.7.

Total C 1.9; Org. C 0.5; $CaCO_3$ 11.7.
Water content 48.8.

Figure 15. *Site 1, Piston Core 1, Section 2.*

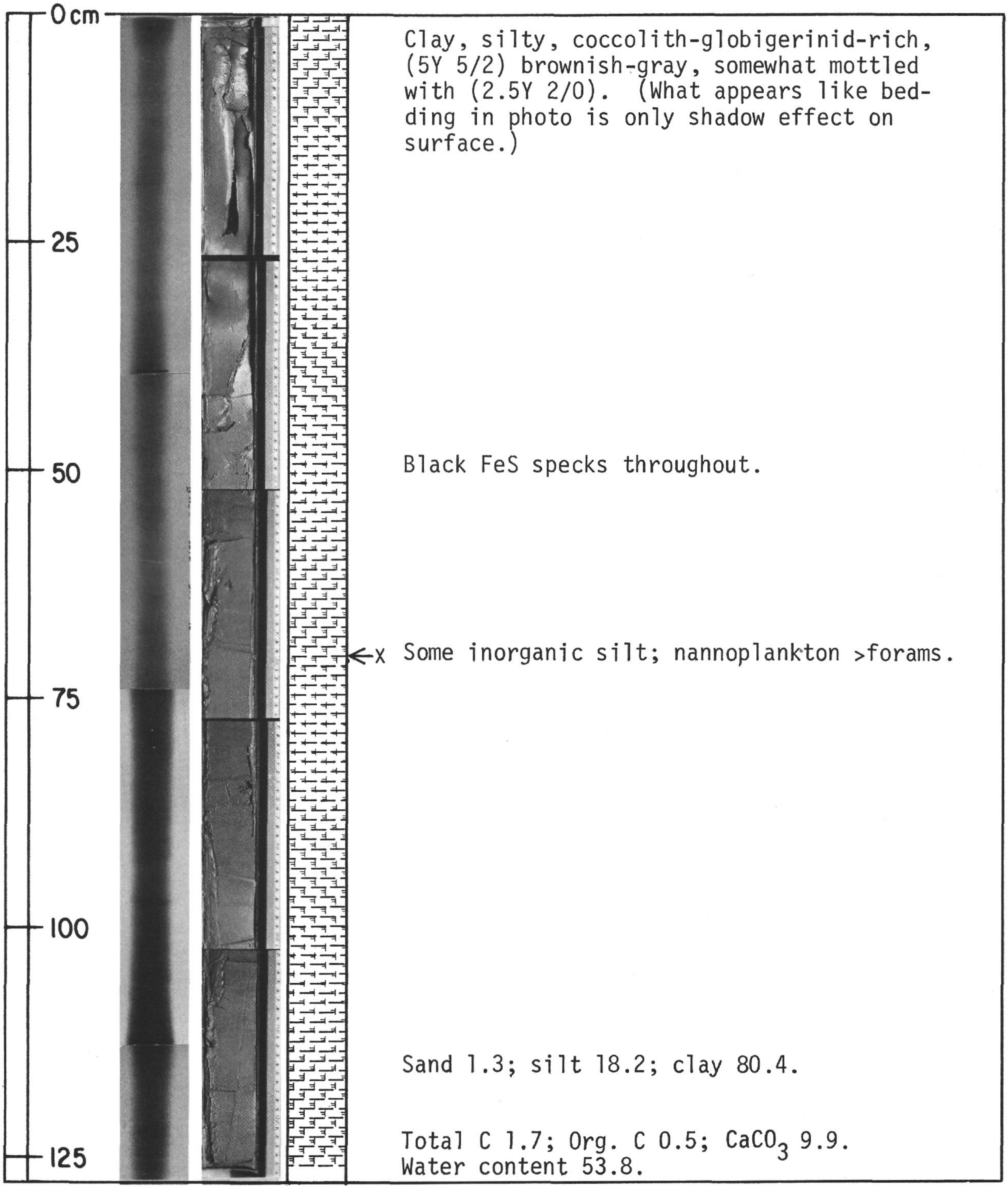

Figure 16. *Site 1, Piston Core 1, Section 3.*

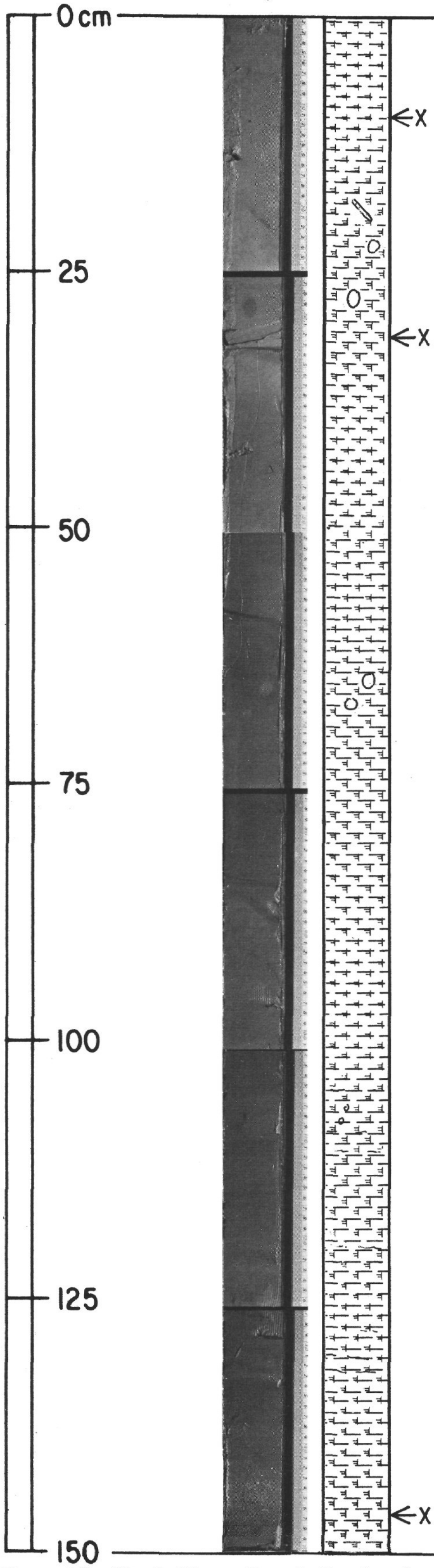

Clay, silty, coccolith-globigerinid-rich, brownish-gray.
Sand 0.0; silt 57.8; clay 42.2.
Some inorganic silt; nannoplankton >forams.

(10R 6/1).
Burrows, (2.5YR 4/0).
(10R 6/3).

(2.5Y 6/2).
Large burrows (2.5Y X 5/0).
Some inorganic silt; nannoplankton >forams.

(10YR 6/2).

(10YR 6/2).

(10YR 4/0).
Large burrows (2.5Y 6/2).

Laminated in various shades

Total C 2.3; Org. C 0.9; $CaCO_3$ 11.7.
Water content 40.1.
Some inorganic silt; nannoplankton >forams.

Figure 17. *Site 1, Piston Core 1, Section 4.*

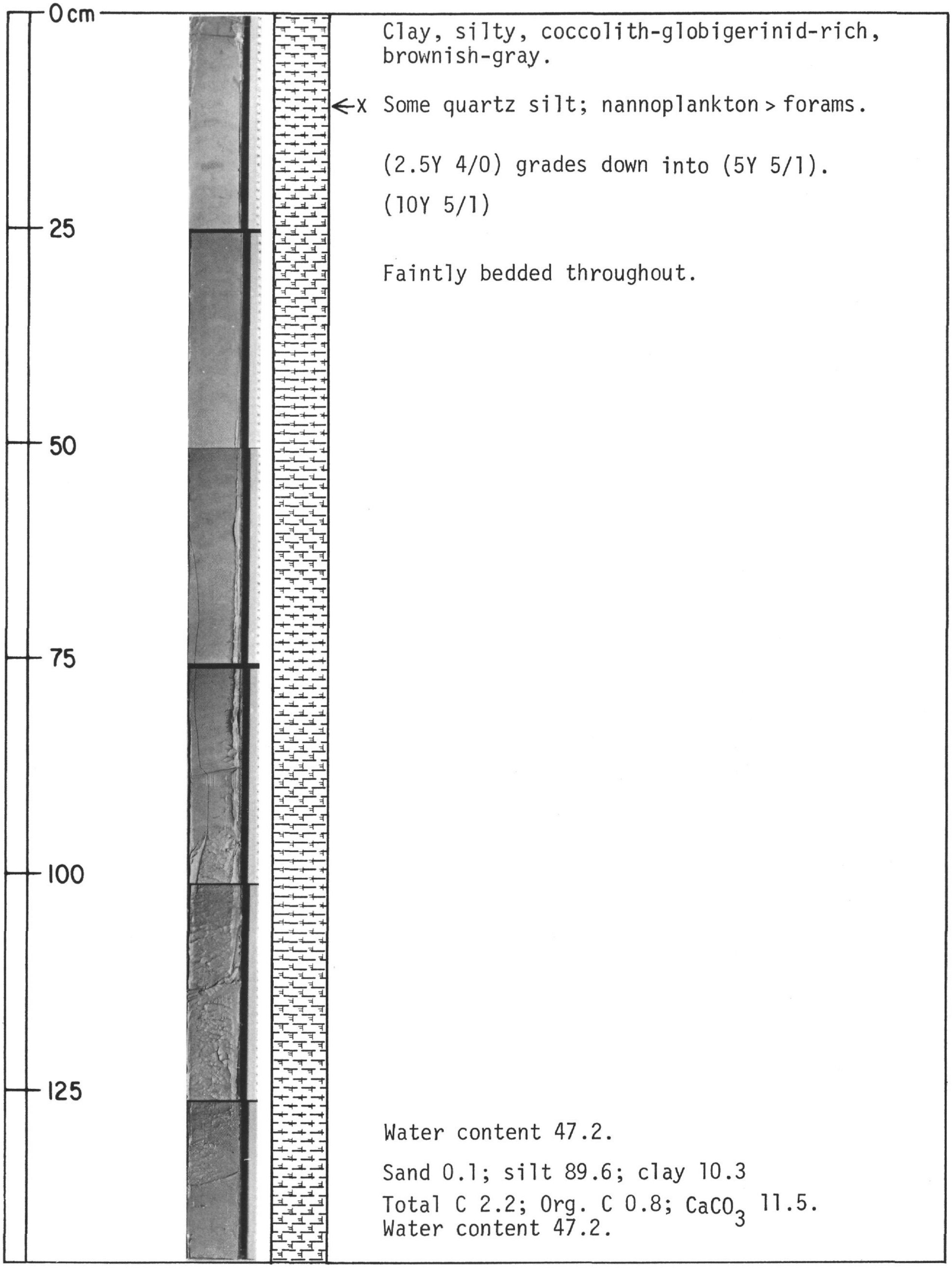

Figure 18. *Site 1, Piston Core 1, Section 5.*

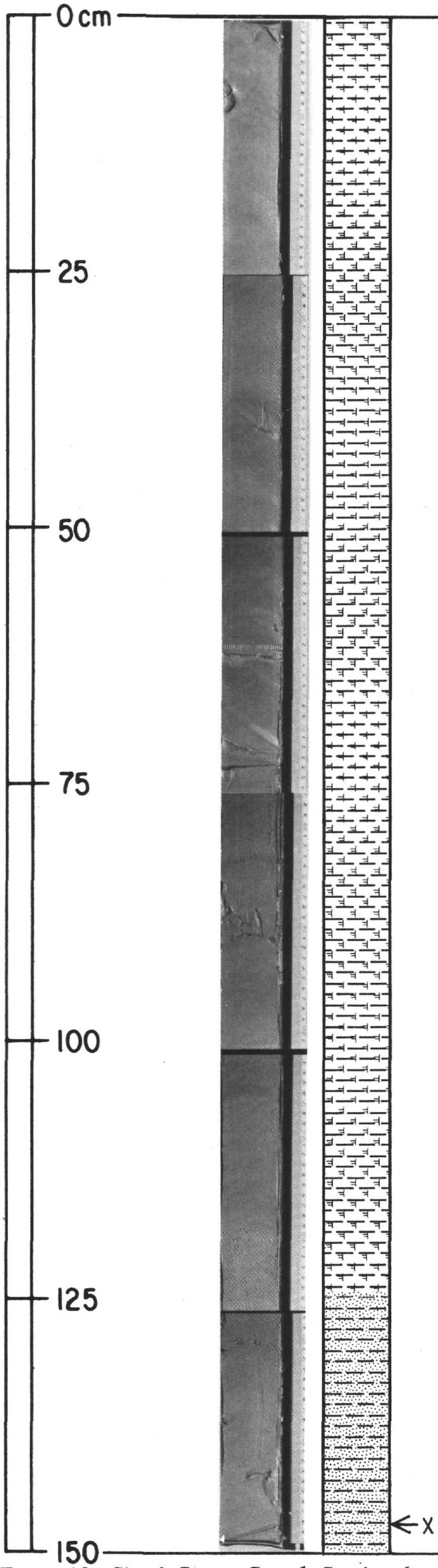

Clay, silty, coccolith-globigerinid-rich, brownish-gray (5Y 4/2), faintly layered throughout with (5Y 3/1), 2 - 30 mm thickness.

Clay, silty, carbonate-rich, terrigenous, olive-gray (5Y 5/1).

Sand 0.2; silt 22.5; clay 77.3.

Total C 2.4; Org. C 0.6; $CaCO_3$ 14.8.
Water content 29.1.
Silt of quartz, detrital carbonate, mica; only traces of fossils (nannoplankton, forams)

Figure 19. *Site 1, Piston Core 1, Section 6.*

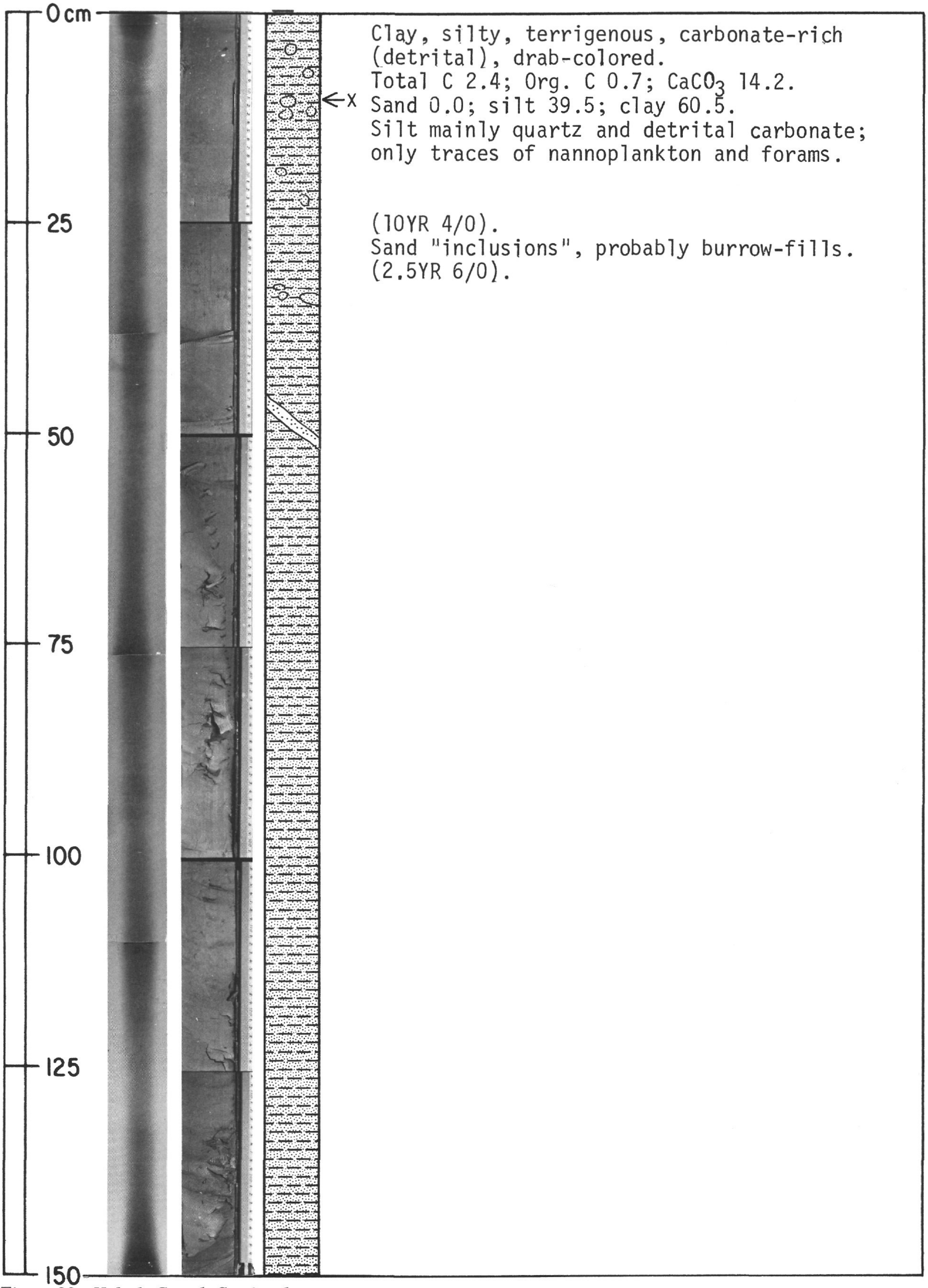

Figure 20. *Hole 1, Core 1, Section 1.*

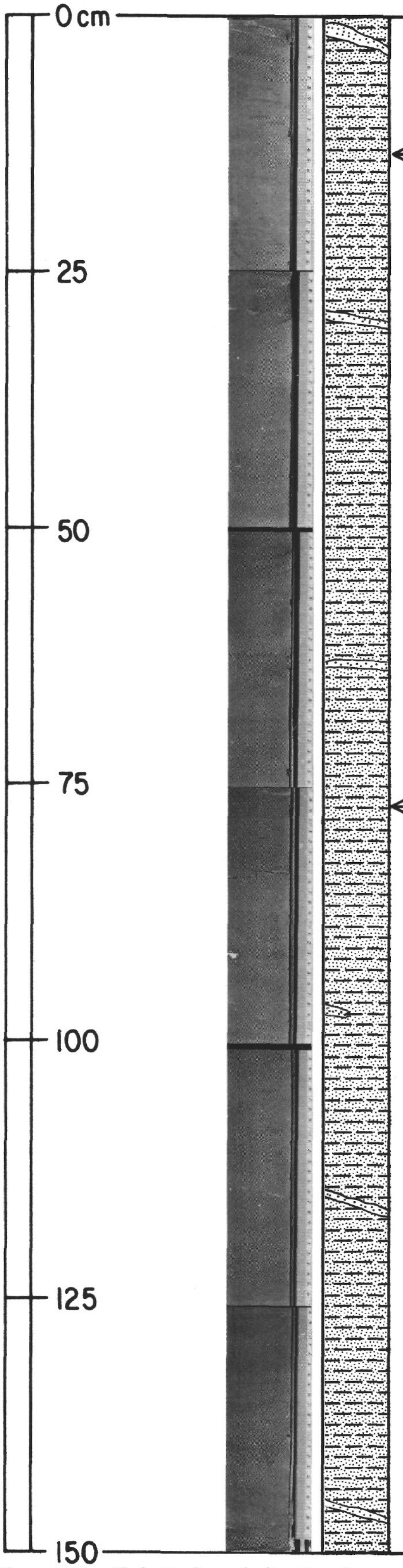

Clay, silty, carbonate-rich, terrigenous, banded, brownish-gray.
Sand 0.1; silt 41.0; clay 58.9.
Total C 2.4; Org. C 0.8; $CaCO_3$ 13.7.

←X Silt mainly quartz and detrital carbonate; traces of nannoplankton.

(2.5YR N 5/0) banded with (10YR 5/1)

Thin lighter beds or discontinuous streaks of silt, commonly dipping 5 - 15^{o}, (5Y 6/1) (burrow fillings?).

←X Silt mainly quartz and detrital carbonate; traces of black minerals and of nannoplankton.

Figure 21. *Hole 1, Core 1, Section 2.*

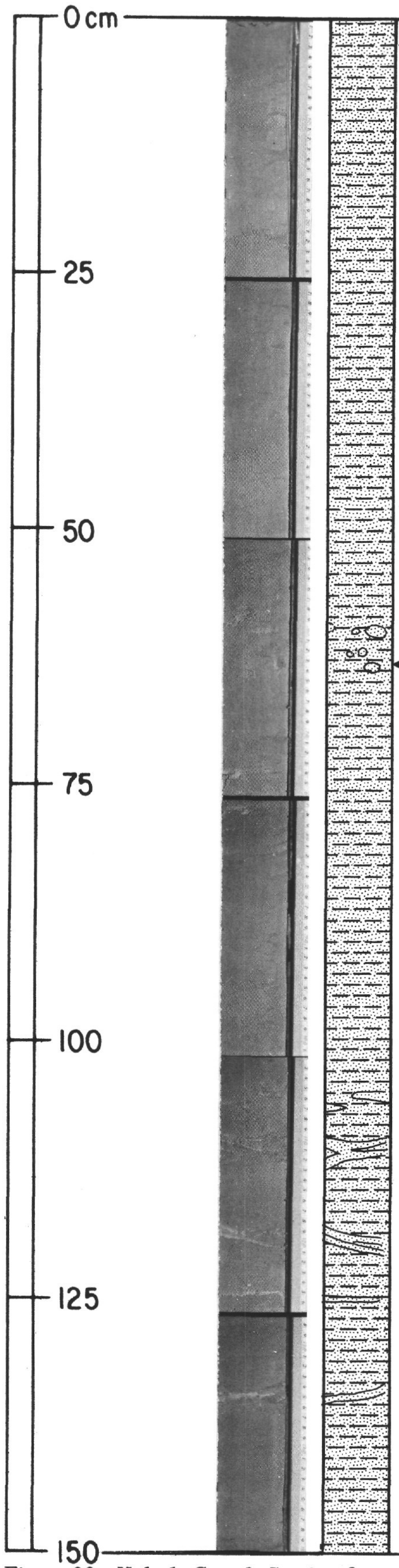

Silt mainly quartz and detrital carbonate; trace nannoplankton.
Total C 3.6; Org. C 0.8; $CaCO_3$ 23.3.
Water content 23.1.
Sand 0.0; silt 33.6; clay 66.4.
Clay, silty, carbonate-rich, terrigenous, drab-colored with laminae and burrow fills of silt.
(5Y 5/1) banded with 2.5Y 5/2), silts (5Y 6/1).

Burrow fillings.
Silt mainly quartz and detrital carbonate; trace nannoplankton.

Silt burrow fills?

Figure 22. *Hole 1, Core 1, Section 3.*

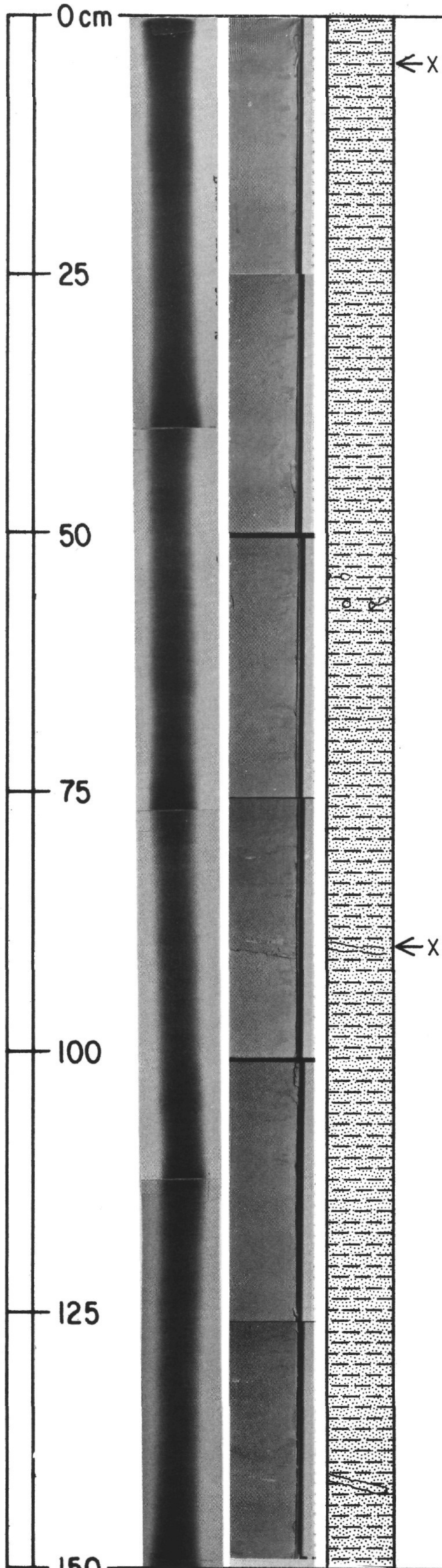

Silty clay and clayey silt, olive-gray (5Y 5/1) banded with dark olive (5Y 2/1) and yellowish-brown (10YR 5/2), speckled with black FeS; silt burrow-fills.
Silt mainly quartz and detrital carbonate.
Total C 2.8; Org. C 0.9; $CaCO_3$ 16.1.
Sand 0.1; silt 84.8, clay 15.1.

Zone of silt-filled burrows.

Silt band (5Y 6/1).
Silt mainly quartz; some detrital carbonate.

Silt band (5Y 6/1).

Figure 23. *Hole 1, Core 1, Section 4.*

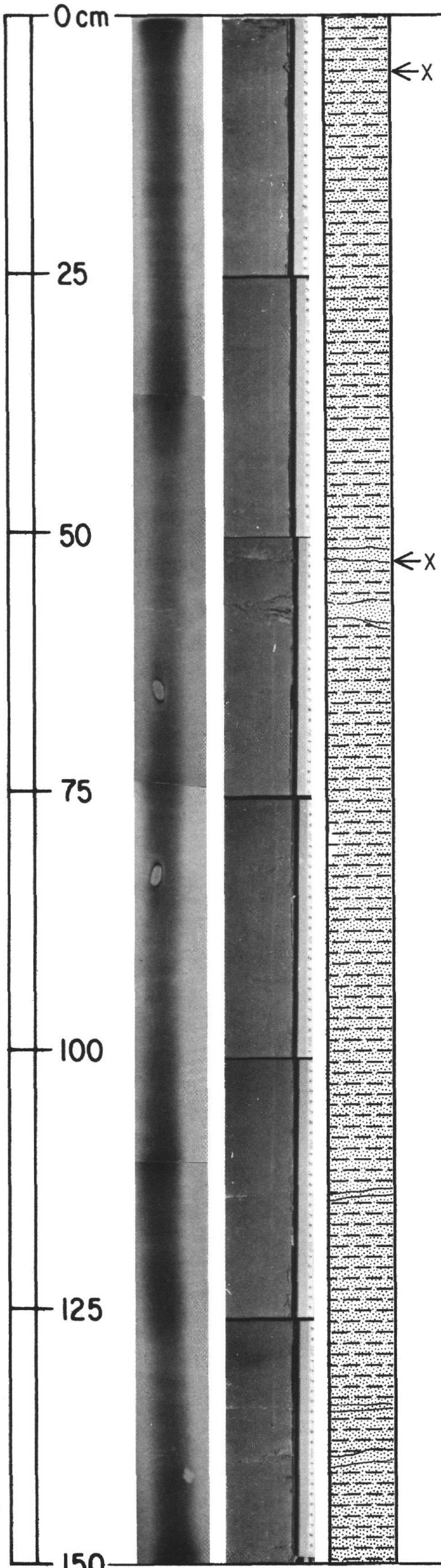

Total C 5.4; Org. C 0.7; $CaCO_3$ 39.6.
Silt mainly detrital carbonate and quartz; trace nannoplankton.
Sand 0.0; silt 40.5; clay 59.5.

Silty clay and clayey silt, carbonate-rich, terrigenous, with sparse bands of silt. Yellowish-brown (10YR 5/2), silt bands pale olive (5Y 6/1), some dark FeS mottling.

Silt mainly quartz and detrital carbonate.

Figure 24. *Hole 1, Core 1, Section 5.*

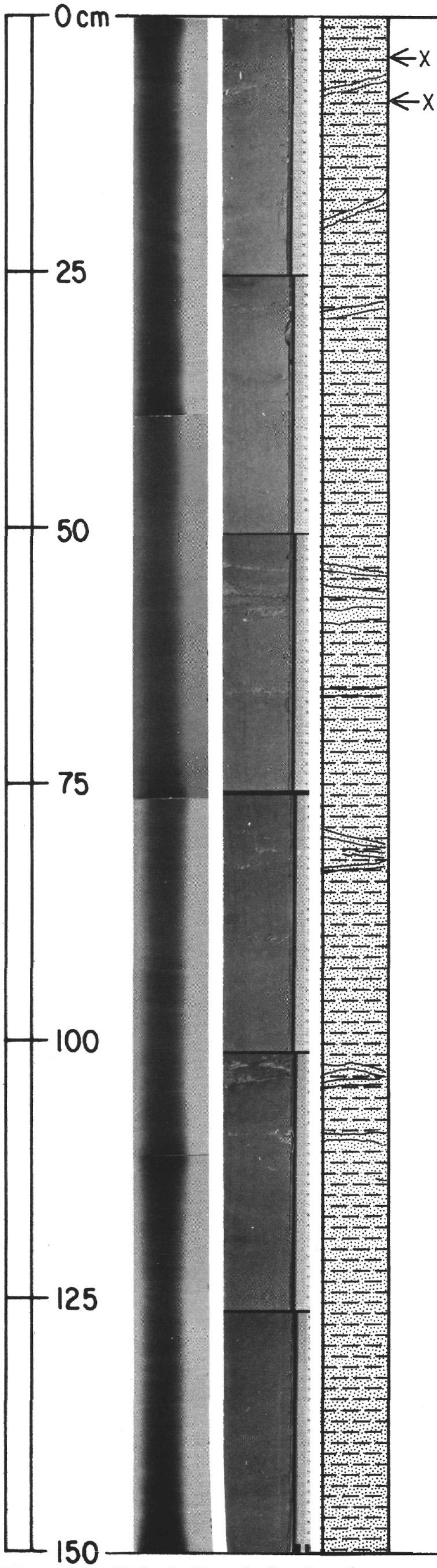

Total C 2.9; Org. C 0.8; $CaCO_3$ 17.2.
Water content 27.3.
Silt mainly quartz and detrital carbonate; trace nannoplankton.
Sand 0.3; silt 58.2; clay 41.5.
Silt mainly quartz, some detrital carbonate; trace nannoplankton.
Silty clay and clayey silt, carbonate rich, terrigenous, with thin (mostly 1 mm) and irregular silt laminae as shown.
Dominant color yellowish-brown (10YR 5/0), silts pale olive (5Y 6/0).

Figure 25. *Hole 1, Core 1, Section 6.*

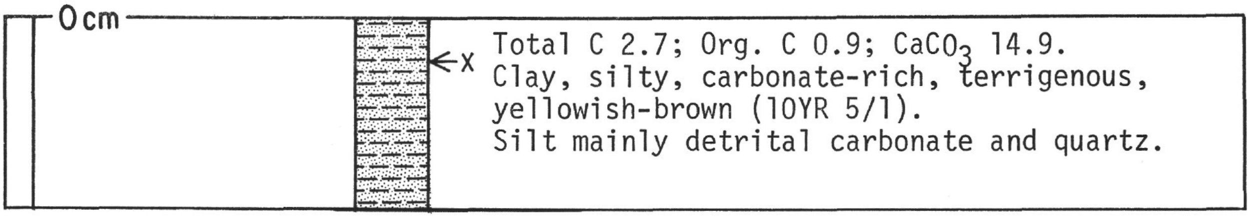

Figure 26. *Hole 1, Core 1, Section 7.*

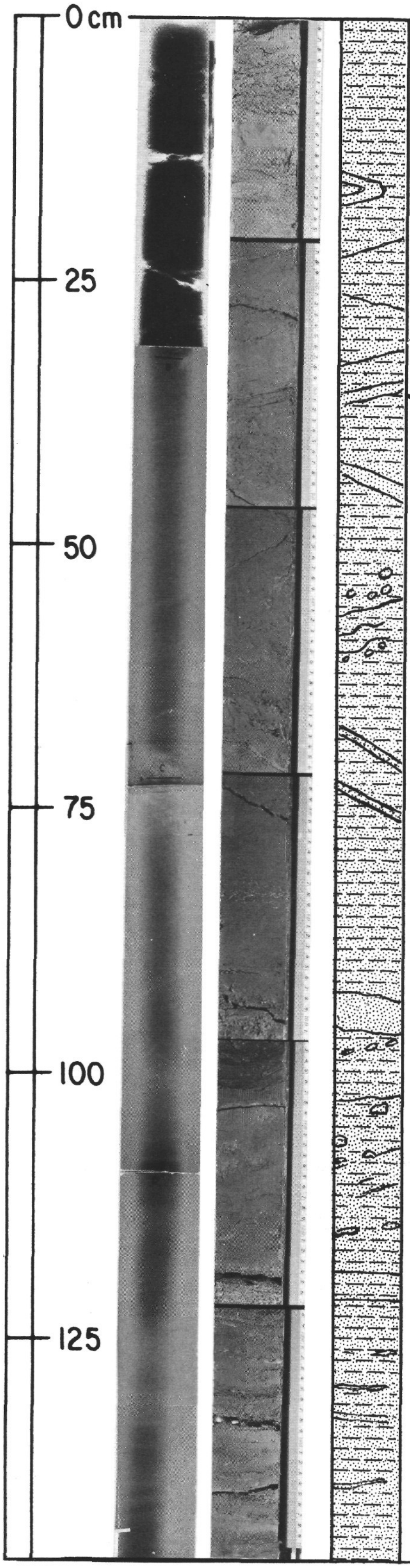

Silt, clayey, carbonate-rich, terrigenous, light olive-brown with lighter (5Y 6/1) thin beds and pockets (burrow-fills) of silt and sandy silt. Semiconsolidated. Upper part contains 3 - 4 horizontal slump-folds.

←X Silt mainly quartz, some detrital carbonate.

Sand 0.1; silt 59.1; clay 40.8.

Total C 2.8; Org. C 0.6; $CaCO_3$ 18.1.
Water content 24.7.

Sandy silt pockets and layers very numerous.

Figure 27. *Hole 1, Core 2, Section 1.*

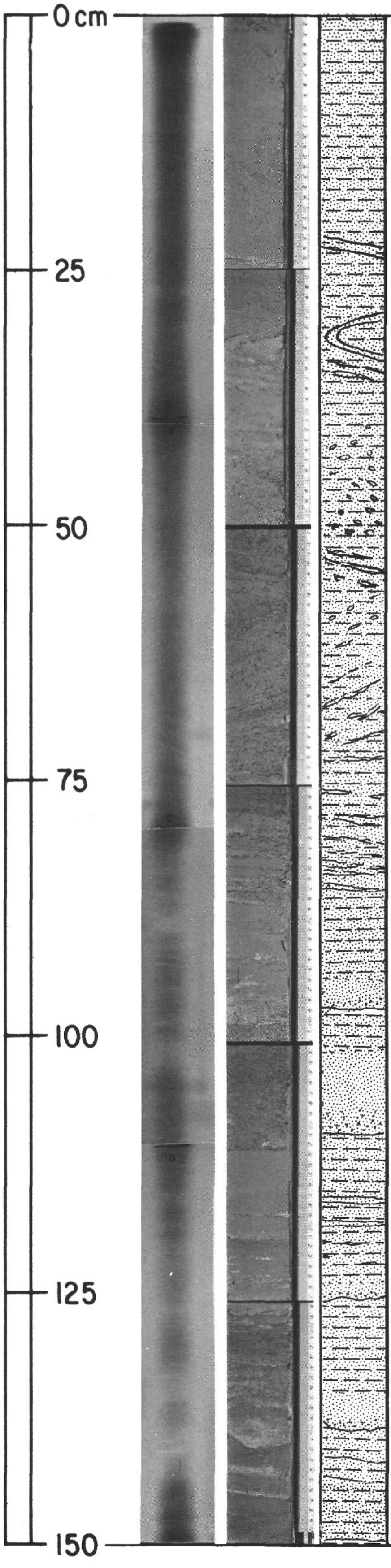

Sand 0·1, Silt 61.9, Clay 38.0
Silt mainly detrital carbonate and quartz;
Total C 2.6; Org. C 0.6; $CaCO_3$ 16.4.
Water 18.7.

Silt, clayey, carbonate-rich, terrigenous, semiconsolidated, yellowish-brown (10YR 4.5/1), with more yellowish silt layers (2.5Y 6/2). Beds thrown into recumbent (horizontal) isoclinal folds.

Horizontal fold axis; cf Plate...Fig. 2.
Silt partly in thin beds, partly in pockets and lenses which probably represent burrow-fillings.

Horizontal fold axis?

Sand and silt mainly quartz, some detrital carbonate.
Horizontal fold axis?

Silt beds graded, with sharp, sandy base.

Figure 28. *Hole 1, Core 2, Section 2.*

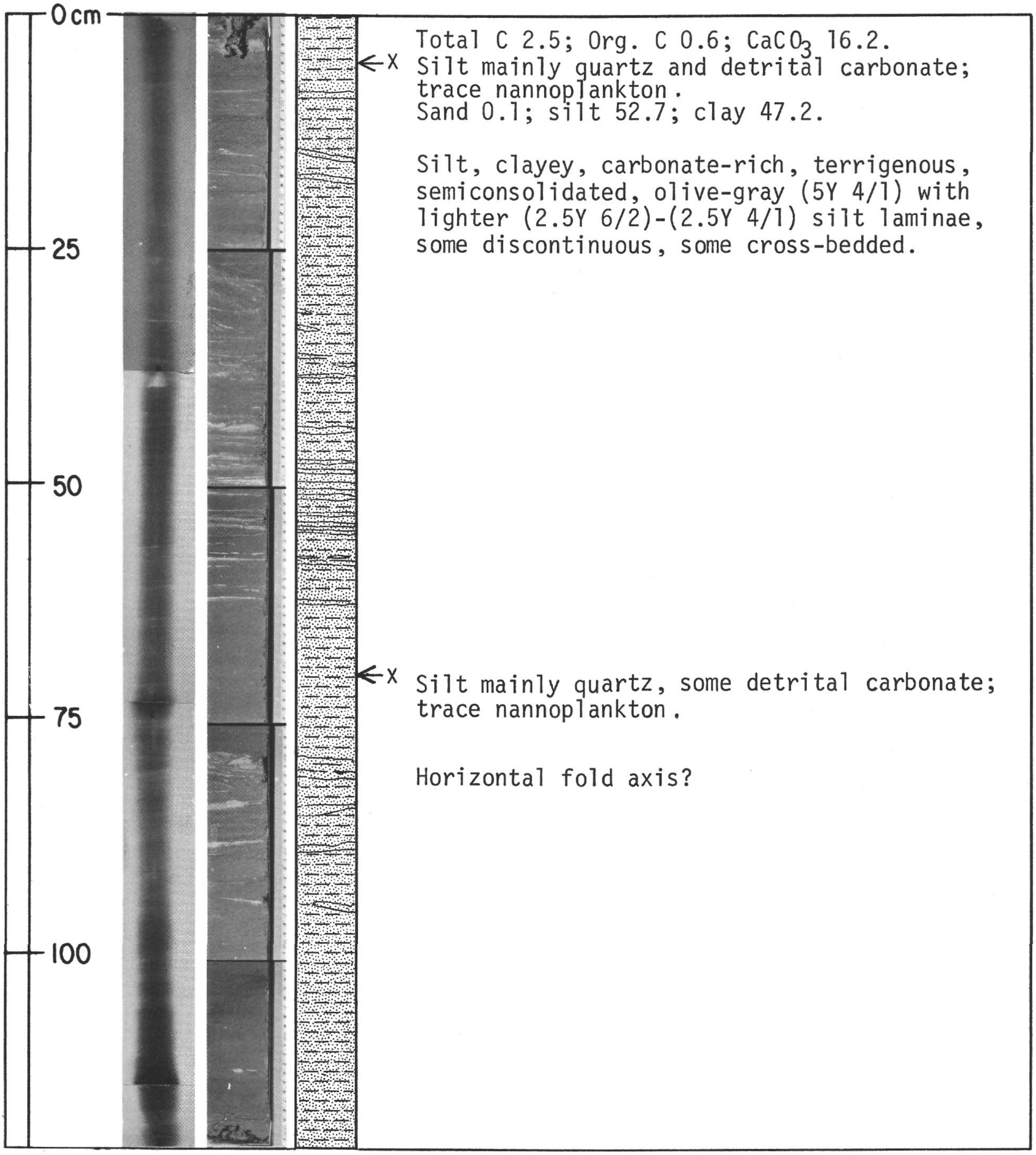

Figure 29. *Hole 1, Core 2, Section 3.*

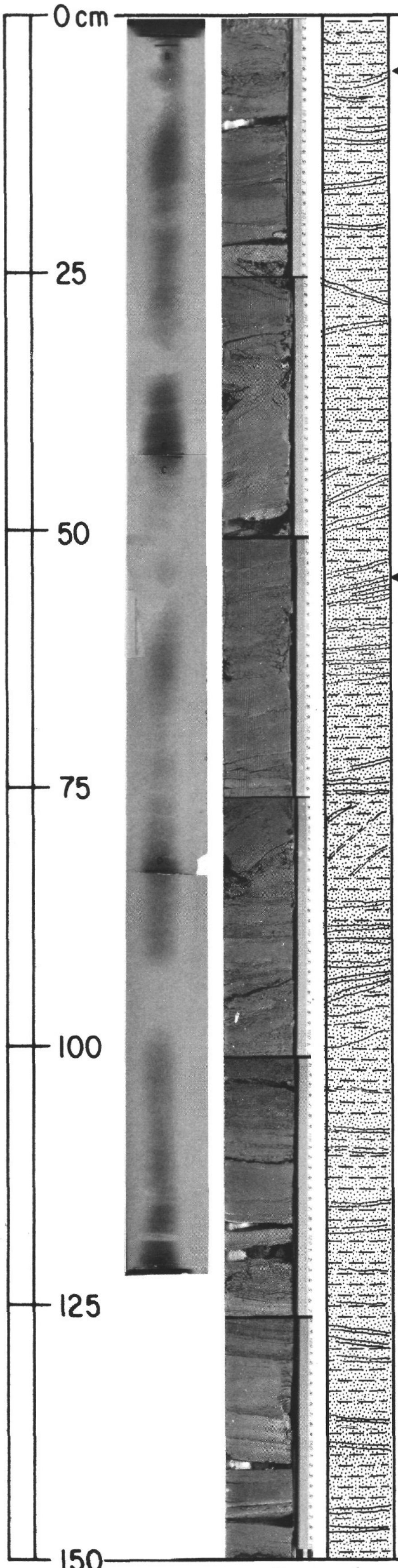

←X Silt mainly detrital carbonate and quartz; trace nannoplankton.
Sand 0.0; silt 48.9; clay 51.1.

Clay, silty, carbonate-rich, terrigenous, light olive-gray (5Y 5/0) laminated with lighter (5Y 7/0) layers of silt (1-2 mm). Beds contorted, with some horizontal fold axes.

←X Silt mainly quartz, some detrital carbonate; trace nannoplankton.

Figure 30. *Hole 1, Core 3, Section 1.*

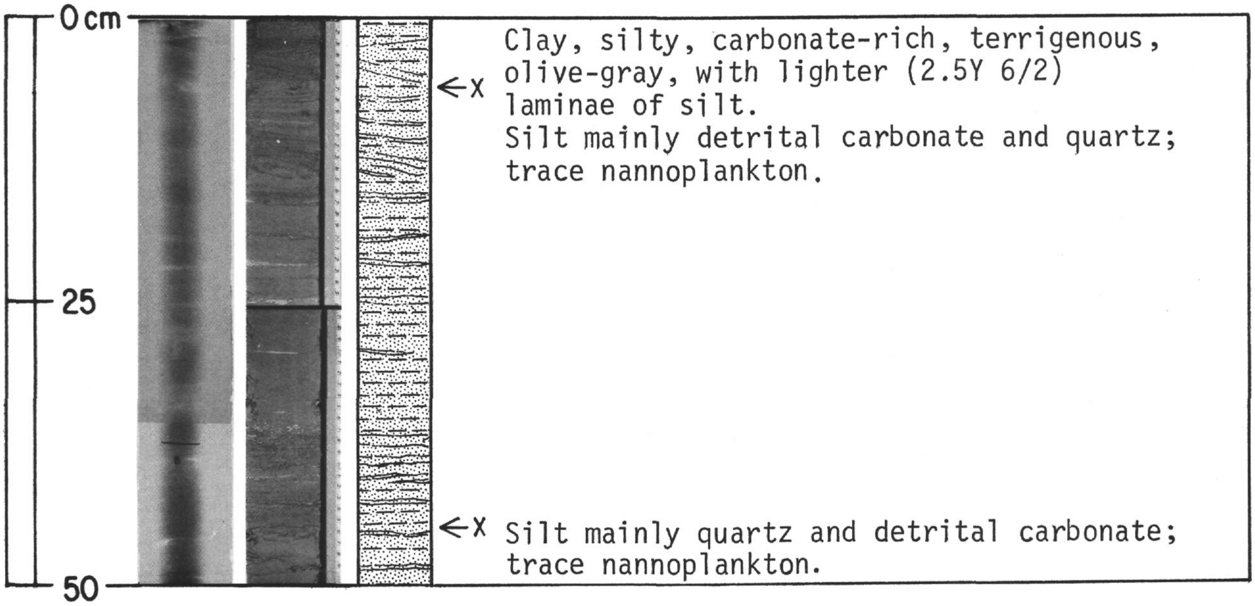

Figure 31. *Hole 1, Core 3, Section 2.*

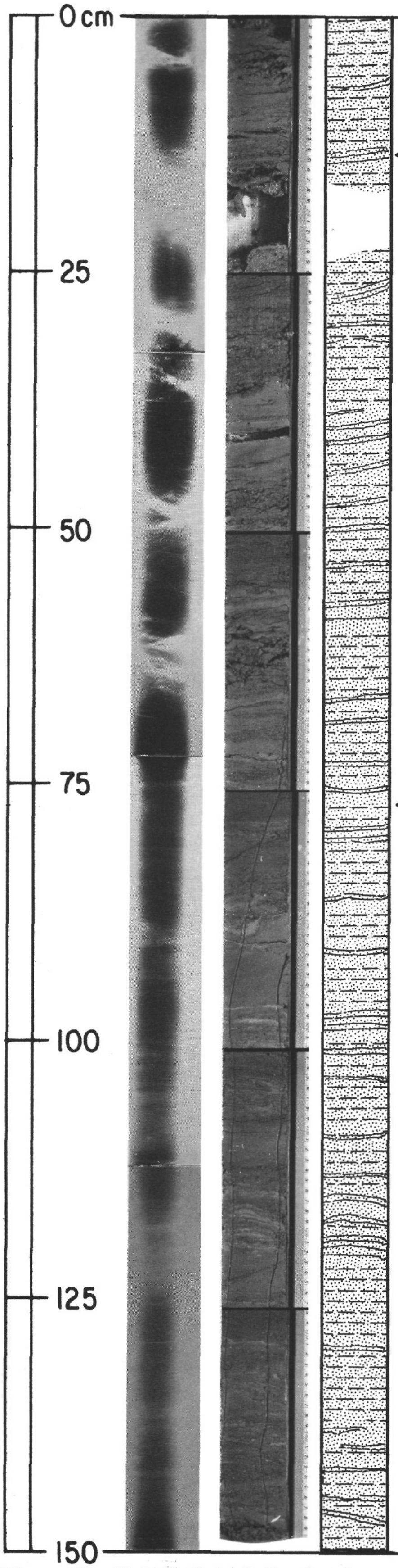

Clay, silty, carbonate-rich, terrigenous, olive-gray (5Y 4/1) with many lighter (5Y 6/1) silt laminae.
Total C 2.7; Org. C 0.6; $CaCO_3$ 17.2.
← X Water content 22.7.
Silt mainly quartz and detrital carbonate; trace nannoplankton.

Sand 0.2; silt 42.0; clay 57.8.

← X Silt mainly detrital carbonate and quartz.

Figure 32. *Hole 1, Core 5, Section 1.*

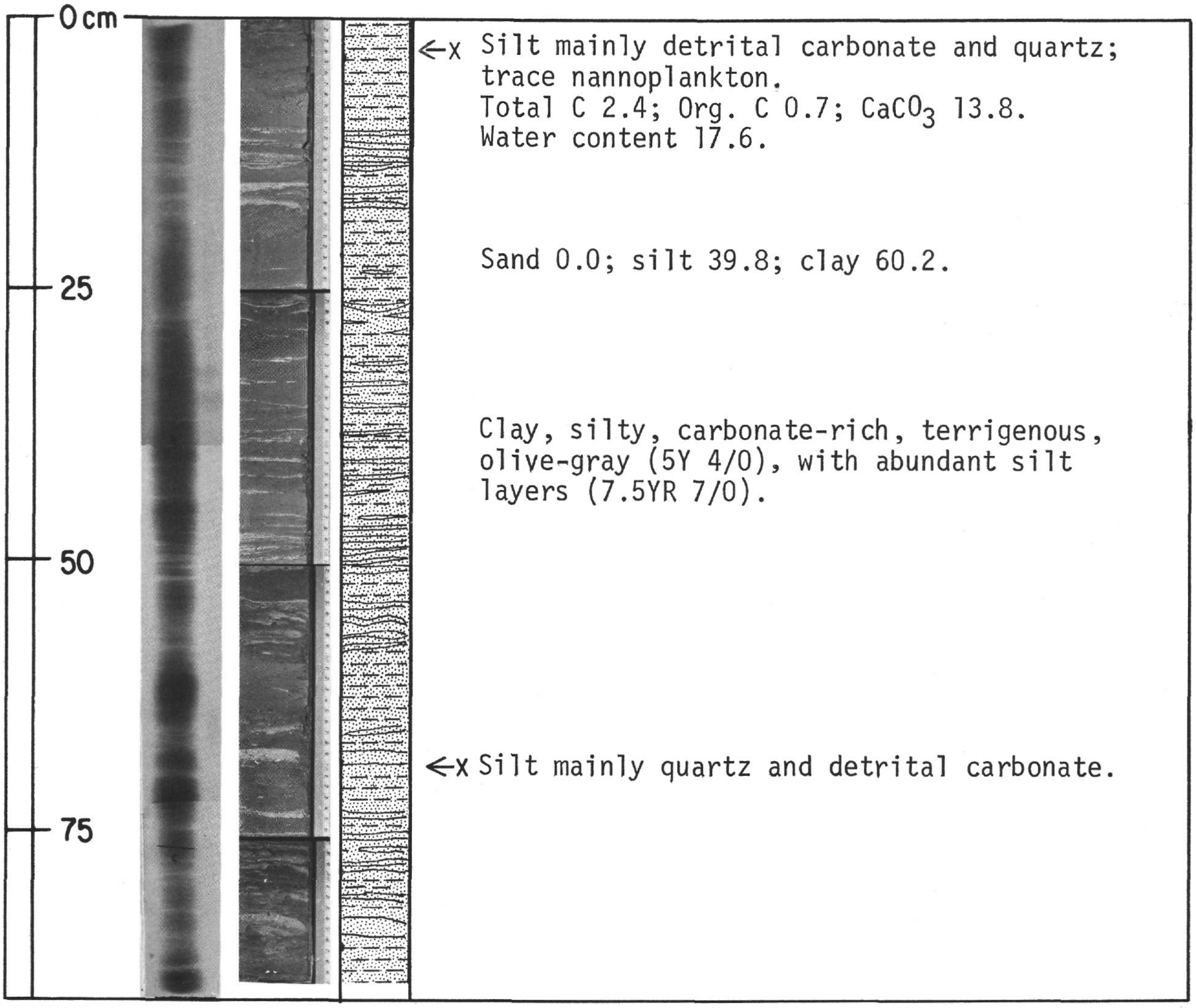

Figure 33. *Hole 1, Core 5, Section 2.*

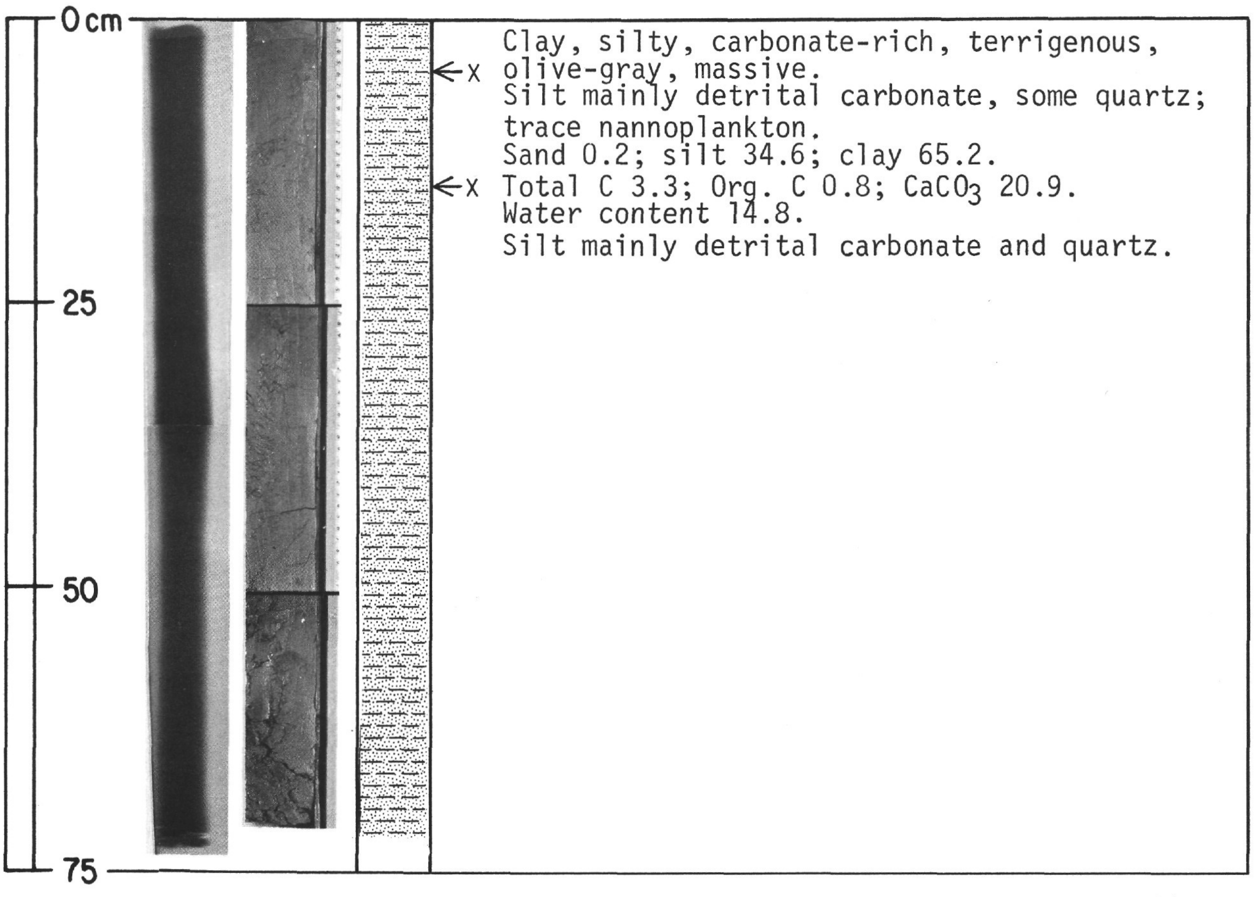

Figure 34. *Hole 1, Core 6, Section 1.*

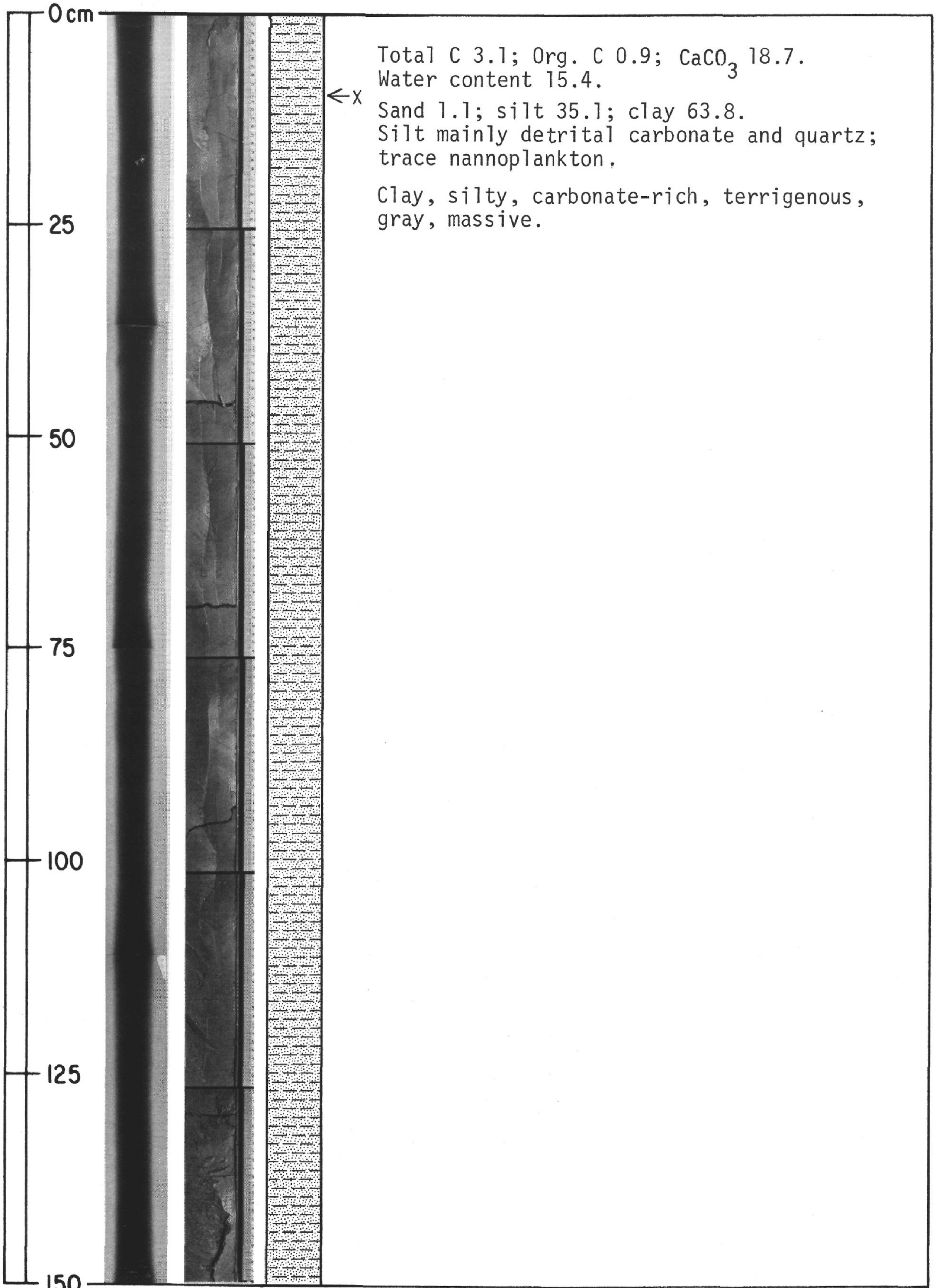

Figure 35. *Hole 1, Core 6, Section 2.*

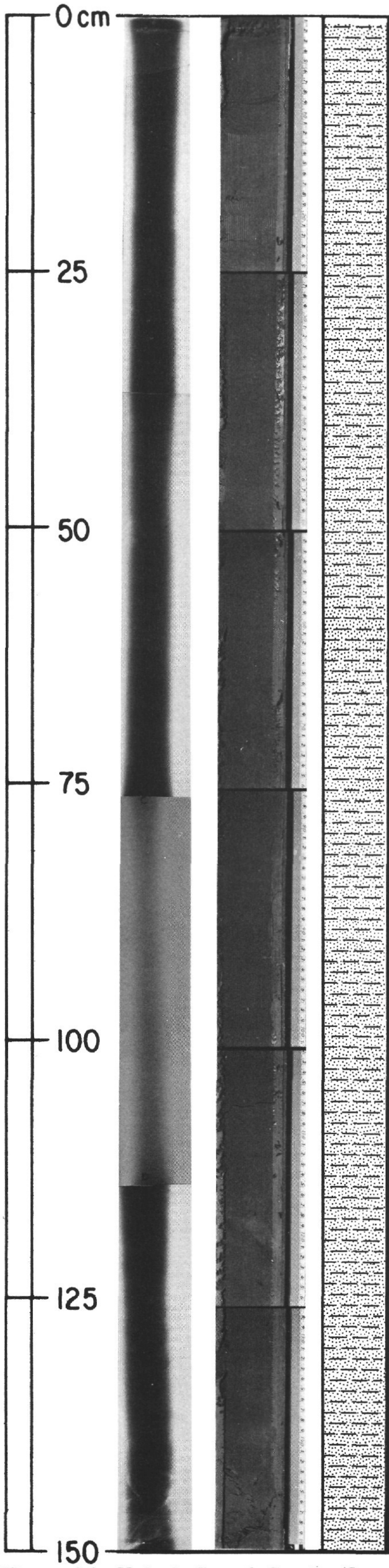

←X Total C 3.3; Org. C 0.9; $CaCO_3$ 19.9.
Water content 18.0.
Silt mainly detrital carbonate, some quartz; trace nannoplankton.
Clay, silty, carbonate-rich, terrigenous, gray (5Y 3/1); massive, but finely speckled with light spots (silt?) and some dark FeS specks.

←X Silt mainly detrital carbonate, some quartz; trace nannoplankton.
Many small silt spots (burrows?).

Figure 36. *Hole 1, Core 6, Section 3.*

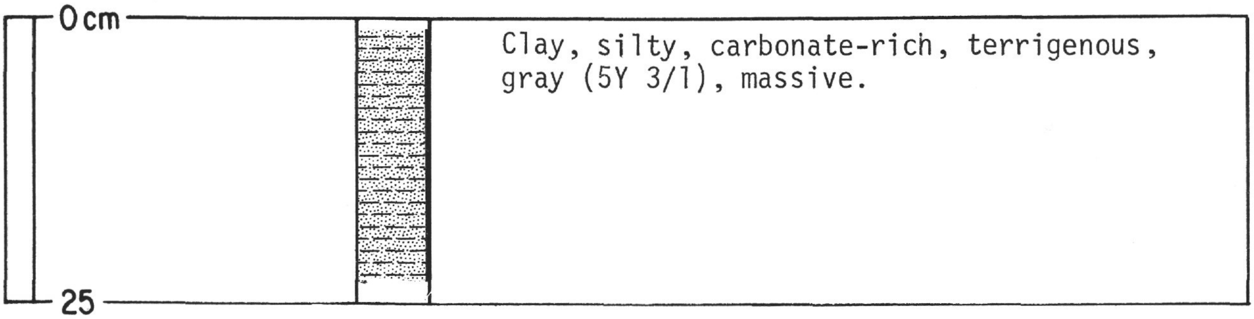

Figure 37. *Hole 1, Core 7, Section 1.*

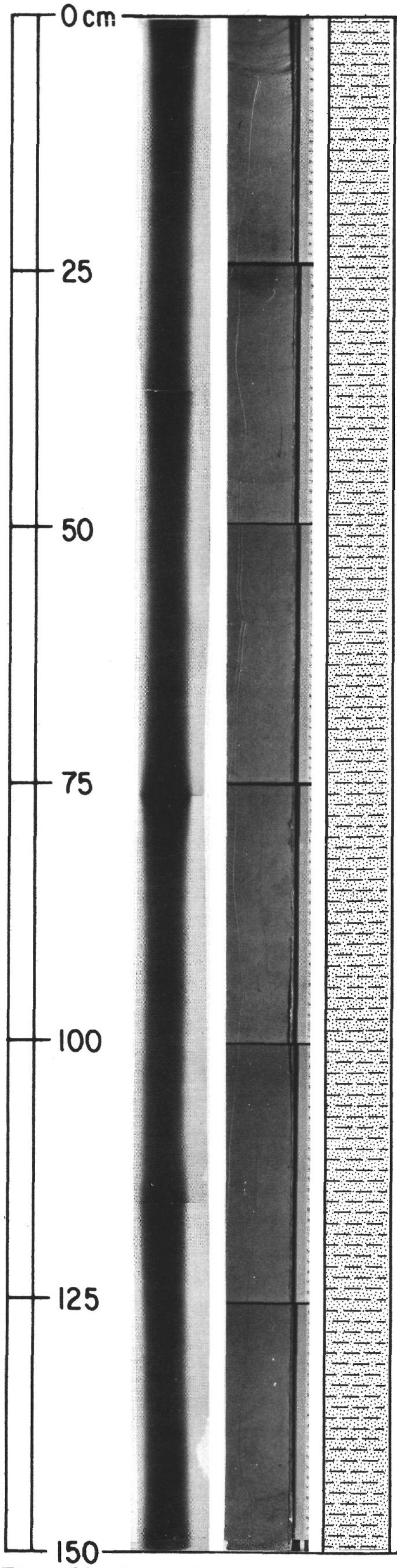

Total C 2.8; Org. C 0.4; $CaCO_3$ 20.1.
Water content 16.0.

← X Sand 0.1; silt 34.7; clay 65.2.
Silt mainly detrital carbonate, some quartz; trace nannoplankton.
Clay, silty, carbonate-rich, terrigenous, olive-gray (5Y 3/2), with lighter (5Y 6/2) specks of silt; spots of blackish FeS_2 at 44.5 and 96 cm. Core vaguely mottled (5Y 6/2).

Figure 38. *Hole 1, Core 7, Section 2.*

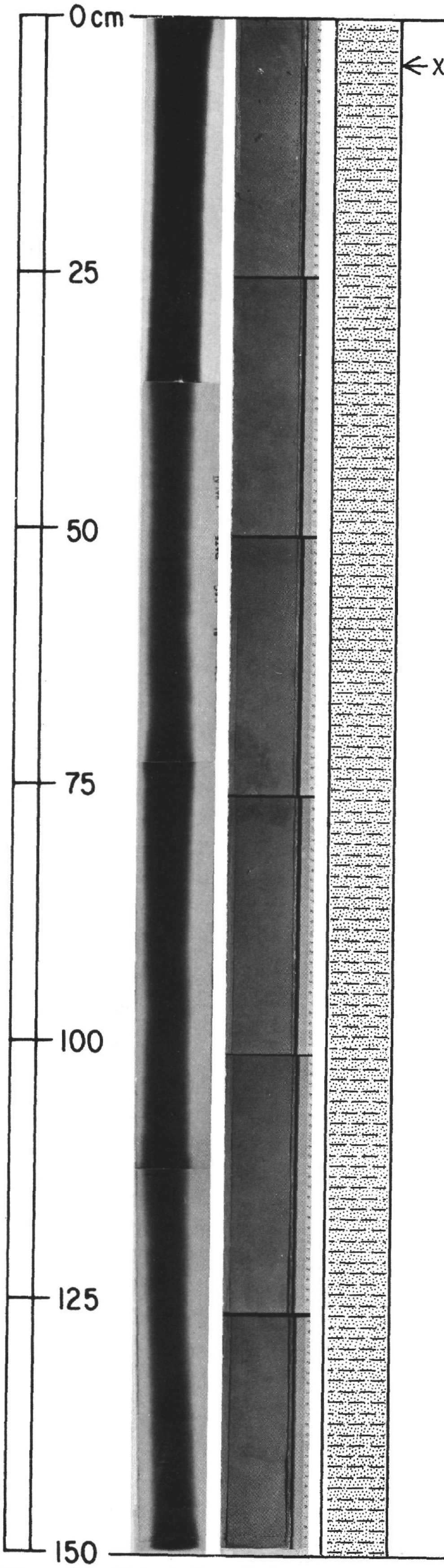

Total C 2.2; Org. C 0.7; $CaCO_3$ 12.8.
Water content 16.4.
Sand 0.8; silt 33.1; clay 66.1.
Silt mainly detrital carbonate and quartz; trace nannoplankton.

Clay, silt, carbonate-rich, terrigenous, gray (5Y 3/1), with vague mottling and fine silt specks, lighter (5Y 6/1).

Specks of dark FeS (2.5Y /0) throughout core.

FeS patches abundant.

Figure 39. *Hole 1, Core 7, Section 3.*

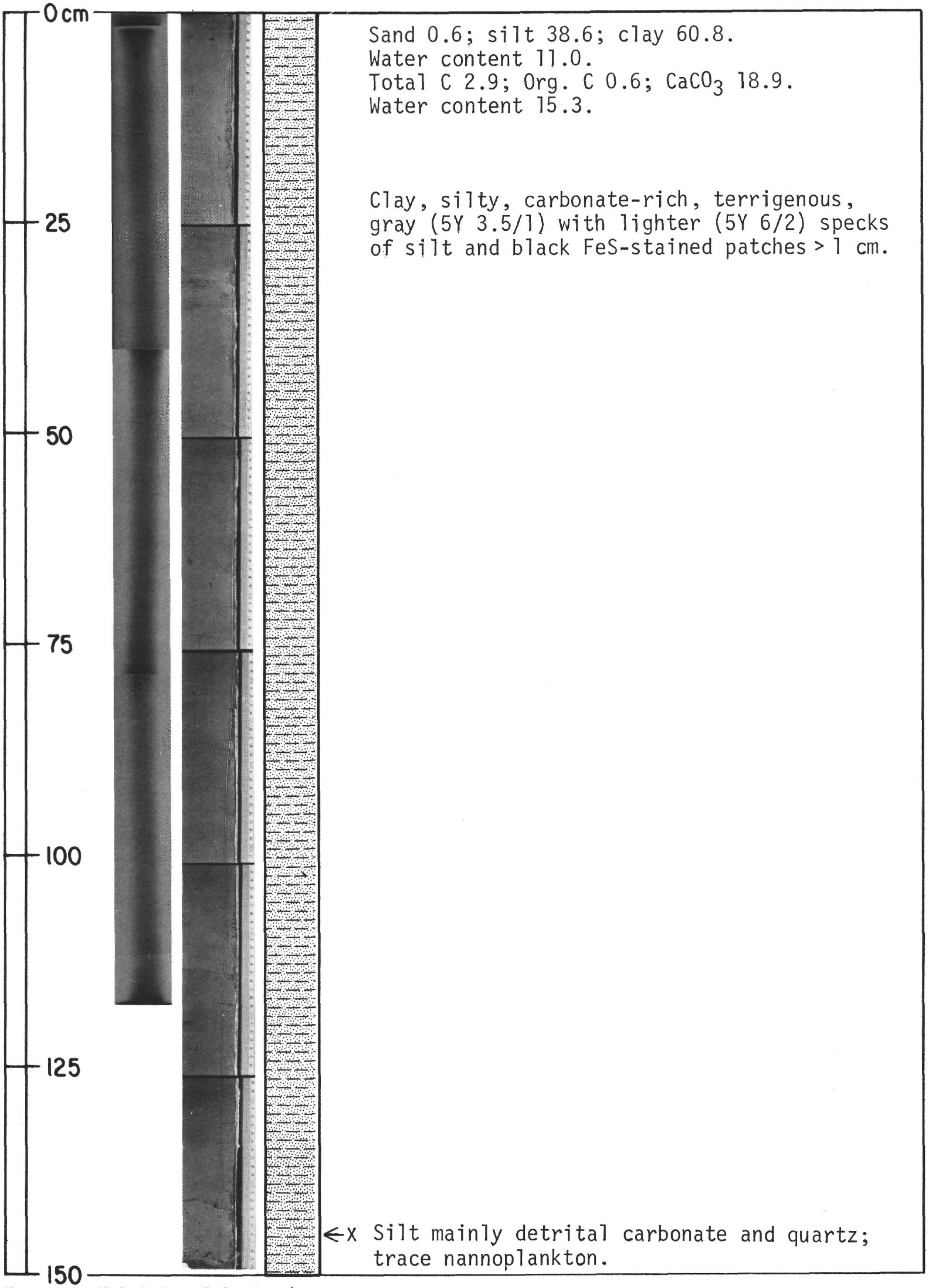

Figure 40. *Hole 1, Core 7, Section 4.*

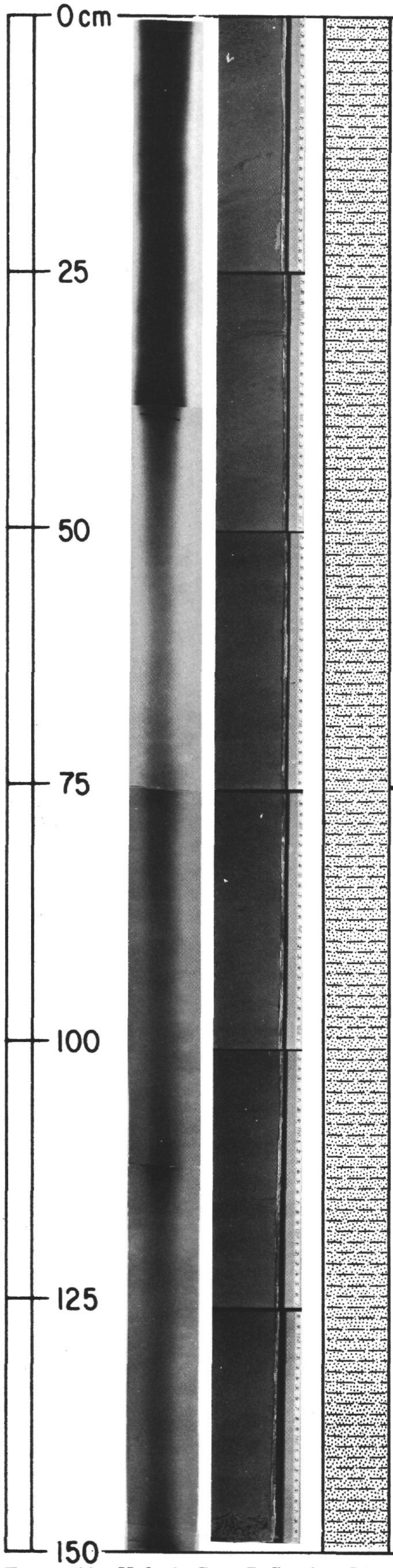

Total C 2.9; Org. C 0.8; $CaCO_3$ 17.6.

←x Sand and silt mainly quartz and detrital carbonate.

Sand 0.1; silt 30.8; clay 69.1.

Clay, silty, carbonate-rich, terrigenous, gray (5Y 3.5/1), speckled throughout with light (5Y 6/2) silt specks and black FeS patches < 3 mm.

←x Sand, quartz; silt, mixed detrital carbonate and quartz; trace nannoplankton.

Figure 41. *Hole 1, Core 7, Section 5.*

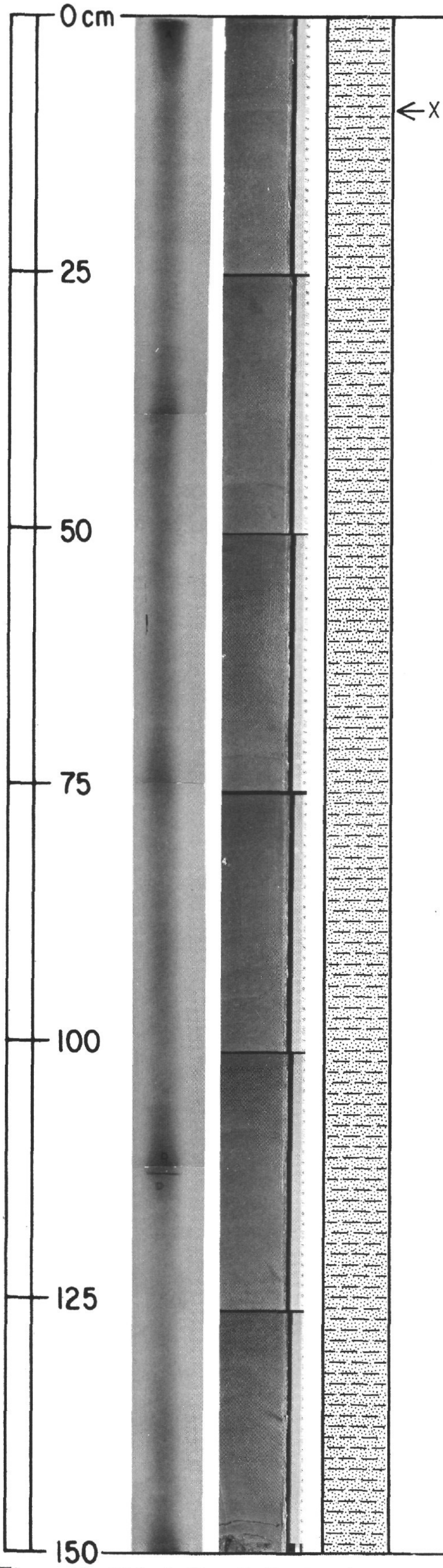

Total C 3.2; Org. C 0.5; $CaCO_3$ 22.5.
Water content 13.3.
Sand 0.0; silt 32.5; clay 67.5.
Silt mainly detrital carbonate and quartz.

Clay, silty, carbonate-rich, terrigenous, gray (5Y 3/1) with lighter (5Y 6/2) silt specks and black FeS-stained specks and patches $<$ 1 mm to $>$ 1 cm.

Figure 42. *Hole 1, Core 7, Section 6.*

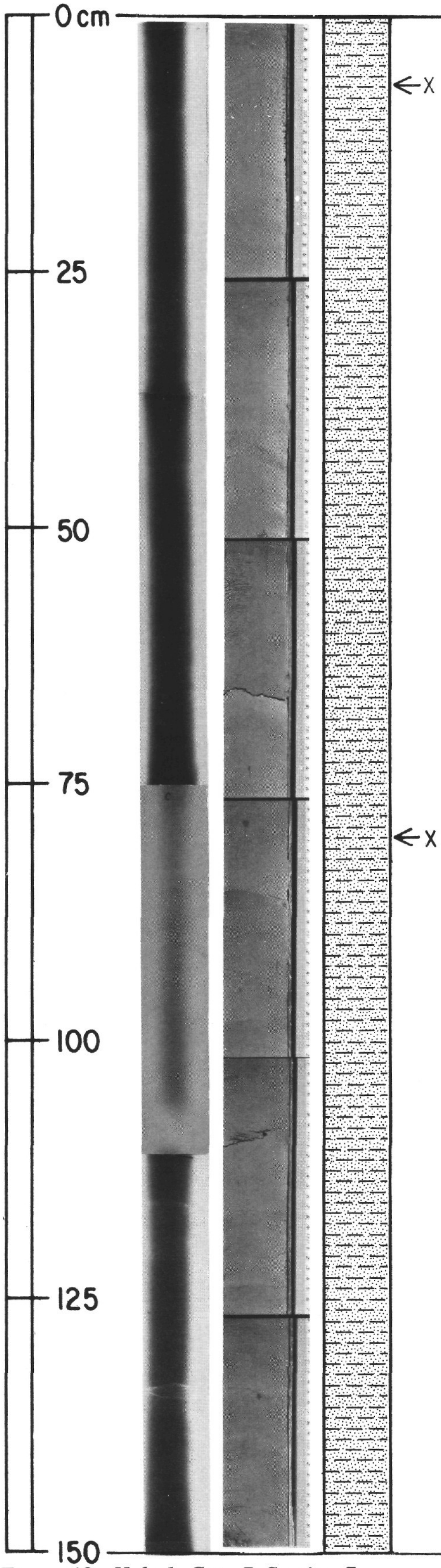

Silt mainly detrital carbonate and quartz; some opaque grains.
Total C 2.9; Org. C 0.7; $CaCO_3$ 18.2.
Water content 15.5.
Sand 0.1; silt 33.1; clay 66.8.

Clay, silty, carbonate-rich, terrigenous, gray (5Y 3/1) with small wisps of lighter silt (5Y 6/2), and abundant black specks and patches stained by FeS, 1 mm - 1 cm.

Silt mainly quartz and detrital carbonate.

Figure 43. *Hole 1, Core 7, Section 7.*

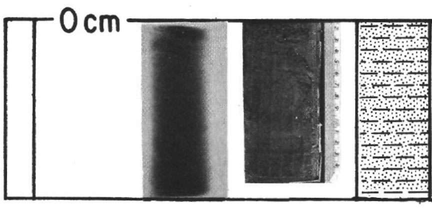

Clay, silty, carbonate-rich, terrigenous, gray (5Y 5/1), slightly mottled.

Figure 44. *Hole 1, Core 8, Section 1.*

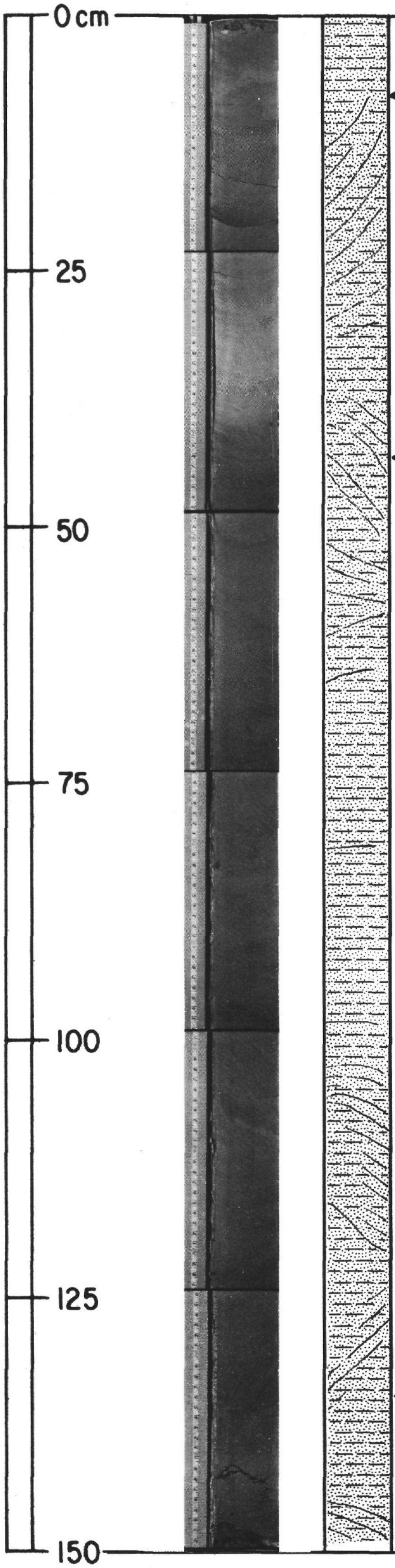

←X Silt mainly detrital carbonate, some quartz; trace nannoplankton.
Sand 0.5; silt 31.3; clay 68.2.

Total C 3.2; Org. C 0.6; $CaCO_3$ 21.3.
Water content 15.5.

Clay, silty, carbonate-rich, terrigenous, gray - top 10 cm (5Y 5/1) remainder (5Y 4/1) - with darker bands which show sharp reversals in dip: A chevron-folded sequence with horizontal fold-axes.

←X Silt mainly detrital carbonate, some quartz; trace nannoplankton.

Sediment speckled with light silt specks.

←X Sandy, mainly quartz but includes feldspar, silicates, rock fragments, opaque minerals.

Note: Arcuate marks on photo are cutting marks, not bedding.

Figure 45. *Hole 1, Core 8, Section 2.*

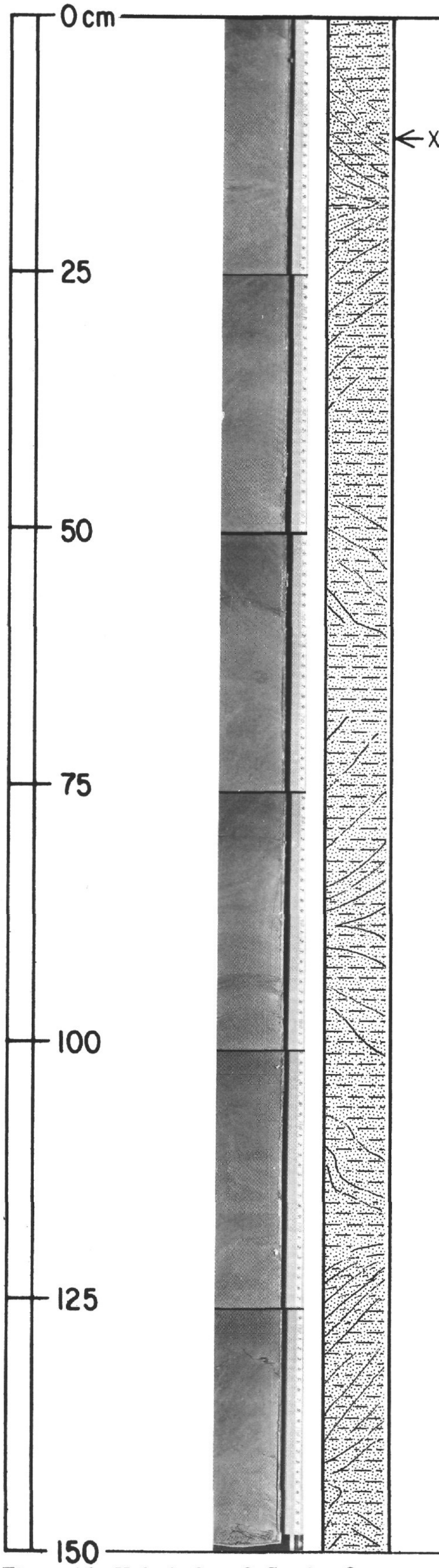

Total C 2.4; Org. C 0.5; $CaCO_3$ 16.2.
Water content 15.2.
Sand 2.0; silt 30.6; clay 67.4.
Silt, mainly detrital carbonate and quartz.
Axis.

Clay, silty, carbonate-rich, terrigenous, gray (5Y 4/1), banded dark gray (5Y 2/1) in 1 mm - 1 cm layers. Chevron folds with horizontal axes.

Jumbled zone.

Figure 46. *Hole 1, Core 8, Section 3.*

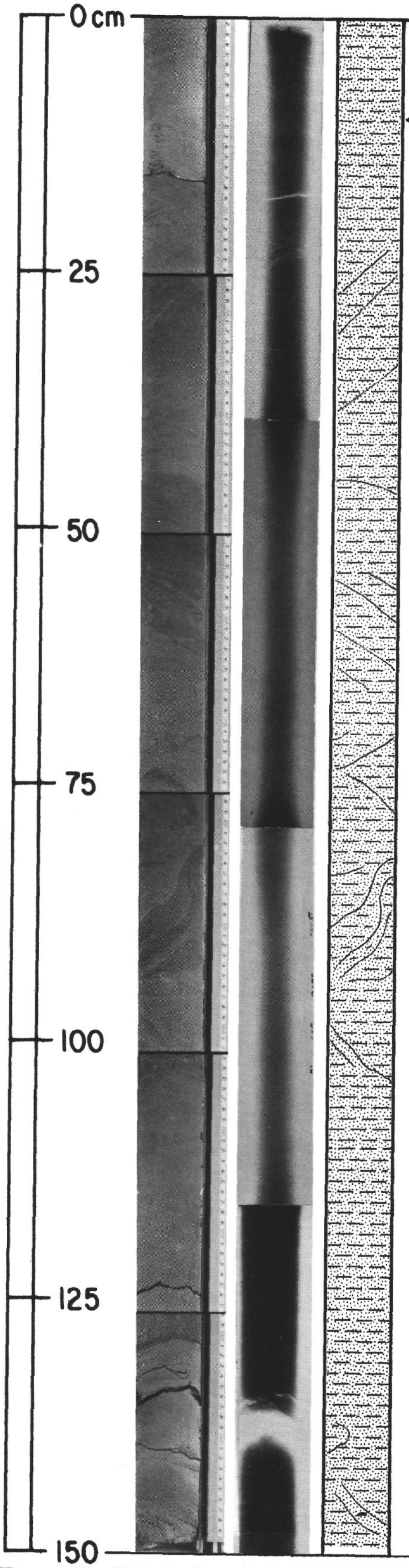

Total C 2.2; Org. C 0.4; $CaCO_3$ 14.8.
Water content 11.6.
Silt mainly detrital carbonate, some quartz.
Sand 1.1; silt 31.8; clay 67.1.

Clay, silty, carbonate-rich, terrigenous, gray (5Y 3/1 banded with 2/1 and 4/1), in recumbent chevron folds.

Irregularly contorted.

Figure 47. *Hole 1, Core 8, Section 4.*

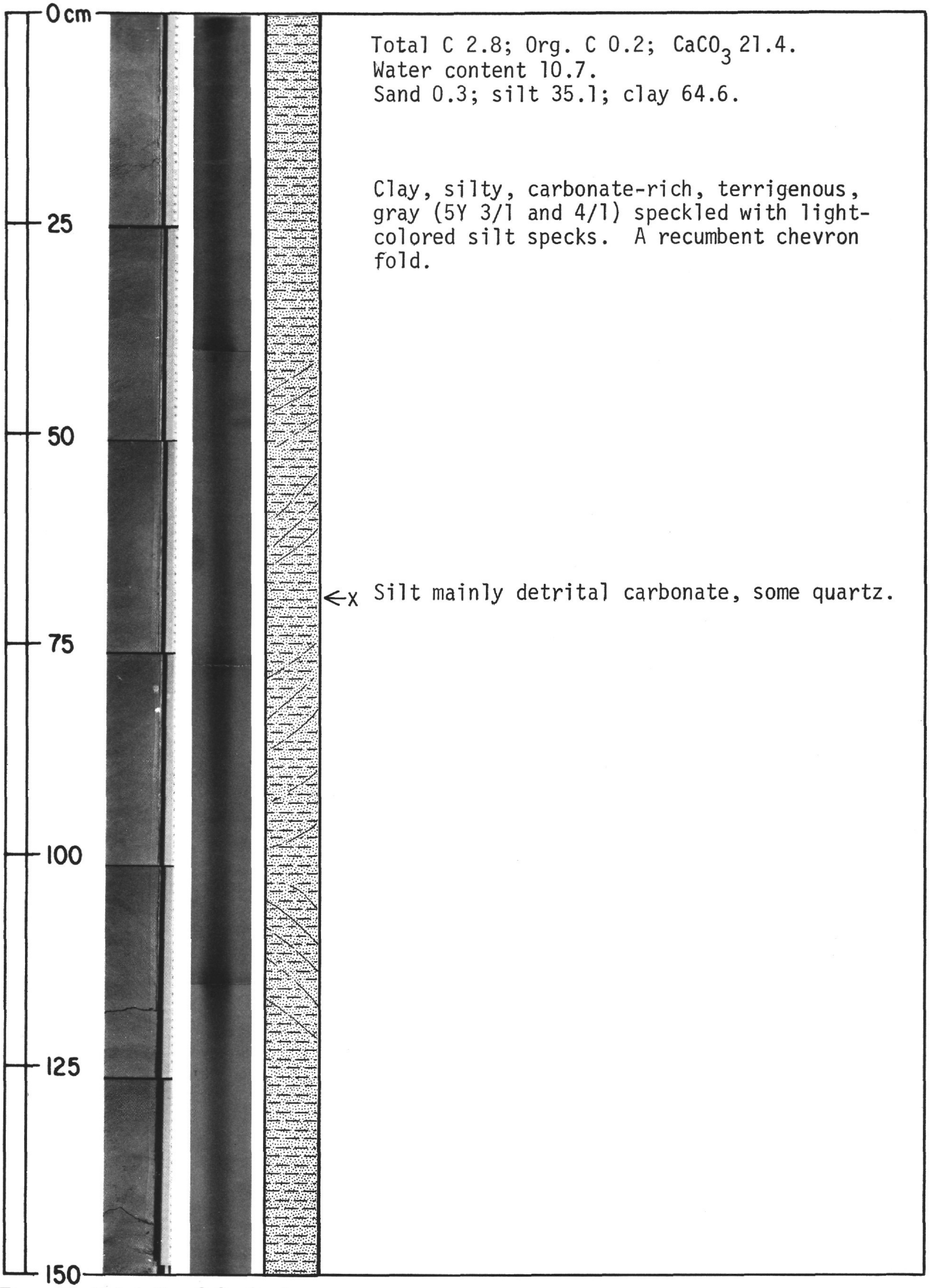

Figure 48. *Hole 1, Core 8, Section 5.*

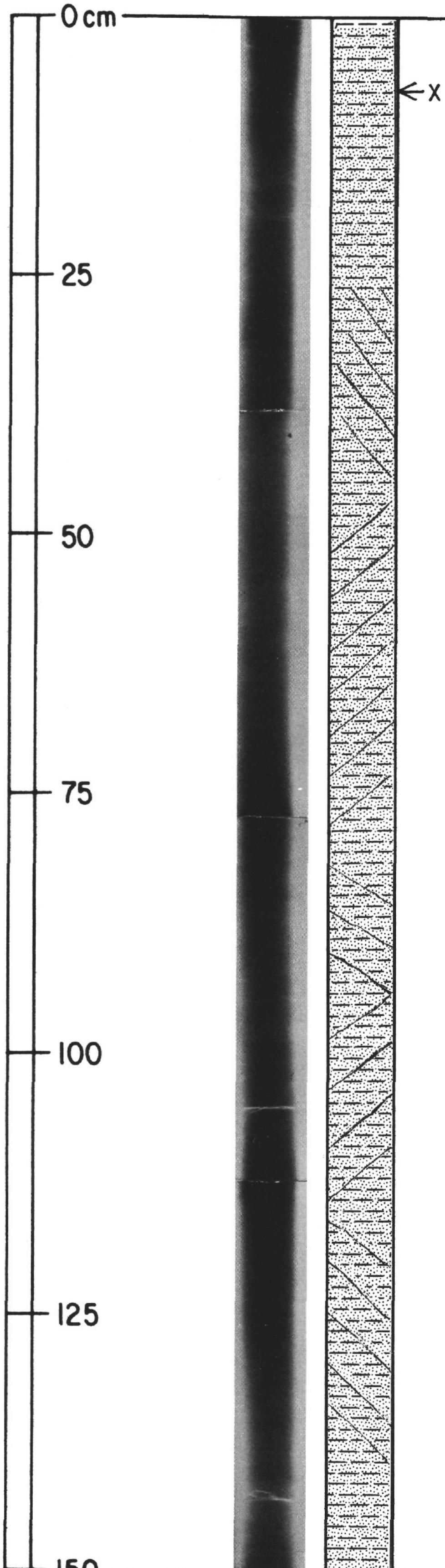

Total C 2.6; Org. 0.1; $CaCO_3$ 21.1.
Water content 12.1.
Silt mainly detrital carbonate and quartz; trace nannoplankton.
Sand 0.2; silt 32.7; clay 67.1.

Clay, silty, carbonate-rich, terrigenous, gray (5Y 4/) with slightly lighter and darker streaks and wisps, thrown into recumbent chevron folds.

Figure 49. *Hole 1, Core 8, Section 6.*

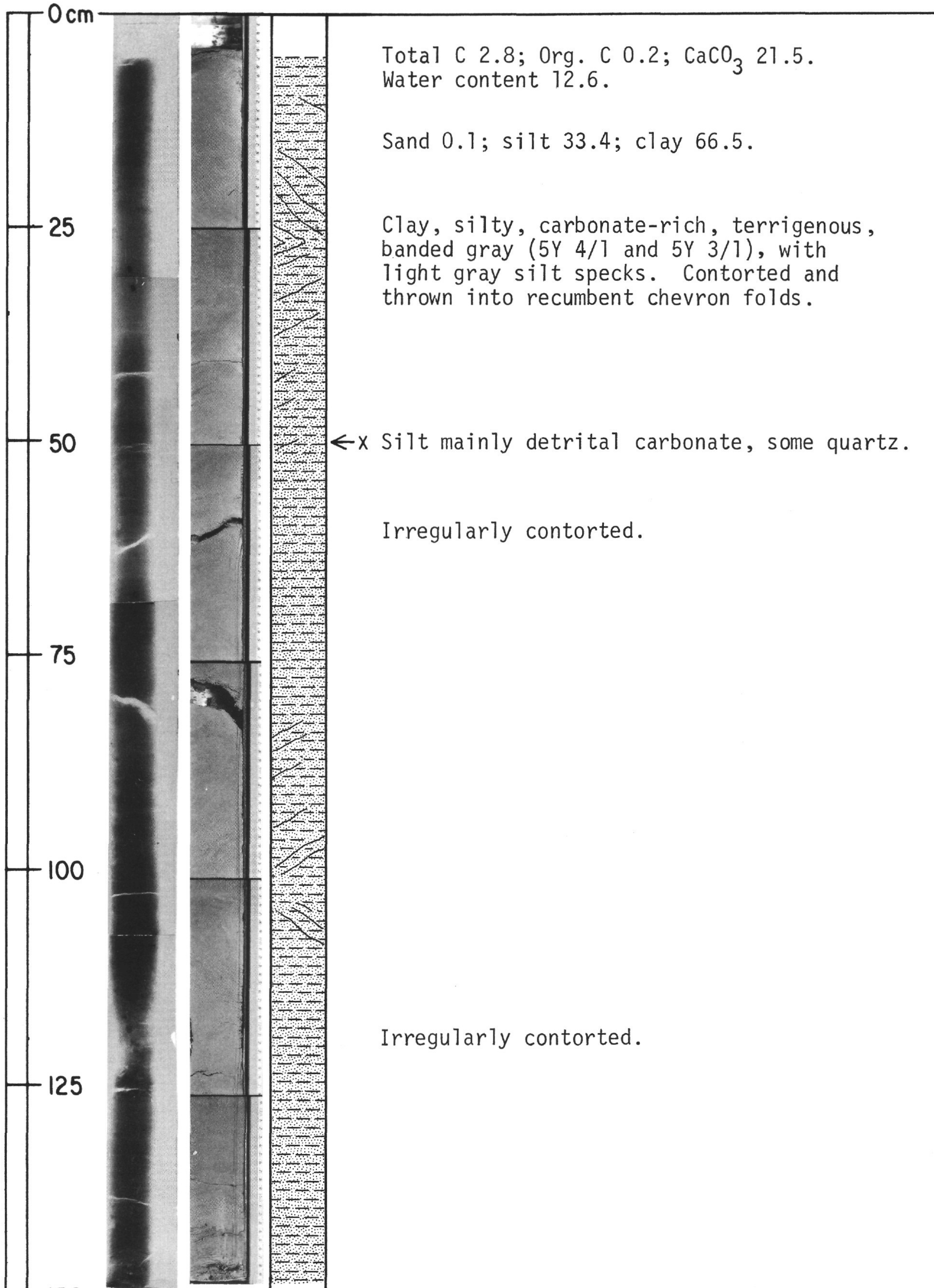

Figure 50. *Hole 1, Core 8, Section 7.*

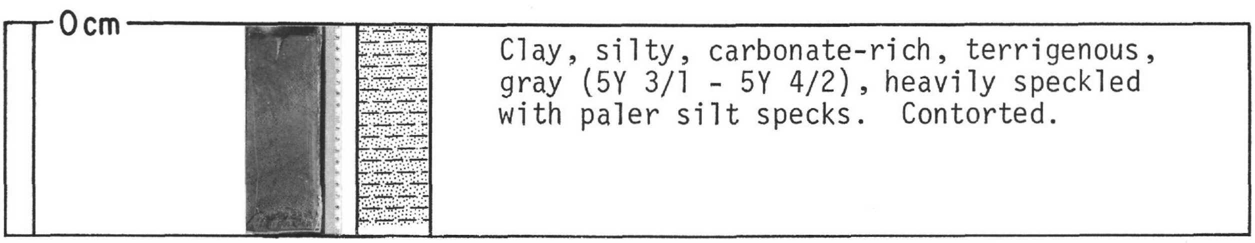

Figure 51. *Hole 1, Core 9, Section 1.*

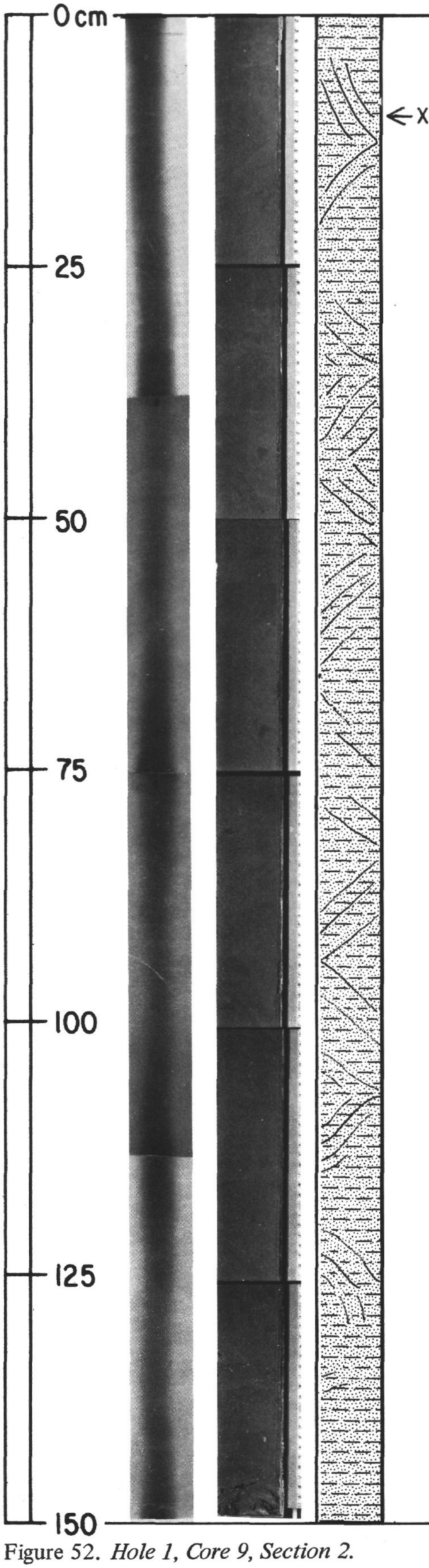

Sand 0.2; silt 31.8; clay 68.0.
Water content 15.6.

Silt mainly detrital carbonate, some quartz; trace nannoplankton.

Clay, silty, carbonate-rich, terrigenous, gray (banded 5Y 3/1 and 4/2), the (5Y 4/2) arcs due to heavy speckling with light silt specks sparse black FeS specks. Thrown into closely spaced recumbent chevron folds.

Figure 52. *Hole 1, Core 9, Section 2.*

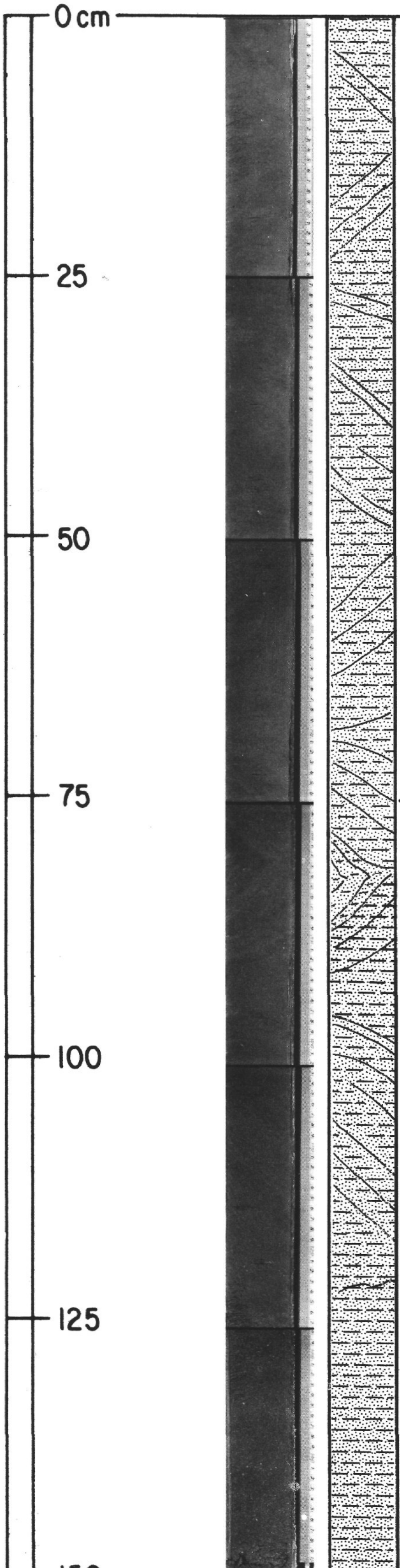

Total C 1.3; Org. C 0.8; $CaCO_3$ 4.3.
Water content 15.1.

Sand 0.3; silt 30.7; clay 69.0.

Clay, silty, carbonate-rich, terrigenous, gray (5Y 3/1 - 5Y 4/2), with abundant paler silt specks and some black FeS specks. Thrown into recumbent chevron folds.

<-X Silt mainly detrital carbonate, some quartz; trace nannoplankton.

Figure 53. *Hole 1, Core 9, Section 3.*

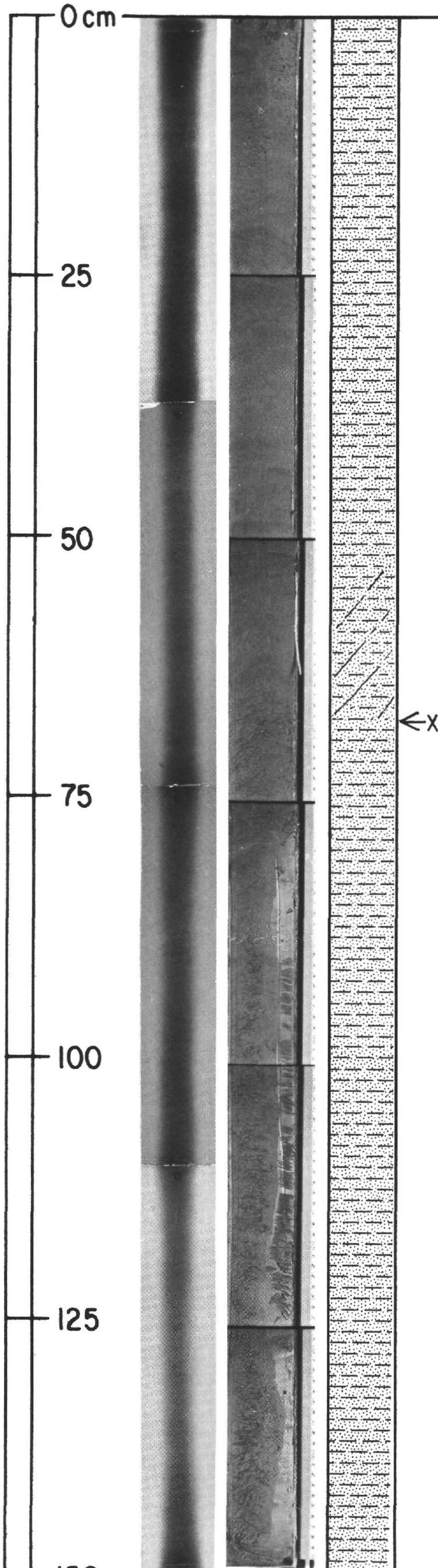

Total C 3.7; Org. C 0.7; $CaCO_3$ 24.6.
Water content 11.0.
Sand 0.2; silt 30.6; clay 69.2.

Clay, silty, carbonate-rich, terrigenous, gray (5Y 4/1) with light silt specks, massive.

Steep dip.

←x Silt mainly detrital carbonate and quartz.

Figure 54. *Hole 1, Core 9, Section 4.*

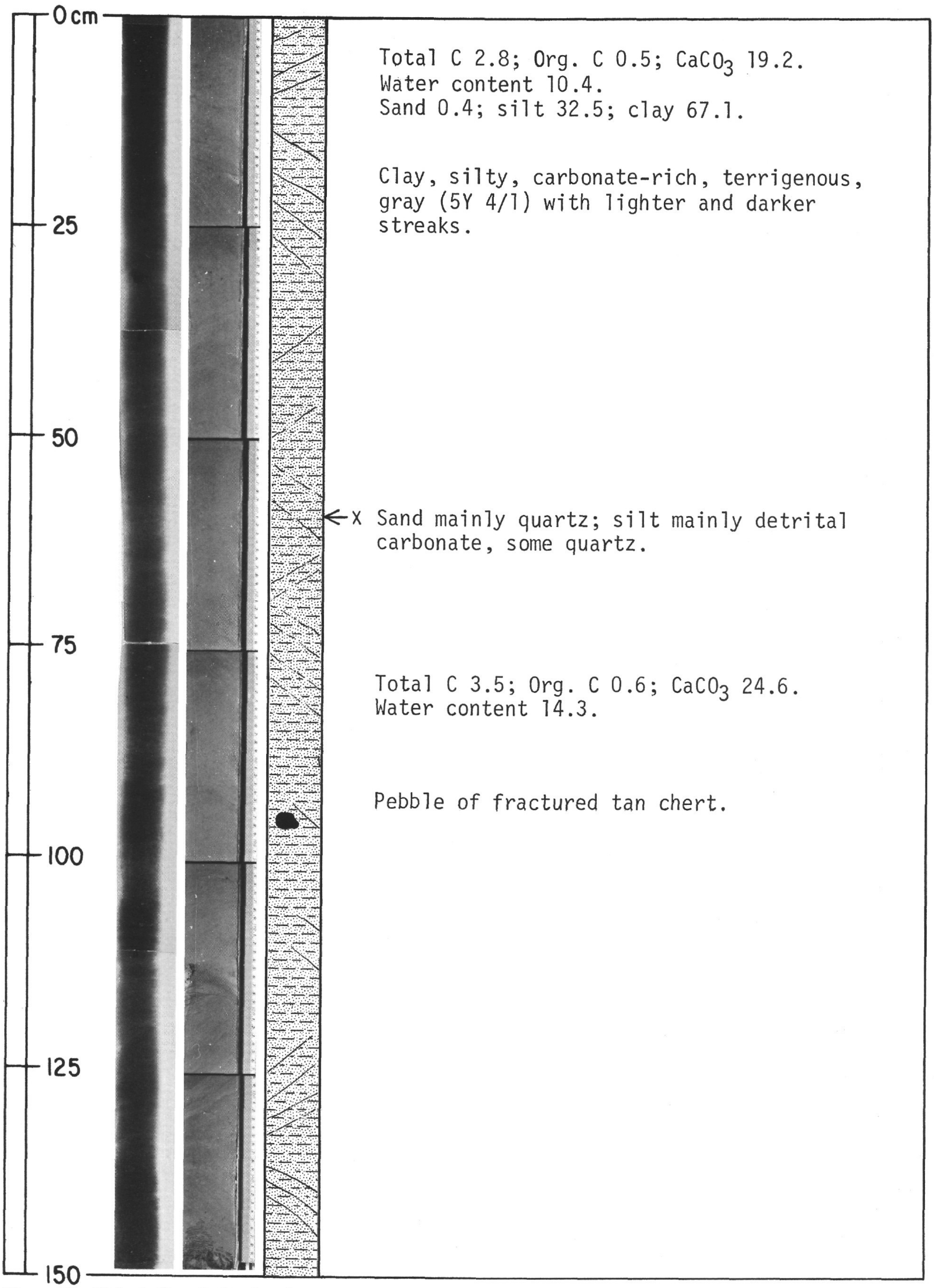

Figure 55. *Hole 1, Core 9, Section 5.*

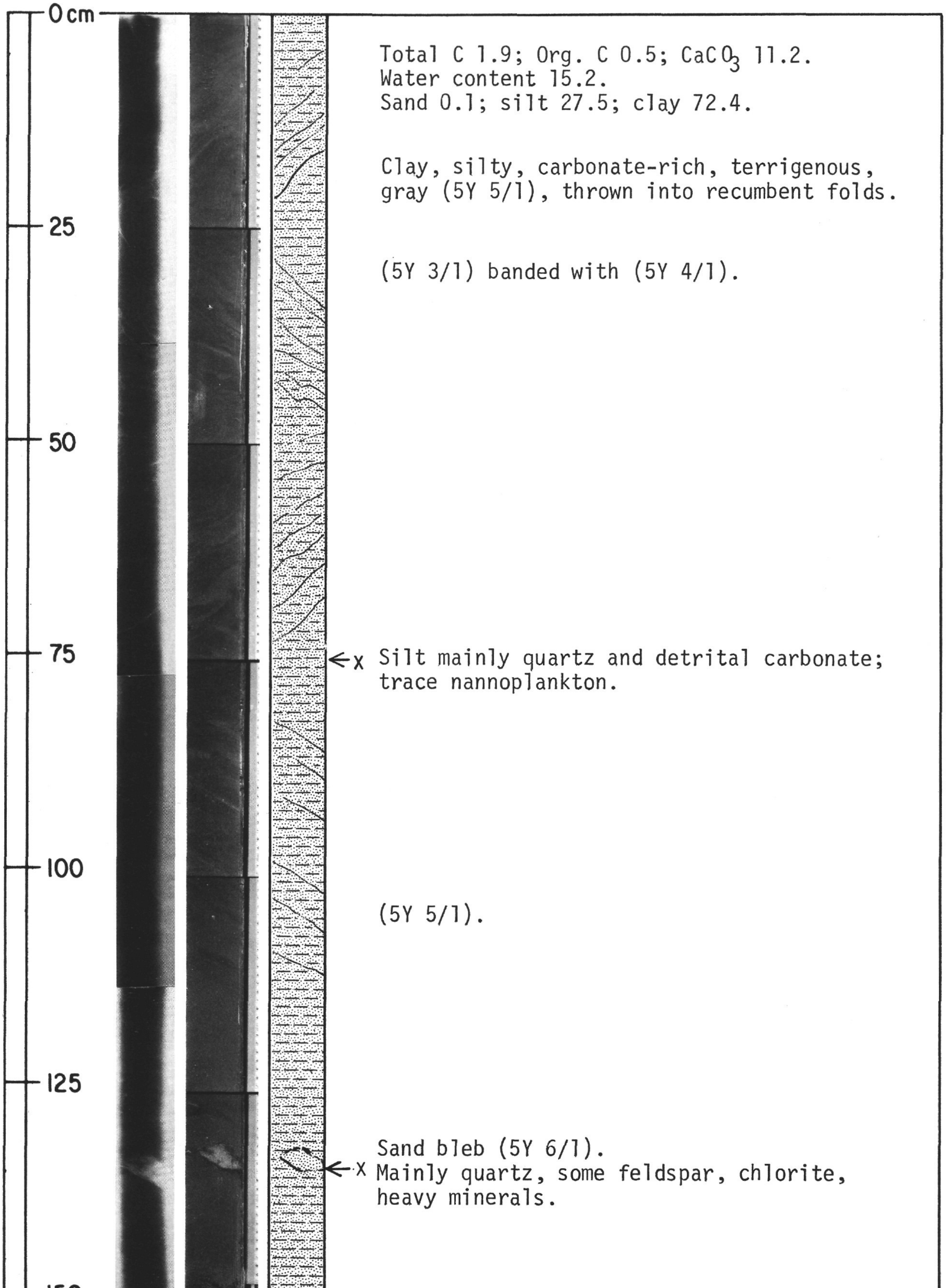

Figure 56. *Hole 1, Core 9, Section 6.*

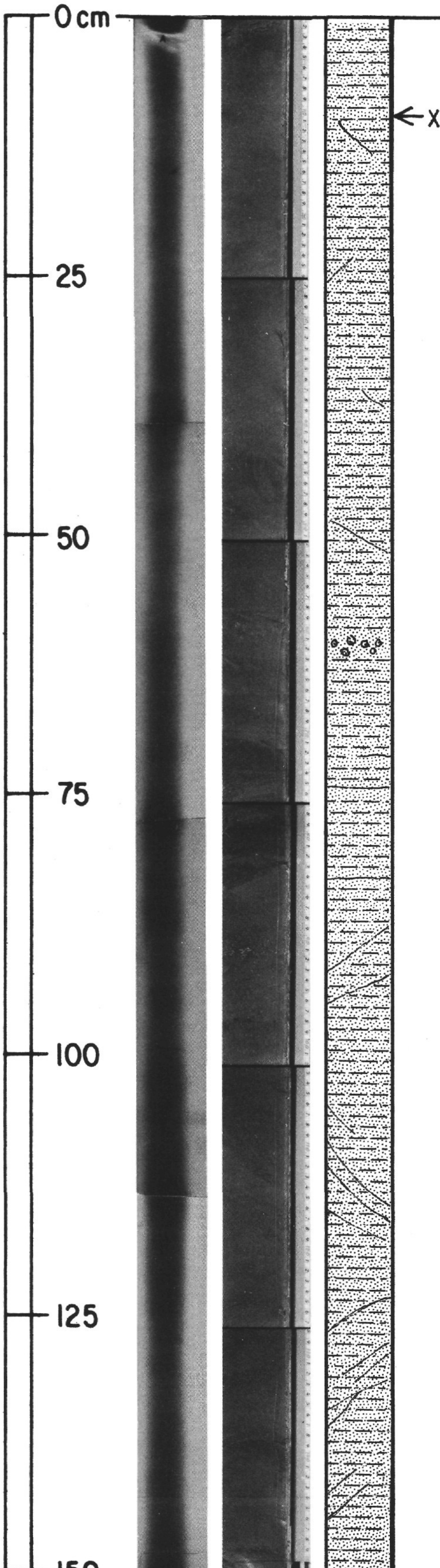

Total C 2.6; Org. C. 0.6; $CaCO_3$ 17.1.
Water content 13.3.
X Sand 4.3; silt 41.8; clay 53.9.
Sand mainly quartz; silt quartz and detrital carbonate.

Clay, very silty, carbonate-rich, terrigenous, gray (5Y 4/1), irregularly convoluted, with two recumbent folds in lower part.

Zone of sandy blebs (burrows?).

Dark zone (5Y 2/1).

Figure 57. *Hole 1, Core 9, Section 7.*

The Nature of the Sediments

General Description of the Sediments

Sediments recovered at Site 1 are dominantly brownish-gray silicate clays with a variable admixture of silt and sand particles (see Plate 6A, Chapter 24), and varied lamination with silt and sand beds. The main (Pleistocene) part of the section cored is of terrigenous origin throughout, whereas the uppermost (Holocene or Recent) core contains an appreciable admixture of nannofossils and pelagic foraminifera.

The basal cores of the Pleistocene sequence (Cores 6 through 9) consist of rather well consolidated, massive to obscurely laminated silty clays with up to about 20 per cent calcium carbonate, most of which appears to be terrigenous rock flour, dolomite exceeds calcite (see Figure 1, Chapter 24). Of the scarce fossils present, most are Cretaceous coccoliths, presumably derived from the Cretaceous outcrop belts on the continent, but some pelagic foraminifera and nannofossils date the cores as Pleistocene.

The upper drilled cores (1 through 5) and the base of the piston core are rather similar in general composition, both contain many beds of clayey quartz silt, ranging in thickness from a few silt grains to several centimeters (see Plate 3, A, B & C, Chapter 24). These beds normally have a sharp base and a less distinct top. Some of these silt beds show horizontal to sub-horizontal lamination, and a few show ripple lamination. The massive to laminated clays also show scattered sand-filled burrows, cutting the bedding at oblique angles, but extensive burrowing is not observed and pelagic foraminifera are absent. The silt lamination is so characteristic of these sediments that they merit Lombard's (1963) term "laminite." The silty clays of this sequence also differ from the underlying massive mudstones by having a higher silt content, but fewer and finer sand grains; whereas the sand grains in the underlying beds commonly reach a diameter of 0.5 millimeter, those of the laminite clays are generally below 0.25 millimeter.

The uppermost stratigraphic unit, comparing the top 8.7 meters of the piston core, is of clay containing 10 to 25 per cent nannoplankton and planktonic foraminifera.

Discussion

Both the basal massive mudstones and the overlying laminites are: chemically immature sediments, lacking in skeletal materials, full of carbonate rock flour, and may represent paraglacial sediment. Sedimentation throughout the time period represented by the cored section was rapid (see Paleontology notes). The basal sediments seem to have been deposited in an area out of reach of most currents – quite possible on the face of the Sigsbee Scarp, or on the lower edge of the slope; the laminite facies, sediments, on the other hand, were deposited on a surface swept time and again by currents strong enough to carry silt – presumably low-energy turbidity currents. In this they are typical of abyssal plain or abyssal fan turbidity current sedimentation. The tortuous path which such currents would have had to follow from the north through the hummocky continental slope would have slowed them down. This would explain the limited contribution of coarse detritus.

The uppermost stratigraphic unit clearly represents the postglacial sequence with its warmer waters and slower, though still comparatively rapid, sedimentation rate.

It cannot be certain that the cores are representative of the section penetrated; the gaps between cores might well contain other interglacial pelagites—the electric log suggests this possibility. On the other hand, there is no certainty that the section penetrated is a normal stratigraphic sequence. The reflection profiles show that the sediments of this area are disturbed, and this is born out in some of the cores – specifically in parts of Cores 2, 8 and 9. The deformation shown by these cores consists of an intense chevron folding with horizontal axial planes, as shown in the core descriptions and in X radiographs (see Plate 3, A & B, Chapter 24). Some of the more strongly consolidated cores also show peculiar sub-horizontal, intersecting hackly fractures (see Plate 3C, Chapter 24) but it is not certain whether these represent a kind of natural fracture cleavage, or something due to drilling. This deformation is clearly a soft-sediment deformation and presumably the chevron folds mark the noses of recumbent nappe-like bodies, moving or moved in a down-dip direction, i.e., away from the Sigsbee Scarp. The authors suggested above that the lower massive muds might have come from the scarp itself; the laminites could not have, and yet they, too, show similar deformation. Also, the belt of disturbed sediments indicated by the reflection profiles is rather too voluminous to have come from the scarp itself; thus, the origin of this deformation remains obscure.

Physical Properties of the Sediments

Determinations of bulk density (and porosity) by the GRAPE device were not made on all the Hole 1 Cores due to mechanical malfunctions during processing of this suite of cores. Cores 1 and 2 show small variations in bulk density which are interpreted as reflecting the presence of thin silt laminae. Unfortunately, it was not possible to obtain detailed descriptions of these cores in order to compare curve response directly with lithology. One section of Core 8 was also analyzed. Small scale variation of bulk density in the latter is thought to reflect variation in sediment core diameter, a variable which can not be controlled in semi-consolidated sediment.

By averaging bulk density data for each core barrel determined, an average bulk density curve was prepared and is shown in Figure 4. (No data are available for Cores 3, 5, 6, 7, and 9). Although the data are sparse, a generalized curve showing an increase of density with depth is easily constructed with the largest changes occurring near the sea floor in the upper 200 meters of sediment. Density values, however, were initially abnormally high. After several attempts to recalibrate the GRAPE unit, an aluminum standard was prepared for use as an intermittent calibration check. Based on preliminary results, the GRAPE readings were thought to be approximately 0.3 g/cc too high. Thus, both the barrel plots and the average curve have been adjusted downward 0.3 g/cc.

Using the correction outlined above, a bulk density of approximately 1.8 g/cc (extrapolated) near the surface down to approximately 2.2 g/cc in the bottom of the boring is in fair agreement with extrapolations, which were based on seismic data made prior to drilling, of approximately 1.96 g/cc average bulk density.

Determination of natural gamma-ray intensity is considerably more complete than the GRAPE determinations for Site 1 cores. Averaged gamma-ray readings for Cores 1, 2, 3, and 5 are quite comparable, especially when contrasted to readings for the upper part of the piston core that average around 5800 counts per 2.5 minutes in the foraminiferal clay. Cores 6, 7, 8, and 9 show readings consistently higher than 9000 counts per 2.5 minutes forming a third distinctive grouping as based on natural gamma-ray determinations. These subdivisions agree well with previously made lithological subdivision based on conventional data.

Percentage difference between high and low natural gamma-ray counts cannot be directly compared to determinations from the down-hole (open hole), gamma-ray log. As previously discussed in the section on down-hole logging, grossly relative differences of gamma-ray values appear somewhat comparable. This also apparently holds true for the density logs.

Penetrometer readings, taken for each core section, were averaged for each core barrel in an attempt to show gross consolidation. For this purpose, an arbitrary consolidation scale is proposed here. Penetrometer values of 0 to 10 qualify a sediment as a stone; readings between 10 to 30 categorize sediment as semi-consolidated; and readings greater than 30 related to unconsolidated sediment. These terms refer to fine-grained sediment or mud only. Variability and consequent reduction of reproducibility in coarse-grained sediment reduces usefulness of the measurement.

Using the scale above, the cored sediments in Site 1 show a general trend toward becoming more consolidated with depth. This trend, however, appears less obvious than the noticeable difference in penetrometer values of semi-consolidated sediment in the lower portion of the hole as compared to the unconsolidated sediment above.

The difference in state of consolidation may be partially reflected in the down-hole logs as an increase in resistivity or increase in gamma-ray counts and gamma-gamma density. These differences are also reflected by limited GRAPE determinations, and has been pointed out previously.

The section shown in Figure 4 is interpreted as representative of a rather thick section of Pleistocene laminite mud which is overlain by a very thin unit of Holocene (?) and upper Pleistocene foraminiferal clay. It seems quite likely that similar pelagic clays, representing interglacial, eustatic high stands of sea level, are present (but not cored) and interbedded with the dominantly maninite facies. This general sequence overlies and is apparently transitional downward into a massive to laminated sequence of semi-pelagic clays near the base of the borehole.

Various lines of evidence from density, penetrometer, and down-hole logs indicate that sediments at Site 1 are overconsolidated as compared to normally pressured, normally consolidated Pleistocene continental shelf sediments of the northern Gulf of Mexico. This will be discussed further in Chapter 24. It is suggested that the deformation of sediment at Site 1 had the effect of remolding the sediment and that the new equilibrium state is a more consolidated condition than the original state, thus forming conditions for continued consolidation of the entire section at a rate in excess of that attained by contemporaneous shelf sediments. It is further suggested that this deformation is related by proximity to the Sigsbee Scarp. The ultimate origin of forces of deformation and how such forces might be transmitted by such incompetent sediment is not known. Further analysis is suggested.

Biostratigraphy

Foraminifera

In the Site Reports (Chapters 1 through 7) brief faunal lists are presented of the significant foraminiferal species observed in cores from the seven holes drilled by the first Leg of the Project. These lists are not be to construed as complete or representative of the total fauna in any given sample. The identification lists include those species which are either abundant, or are of stratigraphic importance, or, in some instances, may have some climatic significance. Benthonic species of foraminifera have been listed in some samples where they are of general interest. A relatively diverse benthonic foraminiferal fauna has been observed in the Pliocene and Pleistocene of the Gulf of Mexico. Most of these forms can be identified by referring to the Challenger Expedition Reports, Volume 9 (Foraminifera).

In the listing presented below, the abbreviations (D) and (S) stand for dextral and sinistral, respectively, and refer to the mode of coiling of a specific species of planktonic foraminifera.

Sample 1(1-1-1-1, 136-137 cm):
Globigerinoides rubra (including pink variant), *G. conglobata, G. sacculifera, Globorotalia truncatulinoides, G. inflata, Globigerina bulloides, Hastigerina siphonifera, Globoquadrina dutertrei.* Benthonics: *Planulina bradyi, Bulimina marginata, Uvigerina peregrina, Cibicides* sp., *Laticarinina* sp.
Age: Pleistocene.

Sample 2(1-1-1-2, 124-126 cm):
Globigerinoides rubra (including pink variant), *G. sacculifera, G. conglobata, Globorotalia truncatulinoides, G. menardii, G. tumida, G. inflata, Globoquadrina altispira.*
Age: Pleistocene.

The cores taken at Site 1 penetrated a thick sequence of late Pleistocene turbidites. A few scattered carbonate intercalations were observed and two of these are recorded here. Similar late Pleistocene faunas were observed at the following two levels, as well: Section 3, 109-110 centimeters, and Section 4, 127-129 centimeters. The faunas are essentially subtropical in nature and suggest that these layers may represent accumulations during interglacial periods. The turbidites are essentially nonfossiliferous, although scattered juvenile specimens of buliminids, bolivinids, uvigerinids and various rotaliids were observed in some samples.

Calcareous Nannoplankton

For detailed correlation and discussion of individual samples see the report by Bukry and Bramlette (Chapter 15). In summary, the nannoplankton samples examined indicate the entire section cored to be Pleistocene in age.

SUMMARY: HISTORICAL AND REGIONAL ASPECTS

Site 1 saw selected and drilled largely as an engineering test of the drilling equipment and operating procedures; nevertheless, it provided some valuable geological data. The site was about two miles south of the Sigsbee Scarp in 2878 meters (9275 feet) of water, and the hole penetrated 770 meters (2528 feet) below the sea floor. It is possible that the site was situated in a slight embayment into the Sigsbee Escarpment.

A thin surficial interval at the sea floor contains a mixture of Pleistocene and Upper Cretaceous nannoplankton, but most of this sequence contained only sparse, reworked Upper Cretaceous nannoplankton. The section cored is interpreted to be entirely of Recent to Pleistocene age. Well logs suggest the possible presence of lithologies different from those of the cored intervals; it is possible that these may represent interglacial stages.

It appears most probable that the section cored is part of the Sigsbee Abyssal Plain at a point near where it abuts the bordering scarp. The sediments consist of unconsolidated silt and clay, poorly fossilferous but rich in detrital carbonates of unknown origin. Several cores expanded within the plastic liners and were described as "gassy". Shipboard studies of natural gamma-radiation indicates that the clays are fairly homogenous throughout the cores, suggesting the possibility that all were derived from a single source. There is a notable absence of pelagic foraminifera and a general absence of burrowing. There is no evidence of shallow-water sediments or sedimentary processes in any of the cored intervals. The sequence is partly laminated by silt in thin graded beds.

Thus, all of the data available suggest that the sediments cored represent a Recent to Pleistocene sequence of suspended debris from the adjacent continental slope and/or turbidites derived perhaps from a more distant source, such as the Mississippi Fan. This deep-water sediment accumulated very rapidly. A minimum rate of accumulation is 38 cm/10^3 years, assuming that the entire two million years since the close of the Pliocene was represented in the interval drilled; for the purposes of the present discussion, it seems necessary to make allowances for the repetition of beds due to chevron folding. These are all features characteristic of abyssal plains in general, and of the Sigsbee Abyssal Plain in particular.

Perhaps the feature in these cores of greatest regional significance is the prominent deformation which is displayed in them. The near-surface clays and silts appear to be entirely undisturbed, but many of the cores, especially in the lower part of the hole, contain abundant chevron folds. These have a wave length of commonly less than one meter, with essentially horizontal axial planes (assuming that the hole was vertical). No definite faulting was apparent, but in many of the cores these chevron folds are stacked in a series, one on top of another.

The seismic reflection data provided by the petroleum industry in the vicinity of Site 1 shows an interval of strongly diffracted arrivals overlying a sequence of uniformly- and evenly-layered reflectors. This diffracted interval extends for a considerable distance south of the Sigsbee Scarp (Figure 59).

On possible origin for these small, tight folds is that they owe their origin to tectonic stresses generated by movements within the adjacent continental slope. In fact, the industry data provided do suggest the presence of a sill-like diapir north of the Sigsbee Scarp which could confine lateral compressive stresses to the upper part of the adjacent abyssal plain sediments. However, it does not seem at all reasonable to expect these uncemented and poorly consolidated sediments to be able to transmit such stresses for any significant distance away from the scarp, as suggested by the diffracted interval in the seismic reflection records.

A more likely explanation may be that these water-saturated sediments moved laterally under the force of gravity for only short distances due to the slight steepening of the slope of the depositional surface (perhaps also triggered by tectonic movements within the adjacent slope). The seismic reflection data suggest such tilting of the sea floor adjacent to the scarp since the deeper reflectors do not diverge markedly northward toward the slope, as would be expected if subsidence were continuous.

It also seems unlikely that these sediments could remain intact during transport over log distances, as would be necessary if they owed their origin to mass movement of debris down the very irregular slope. There is also no indication of a random or irregular strike of the axes of these small folds. Alternatively, these beds could have been emplaced by mass movement down the slope before formulation of the Sigsbee Scarp—unless it can be shown that the scarp is older than these sediments. This type of deformation has not been seen in cores taken elsewhere in the Sigsbee Abyssal Plain.

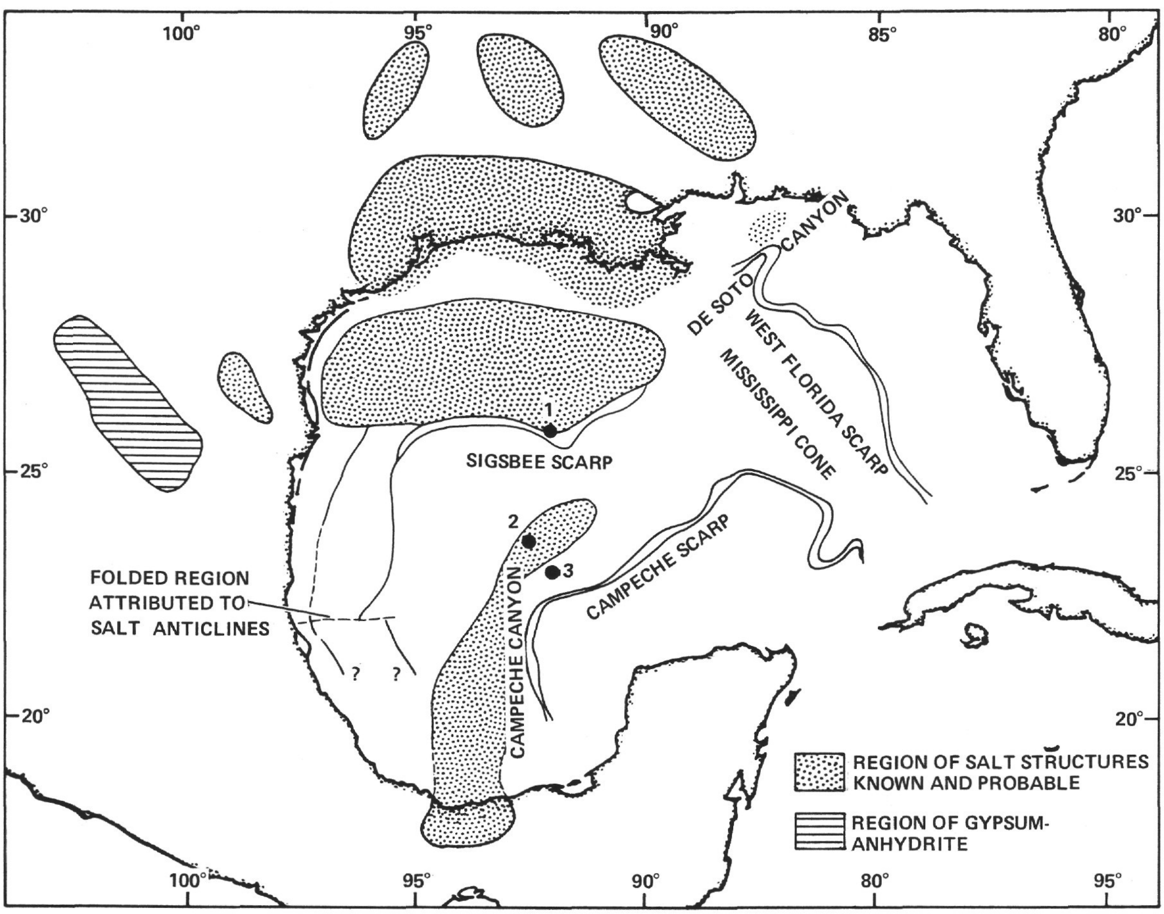

Figure 58. *Physiographic diagram of Gulf of Mexico, showing locations of Sites 1, 2 and 3.*

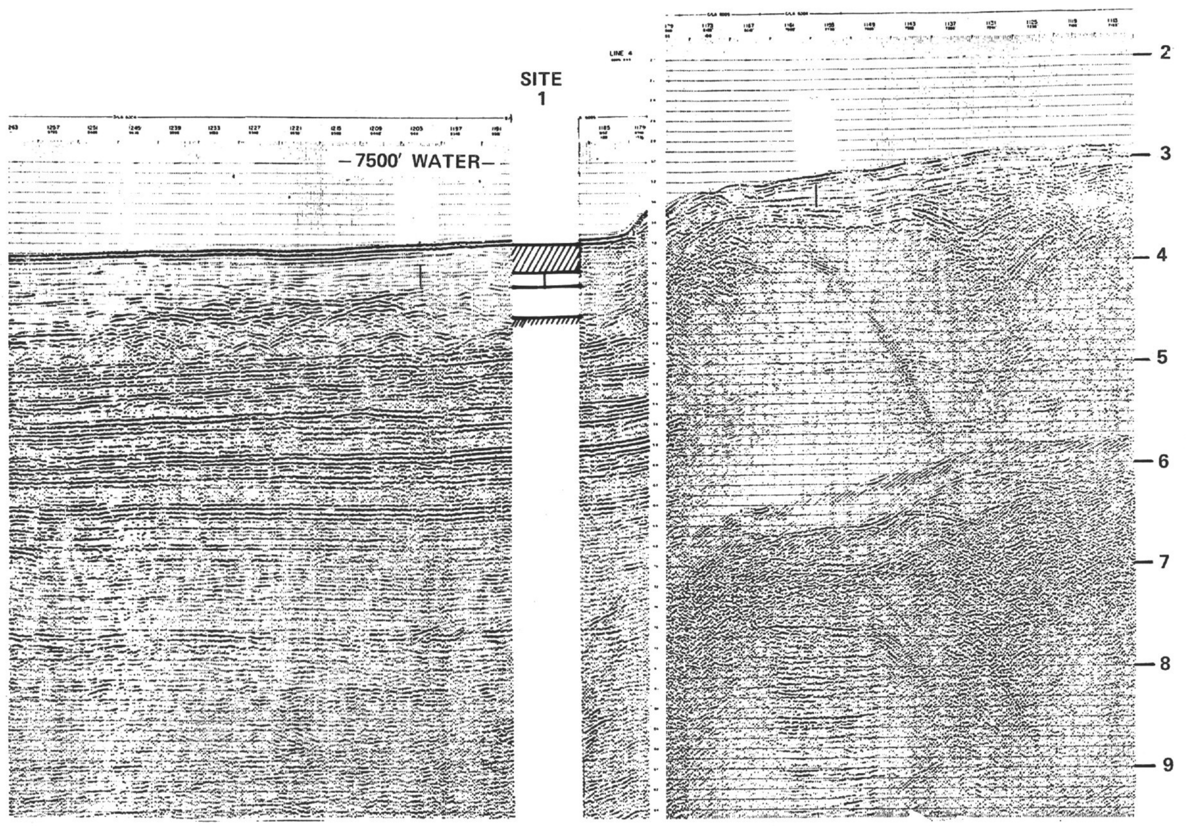

Figure 59. *Profiler record near Site 1.*

REFERENCES

Antoine, J. and Ewing, J., 1963. Seismic refraction measurements on the margins of the Gulf of Mexico. *J. Geophys. Res.* **68** (7), 1975.

Curray, J. R., 1960. Sediments and history of Holocene transgression, continental shelf, northwest Gulf of Mexico. **In** *Recent Sediments Northwest Gulf of Mexico.* F.P. Shepard, F. B. Phleger, and Tj. H. van Andel (Eds).*Bull. Am. Petrol. Geologists,* p. 221.

Eardley, A. J., 1951. *Structural Geology of North America.* New York (Harper & Brothers).

Ewing, J., Antoine, J., and Ewing, M., 1960. Geophysical measurements in the Western Caribbean Sea and in the Gulf of Mexico. *J. Geophys. Res.* **65** (12), 4087.

Ewing, M. and Antoine, J., 1966. New seismic data concerning sediments and diapiric structures in Sigsbee Deep and upper continental slope, Gulf of Mexico. *Bull. Am. Assoc. Petrol. Geologists.* **50** (3), 479.

Ewing, M., Worzel, J. L., Ericson, D. B., and Heezen, B. C., 1955. Geophysical and geological investigations in the Gulf of Mexico, Part I. *Geophysics* **20** (1), 1.

Gealy, E. L., 1955. Topography of the continental slope in northwest Gulf of Mexico. *Bull. Geol. Soc. Am.,* **66**, 203.

Halbouty, M. T., 1967. *Salt Domes Gulf Region, United States and Mexico.* Houston (Gulf Publishing Co.), 425 pp.

Hardin, F. R. and Hardin, G. C., Jr., 1961. Contemporaneous normal faults of Gulf Coast and their relation to flexures. *Bull. Am. Assoc. Petrol. Geologists.* **45**, 238.

Joesting, H. R., and Frautschy, J. D., 1947. Reconnaissance gravity survey in the Gulf of Mexico. U. S. Geol. Survey Geophys. Invest. Prelim. Map, 1 sheet.

Jones, B. and Antoine, J., 1968. Geophysical survey of the Texas-Louisiana continental shelf and slope (Abstract). Soc. Expl. Geophys. Regional Mtgs., Fort Worth, Texas.

King. P. B., 1959. *The Evolution of North America.* Princeton (Princeton University Press), 190 pp.

Lankford, R. R., and Curray, J. R., 1957. Mid-Tertiary rock outcrop on continental shelf, northwest Gulf of Mexico. *Bull. Am. Assoc. Petrol. Geologists.* **41**, 2113.

Lehner, P., 1968. "Salt tectonics and Pleistocene sediments on the Texas-Louisiana portion of the continental slope of the Gulf of Mexico (Abstract). Program Mtg., *Geol. Soc. Am. Spec. Papers,* Mexico City, Mexico, November 11-13, 1968, 172.

Matthews, R. K. 1963. Continuous seismic profiles of a shelf edge bathymetric prominence in northern Gulf of Mexico, *Gulf Coast Assoc. Geol. Soc. Trans.* **13**, 49.

Moore, D. G., and Curray, J. R., 1963. Structural framework of the continental terrace, northwest Gulf of Mexico. *J. Geophys. Res.* **68** (6) 1725.

Murray, G. E., 1961. Geology of the Atlantic and Gulf Coastal Province of North America. New York (Harper & Brothers).

Nettleton, L. L., 1957. Gravity survey over a Gulf Coast continental shelf mount. *Geophysics.* **22** (3), 630.

Newmann, A. C., "The configuration and sediment of Stetson Bank, Northwestern Gulf of Mexico" (unpublished technical report 58-5T, Texas University, 1958), 125 pp.

Parker, R. H., and Curray, J. R., 1956. Fauna and bathymetric of banks on continental shelf, northwest Gulf of Mexico. *Bull. Am. Assoc. Petrol. Geologists.* **40**, 2428.

Shepard, F. P., 1937. 'Salt' domes related to Mississippi Submarine Trough. *Bull. Geol. Soc. Am.* **48**, 1349.

Worzel, J. Lamar (in press) Results achieved and their implications. **In** *Drilling and Coring the Deep-Sea Floor.* Proc. Vetlesen Symposium, November 25, 1968, Columbia University, New York.